Dissertation

Submitted to the

Combined Faculty of Natural Sciences and Mathematics of the Ruperto Carola

University Heidelberg, Germany for the degree of

Doctor of Natural Sciences

Presented by **Pablo Hernández Malmierca**

born in: Madrid, Spain

Oral examination: 14.09.2021

Hematopoietic stem cells - active modulators of immunity and hematopoiesis in health and disease

Referees: **Prof. Dr. Andreas Trumpp**

Dr. Michael Milsom

TABLE OF CONTENTS

SUMMARY

Hematopoietic stem and progenitor cells (HSPCs) are responsible for the life-long production of mature blood and immune cells. These mature cells perform a wide variety of function in the body, from oxygen distribution to defense against external and internal threats. Within the immune system, adaptive immune cells are capable of mounting a highly specific immune reaction against unique pathogenic epitopes. To accomplish this distinctive feature, antigens are presented to T cells by the major histocompatibility complexes (MHC). While MHC class-I (MHC-I) is expressed on the majority of cells and activates $CD8^+$ T cells, $CD4^+$ T cell-activating MHC-II is exclusively expressed by specialized antigen presenting cells (APCs). In fact, antigen presentation via MHC-II to $CD4^+$ T cells constitute the central process in the orchestration of adaptive immune responses.

The data in this thesis uncovered that HSPCs are not only passive receivers of immunological signals but act as antigen presenting cells capable of functionally modulating $CD4^+$ T cells and thus, their immune microenvironment. First, we demonstrated that mouse and human HSPCs express MHC-II at transcript and protein levels. Subsequently, we showed that HSPCs can process and present endogenous and exogenous antigens via MHC-II. Antigen presentation to $CD4^+$ T cells resulted in an efficient T cell activation and immunoregulatory polarization. In detail, these T cells adapted a type 1 regulatory T cell (Tr1)-like state, were capable of suppressing bystander T cells and polarized macrophages into an immunoregulatory state via IL-10. Importantly, HSPCs were induced into cell cycle and myeloid differentiation upon antigen-specific interaction with $CD4^+$ T cells *ex vivo* and *in vivo*. Furthermore, sustained antigen presentation promoted HSPC exhaustion. In acute myeloid leukemia (AML), a hematopoietic malignancy derived from HSPCs, an immature phenotype resembling stem cells correlated with higher MHC-II expression and adverse prognosis. HSC-derived AMLs maintained the $CD4^+$ T cell activation ability. Moreover, HSC exhaustion upon extended antigen presentation protected the organism from AML onset. In summary, the first part of this thesis unveils a previously unknown interaction of HSCs with $CD4^+$ T cells. This interaction induces a tolerance mechanism promoting immune suppression within the bone marrow. Last but not least, the immunosuppressive HSPC-T cell interaction proves to be an immune-mediated protection against AML onset.

Leukemogenesis is a complex process in which a stepwise acquisition of mutations transforms healthy HSPCs into pre-leukemic and, subsequently, into leukemic cells. Leukemic stem cells (LSCs), similar to their healthy counterparts, are resistant to conventional therapy and responsible for AML relapse. However, current methods do not enable a distinction and

systematic comparison between healthy and (pre-)leukemic cell states. Thus, in the second part of this thesis, a method that overcomes this hurdle, MutaSeq, was co-developed.

MutaSeq exploits known mutations in AML samples and combines them with mitochondrial variations in order to map the clonal relationships of single cells. Based on the mutational profile, MutaSeq classifies cells as healthy, pre-leukemic or leukemic. Additionally, cell type identity is inferred from transcriptomic data. Lastly, healthy, pre-leukemic and leukemic HSCs can be molecularly compared to identify potential druggable targets. Taken together, the second part of this thesis describes a novel methodology for a systematic distinction and comparison between healthy, pre-leukemic and leukemic HSCs. Further characterization of AML using such type of approaches will increase the chances to effectively target LSCs and thus, avoid AML relapse and enhance patient survival.

In summary, this thesis has defined a to date unknown function of HSCs orchestrating the immune system with far reaching implications in health and disease. In addition, a new single cell technology is described to better distinguish and explore the functional differences between healthy pre- and leukemic HSC.

ZUSAMMENFASSUNG

Hämatopoetische Stamm- und Vorläuferzellen (HSPZs) sind für die lebenslange Produktion von reifen Blut- und Immunzellen verantwortlich. Diese reifen Zellen erfüllen eine Vielzahl von Funktionen im Körper, welche von der Sauerstoffverteilung bis hin zur Verteidigung gegen äußere und innere Bedrohungen reichen. Innerhalb des Immunsystems sind die adaptiven Immunzellen in der Lage, eine hochspezifische Immunreaktion gegen einzigartige pathogene Epitope auszuführen. Dafür werden den T-Zellen Antigene durch die Haupthistokompatibilitätskomplexe (MHC) präsentiert. Während MHC-Klasse-I (MHC-I) auf der Mehrzahl der Zellen exprimiert wird eine wichtige Rolle bei der Aktivierung von CD8+ T-Zellen spielt, wird MHC-II ausschließlich von spezialisierten Antigen-präsentierenden Zellen (APZs) exprimiert und ist eines der Schlüsselmoleküle während der Aktivierung von CD4+ T-Zellen und damit einhergehender Orchestrierung von adaptiven Immunantworten.

Die Daten dieser Arbeit haben gezeigt, dass HSPZs nicht nur passive Empfänger von immunologischen Signalen sind, sondern als antigenpräsentierende Zellen fungieren, die in der Lage sind, CD4+ T-Zellen und damit deren immunologische Mikroumgebung funktionell zu modulieren. Zunächst konnten wir zeigen, dass HSPZs der Maus und des Menschen MHC-II auf Transkript- und Proteinebene exprimieren. Anschließend zeigten wir, dass HSPZs endogene und exogene Antigene über MHC-II verarbeiten und präsentieren können. Die Antigenpräsentation an CD4+ T-Zellen führte zu einer effizienten T-Zell-Aktivierung und immunregulatorischen Polarisierung. Tiefgehendere Analysen haben offenbart, dass diese T-Zellen einerseits einen Typ 1 regulatorischen T-Zell (Tr1)-ähnlichen Zustand adaptieren. Desweiteren waren sie in der Lage Bystander-T-Zellen zu unterdrücken und Makrophagen über das Zytokin IL-10 in einen immunregulatorischen Zustand zu polarisieren. Dabei ist von Bedeutung, dass HSPZs bei antigenspezifischer Interaktion mit CD4+ T-Zellen *ex vivo* und *in vivo* in den Zellzyklus eintraten und eine myeloische Differenzierung induziert wurde. Außerdem förderte eine anhaltende Antigenpräsentation die Erschöpfung der HSPZs. Bei der akuten myeloischen Leukämie (AML), einer Krankheit des hämatopoetischen Systems die von HSPZs abstammt, korrelierte ein unreifer, stammzellähnlicher Phänotyp mit einer höheren MHC-II-Expression und einer ungünstigen Prognose. HSZ-abgeleitete AMLs behielten die Fähigkeit zur Aktivierung von CD4+ T-Zellen bei. Darüber hinaus schützte die Erschöpfung der HSZ bei längerer Antigenpräsentation vor dem Auftreten von AML. Zusammenfassend deckt der erste Teil dieser Arbeit eine bisher unbekannte Interaktion von HSZs mit $CD4^+$ T-Zellen auf. Diese Interaktion induziert einen Toleranzmechanismus, der die Immunsuppression im Knochenmark fördert. Nicht zuletzt erweist sich die immunsuppressive HSPZ-T-Zell-Interaktion als ein immunvermittelter Schutz vor dem Auftreten von AML.

Die Leukämogenese ist ein komplexer Prozess, bei dem ein schrittweiser Erwerb von Mutationen gesunde HSPZs in präleukämische und anschließend in leukämische Zellen verwandelt. Leukämische Stammzellen (LSZs) sind, ähnlich wie ihre gesunden Gegenstücke, resistent gegen konventionelle Therapien und verantwortlich für AML-Rezidive. Die derzeitigen Methoden ermöglichen jedoch keine Unterscheidung und keinen systematischen Vergleich zwischen gesunden und (prä-)leukämischen Zellzuständen. Daher wurde im zweiten Teil dieser Arbeit eine Methode mitentwickelt, die diese Hürde überwindet: MutaSeq.

MutaSeq nutzt bekannte Mutationen in AML-Proben und kombiniert sie mit mitochondrialen genetischen Variationen, um die klonalen Beziehungen einzelner Zellen zu kartieren. Basierend auf dem Mutationsprofil klassifiziert MutaSeq die Zellen als gesund, präleukämisch oder leukämisch. Zusätzlich wird die Zelltyp-Identität aus transkriptomischen Daten abgeleitet. Schließlich können gesunde, präleukämische und leukämische HSZs molekular verglichen werden, um potenzielle Angriffspunkte für Medikamente zu identifizieren. Insgesamt beschreibt der zweite Teil dieser Arbeit eine neuartige Methodik zur systematischen Unterscheidung und zum Vergleich zwischen gesunden, präleukämischen und leukämischen HSZ. Die weitere Charakterisierung der AML mit solchen Ansätzen wird die Chancen erhöhen, LSZs effektiv zu bekämpfen und damit AML-Rezidive zu vermeiden und das Überleben der Patienten zu verbessern.

Zusammenfassend hat diese Arbeit eine bisher unbekannte Funktion von HSZs bei der Orchestrierung des Immunsystems mit potentiell weitreichenden Implikationen für ein besseres Verständnis vom gesunden Zustand des Knochenmarks als auch im Zusammenhang von malignen hämatologischen Erkrankungen definiert. Darüber hinaus wird eine neue Einzelzelltechnologie beschrieben, um die funktionellen Unterschiede zwischen gesunden prä- und leukämischen HSZ besser zu unterscheiden und zu erforschen.

INTRODUCTION

Hematopoietic stem cells

Stem cells - definitions and concepts

Stem cells are undifferentiated cells with the capacity to further differentiate into other mature functional cell types (Morrison and Kimble, 2006; Clevers, 2015; Rossant and Tam, 2017). They are of extreme relevance during development, when from a single (stem) cell, an organism is formed (Murry and Keller, 2008; Young, 2011; Rossant and Tam, 2017). After the development of organisms, stem cells remain of fundamental importance throughout adulthood. In this context, they ensure the production of functional mature cells to maintain tissue homeostasis (e.g., renew the intestinal epithelium periodically), repair after tissue damage (e.g., wound scarring in the skin) or respond to hazardous situations or stimuli (e.g., production of immune cells to fight an infection) (Clevers, 2015; Post and Clevers, 2019).

Besides being able to produce diverse mature cells, stem cells are characterized by their ability to self-renew. Self-renewal implies the generation of phenotypically identical daughter cells, which means the production of stem cells with the same capacity to generate cellular output as the mother cell (Morrison and Kimble, 2006; Post and Clevers, 2019).

The combination of self-renewal and differentiation capacity defines stem cells. Stem cells can undergo symmetric or asymmetric cell divisions (Figure 1) (Morrison and Kimble, 2006; Neumuller and Knoblich, 2009; Inaba and Yamashita, 2012). In the case of an asymmetric division, one of the daughter cells would remain a stem cell, while the other will differentiate, maintaining the size of the stem cell pool. On the other hand, if the division is symmetric, either both the cells will differentiate or will remain stem cells, reducing or expanding the stem cell pool, respectively (Neumuller and Knoblich, 2009). How the stem cell decides which option to follow is determined by the integration of both, intracellular and extracellular cues (Scadden, 2006; Morrison and Spradling, 2008; Inaba and Yamashita, 2012).

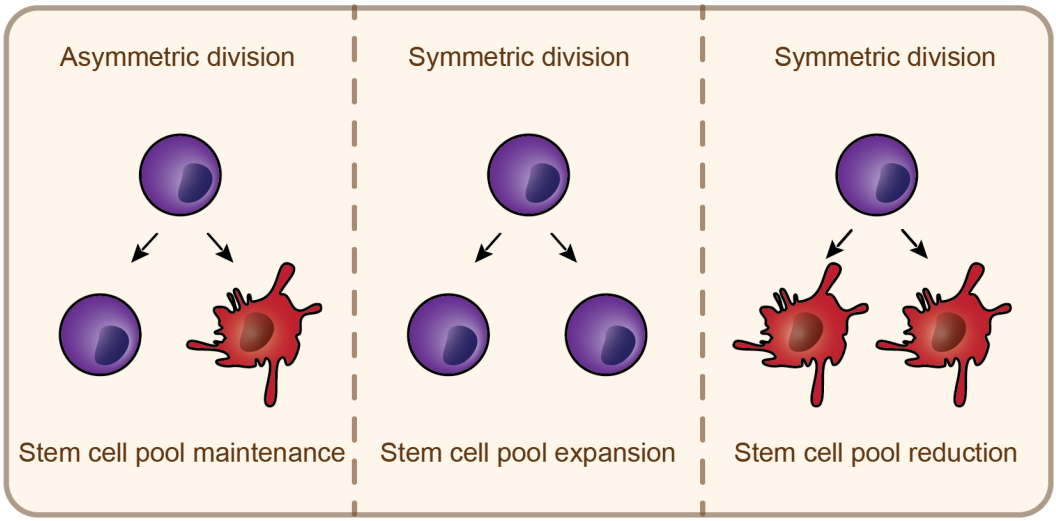

Figure 1. Symmetric and asymmetric stem cell divisions.
Scheme depicting the division possibilities for a stem cell (in purple) to generate other stem or mature cells (in red). On the bottom, the effect that each division type has for the stem cell pool is displayed.

Adult stem cells

Embryonic and adult/somatic stem cells differ in their potency. This means that the amount and type of mature cells they can give rise to vary among different stem cell types. In fact, this variation reaches from being capable of giving rise to all necessary cell types (i.e., totipotent) to only one cell type (i.e., unipotent) (Murry and Keller, 2008; Clevers, 2015).

The most potent stem cells are embryonic, since the process of embryogenesis involves the generation of large amounts of distinct cell types and cell numbers, starting from a single cell (Murry and Keller, 2008; Young, 2011). The critical role of stem cells in embryogenesis and organogenesis changes in somatic stem cells to tissue repair and homeostasis. Therefore, somatic stem cells are specialized and restricted to their tissue and so is their potency (Clevers, 2015; Post and Clevers, 2019).

Despite numerous attempts to find common characteristics to all somatic stem cells other than the previously explained, to date there is mostly evidence of molecular disparities amongst them. The most studied somatic stem cells are intestinal stem cells, that give rise to all cell types in the intestinal epithelium (Clevers, 2013); skin stem cells from hair follicles, glandular epithelia and epidermis (Blanpain and Fuchs, 2009); satellite stem cells that produce skeletal muscle (Tajbakhsh, 2003) and hematopoietic stem cells (Orkin and Zon, 2008).

Hematopoietic stem and progenitor cells

Hematopoietic stem cells (HSCs) are adult stem cells that replenish all cell types present in blood. They are, therefore, multipotent cells with the capacity to differentiate into a wide variety of cells, from red blood cells and platelets to all different cellular components of the immune system (Figure 2) (Orkin and Zon, 2008; Doulatov *et al.*, 2012; Eaves, 2015). In addition to their fate plasticity and as other somatic stem cells, HSCs are characterized by their self-renewing and proliferative capacities (Orkin and Zon, 2008). All these properties combined, allow HSCs to efficiently maintain, renew and restore blood and immune cells during the organism's lifespan.

Despite HSC cycling capacity, during homeostasis, most of them rest in a quiescent state and are activated only upon determined stimuli (Trumpp and Wiestler, 2008; Wilson *et al.*, 2008; Trumpp, Essers and Wilson, 2010). This quiescent state protects HSCs from excessive proliferative stress and thus, from increased mutational risk (Walter *et al.*, 2015). Therefore, at steady-state, blood regeneration is maintained by HSC-derived multipotent progenitors (MPPs). This combination of hematopoietic stem and progenitor cells (HSPCs) share a common and distinctive surface protein profile in mice: Lineage$^-$Sca-1$^+$cKit$^+$, and are therefore also named LSK.

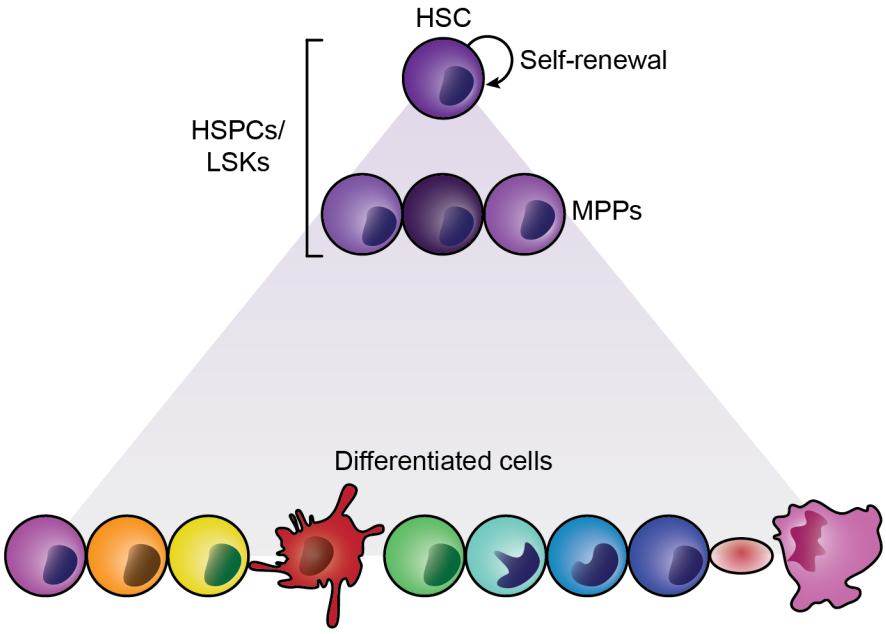

Figure 2. Hematopoietic stem cells and hematopoiesis.
Scheme depicting the process of hematopoiesis, with HSCs on top of the hierarchy, capable of self-renewing and producing the mature differentiated cells displayed on the bottom.

Mature hematopoietic cells and hematopoiesis

As previously mentioned, HSPCs are capable of generating a broad array of functional mature cells, with highly specialized and very distinct functions. Amongst them, erythrocytes, that carry and deliver oxygen throughout the organism; megakaryocytes, that generate platelets; or the immune system, which protects us from both, internal and external threats (Figure 3A). Within the immune system, there are different myeloid and lymphoid cells, all with different and crucial protective functions. The grouping of these different cell types according to common differentiation trajectories from the HSCs is called lineage. In this context, we can distinguish myeloid: eosinophils, neutrophils, basophils, monocytes and different dendritic cells (DCs); lymphoid: T cells, B cells natural killer (NK) cells; erythroid (erythrocytes) and megakaryocytic (megakaryocytes and platelets) lineages (Orkin and Zon, 2008; Doulatov *et al.*, 2012; Eaves, 2015).

How HSCs differentiate to these different lineages, a process termed hematopoiesis, has been studied with great interest over the years and our perspective of how this occurs has evolved accordingly. Some studies suggest that it involves a series of step-wise decisions that generate a defined number of immature but biased intermediates, creating a tree-like structure from HSCs to their mature offspring (Eaves, 2015). Conversely, others suggest a gradual and reversible priming of HSCs towards the final offspring, making hematopoiesis a Waddington-like structure (Schroeder, 2010; Eaves, 2015; Haas, Trumpp and Milsom, 2018). Last but not least, an equilibrium between the two former theories has been proposed, where gradual priming events will result in defined intermediates that can again, gradually, transition towards the final mature cell (Haas, Trumpp and Milsom, 2018; Liggett and Sankaran, 2020). Regardless of the actual events occurring, all theories are in absolute agreement about the HSC being at the apex and the mature lineages placed on the bottom of the hematopoietic hierarchy.

Moreover, the recent studies suggesting gradual transitions in hematopoiesis, have highlighted the fact that HSCs are not a homogenous cell population as previously thought. In turn, they are a heterogeneous mix of transcriptionally diverse cells, with the potential to generate all hematopoietic lineages but primed to one or several of them (Haas *et al.*, 2015; Paul *et al.*, 2015; Velten *et al.*, 2017; Haas, Trumpp and Milsom, 2018; Liggett and Sankaran, 2020).

Emergency hematopoiesis

As opposed to HSC homeostatic quiescence, different stimuli can trigger HSC activation, measured as cycling activity and cellular output. HSC activation is believed to play a crucial role in a process called emergency hematopoiesis. Emergency hematopoiesis can be promoted by loss of blood, infections or other situations deriving in stress for the hematopoietic compartment (King and Goodell, 2011; Boettcher and Manz, 2017; Hirche *et al.*, 2017; Pietras, 2017; Espin-Palazon *et al.*, 2018). These stressful circumstances derive in the generation of several cytokines, such as interferons (IFNs), interleukin-1 (IL-1) and others (Essers *et al.*, 2009; Baldridge *et al.*, 2010; Matatall *et al.*, 2014; Pietras *et al.*, 2016). In addition to activating HSCs, these signaling molecules shape their hematopoietic cellular output to fit the challenge that the organism is facing, e.g., generate more myeloid cells to fight an infection (King and Goodell, 2011; Pietras, 2017; Chavakis, Mitroulis and Hajishengallis, 2019).

Such robust HSC response to a challenge can either be sensed and integrated directly by HSCs, or by surrounding cells that, subsequently, provide the HSCs with additional cues, modulating the balance between quiescence, self-renewal and differentiation (Scadden, 2006; Morrison and Spradling, 2008). These cells that surround and assist the HSCs compose the so called niche (Crane, Jeffery and Morrison, 2017; Pinho and Frenette, 2019).

The HSPC niche

HSPCs reside in the bone marrow, under the physical and molecular protection provided by the bone and their microenvironment, respectively. This microenvironment, composed by abundant extracellular matrix and different cells types has been characterized in depth under homeostasis and upon diverse stress conditions (Tikhonova *et al.*, 2019; Baccin *et al.*, 2020; Méndez-Ferrer *et al.*, 2020; Man *et al.*, 2021). Many niche-HSPC interactions and signaling mechanisms underlying HSPC regulation have been already described and characterized (Pinho and Frenette, 2019; Zhao *et al.*, 2020). Hence, it is broadly established that the HSPC niche provides necessary cues for hematopoiesis and HSPC fitness and function.

Considering the cellular composition of the HSPC microenvironment, endothelial, mesenchymal and neuronal cells can be found amongst others (Asada, Takeishi and Frenette, 2017; Crane, Jeffery and Morrison, 2017; Wei and Frenette, 2018). Nonetheless, immune cells are, undoubtedly, the most abundant cells surrounding HSPCs. The immune system, therefore, plays a key role with regards to HSPC biology as both, progeny and niche component. In addition, several immune cells, such as macrophages or T cells, have already been shown to regulate stem cell function (Ogawa and Matsunaga, 1999; Dent and Kaplan, 2008; Riether, Schürch and Ochsenbein, 2015; Luo *et al.*, 2018).

While the immune system participates in controlling HSPC biology, its key function is to provide protection. Many adult stem cell niches, including the HSPC one, have been described as immune privileged sites (Mercier, Ragu and Scadden, 2012; Riether, Schürch and Ochsenbein, 2015; Naik *et al.*, 2018). This means that immune reactions are dampened at those particular places. In fact, the bone marrow is the main reservoir for regulatory T cells, Tregs, (Zou *et al.*, 2004; Pierini *et al.*, 2017) the key cell type responsible for immune regulation (Sakaguchi *et al.*, 2008; Tang and Bluestone, 2008).

T cell immunology

Innate and adaptive immunity

In order to protect the organism from the many threats it can face in a lifespan, a diverse repertoire of humoral and cellular immune mechanisms have evolved. These can be segregated into innate and adaptive immune systems (Dempsey, Vaidya and Cheng, 2003). The former is composed by different granulocytes, monocyte, dendritic cells (DCs) or natural killer (NK) cells; and the latter, by B and T cells (Figure 3A). However, DCs and NK cells can be considered as part of both systems due to either being a link between the both systems or sharing traits from both, respectively (Palucka and Banchereau, 1999; Hoebe, Janssen and Beutler, 2004; Sun, Beilke and Lanier, 2009).

The innate immune system is the first line of defense of the organism. It is characterized by a fast and non-specific response (Turvey and Broide, 2010; Gasteiger *et al.*, 2017). Innate immune cells, through pattern recognition receptors (e.g. toll-like receptors (TLRs)), recognize structures common to different pathogens and foreign to the organism, such as bacterial membrane compounds like lipopolysaccharides (LPS), or viral RNA genomes (Akira, Uematsu and Takeuchi, 2006; Fitzgerald and Kagan, 2020). Upon their activation, these receptors trigger diverse actions destined to deplete the potential threat, but also to activate the adaptive immune system. Importantly, the innate immune system reacts similarly upon interaction with the same threat after previous encounters (Figure 3B) (Akira, Uematsu and Takeuchi, 2006; Turvey and Broide, 2010).

On the other hand, the adaptive immune system is slower but specific in its way of action. Each threat, or antigen, will trigger a different response and that response will be specific for that particular antigen and not effective against others (Bonilla and Oettgen, 2010). Immune specificity is achieved through physical modifications of the antigen receptors that, unlike TLRs, undergo genetic recombination and somatic hypermutation during B and T cell maturation (Schatz and Ji, 2011; Aiden and Casellas, 2015). This process, leads to different B and T cell receptors (BCRs and TCRs) in every single B and T cell clone (Alt *et al.*, 1992). Due to

their nearly infinite different specificities, B and T cell clones are present at very low levels prior to antigen exposure, which, at least partially, accounts for the delayed response.

After the first encounter with a recognized antigen, B and T cells generate memory cells (Reinhardt *et al.*, 2001; Hoebe, Janssen and Beutler, 2004; Bonilla and Oettgen, 2010). While memory cells recognize the same antigen that activated them, they enhance their affinity, making their binding stronger and more efficient. In addition, they maintain a different metabolism and phenotype when compared to their naïve counterparts (Berard and Tough, 2002; Youngblood, Hale and Ahmed, 2013; Schenkel and Masopust, 2014). Altogether, these changes account for the immune memory and they allow them to react more efficiently and faster in case of a secondary encounter (Figure 3B) (Cho *et al.*, 1999).

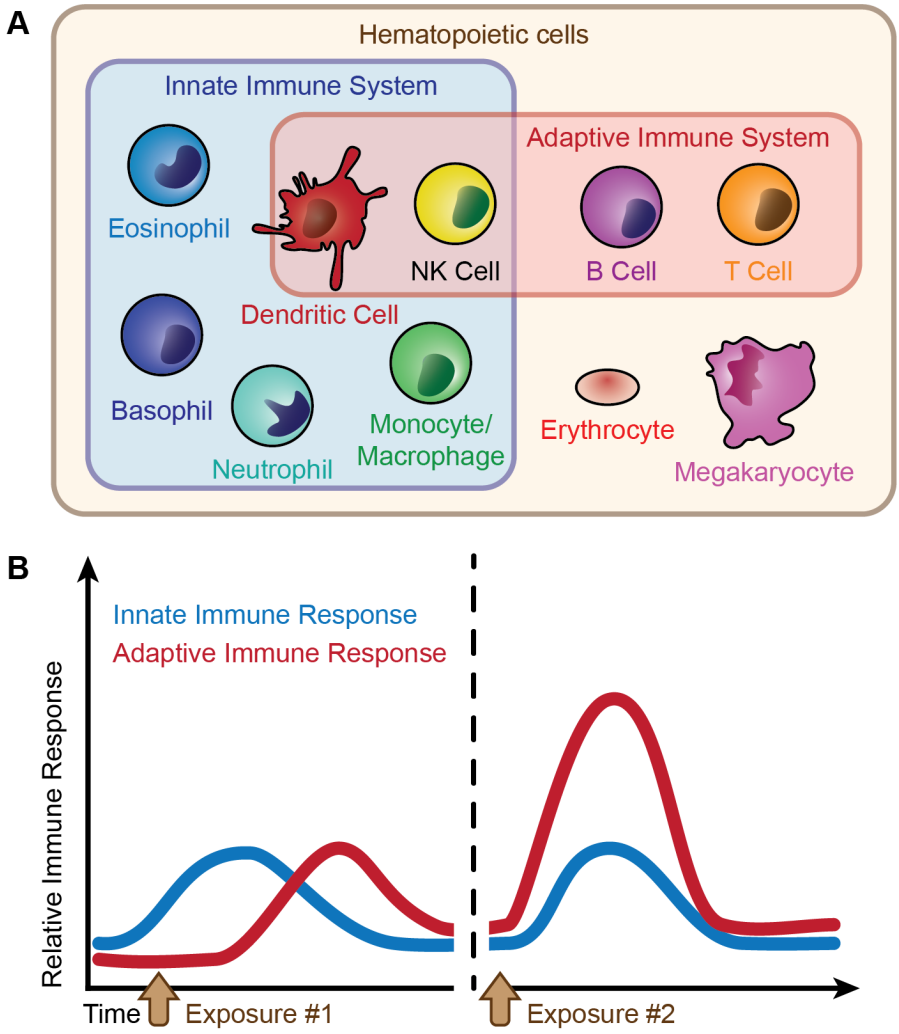

Figure 3. Innate and adaptive immune system.
(**A**) Mature differentiated cells derived from HSCs and how they are characterized within the innate (blue rectangle) or adaptive (red rectangle) immune system. (**B**) Dynamics of activation and response of the innate (blue) and adaptive (red) immune system after a primary (left) or secondary (right) challenge.

Antigen presentation and major histocompatibility complexes

In order to recognize their specific antigens, B and T cells follow different strategies. B cells recognize physical structures, or epitopes, formed by native and unprocessed antigens. Thus, B cells are independent from other cells for that matter (Kwak, Akkaya and Pierce, 2019). On the other hand, T cells recognize small peptides that come from antigen processing, executed by other cells (Germain, 1994; Guermonprez *et al.*, 2002). In addition, for the TCR to identify those peptides, they need to be presented by other molecules on the surface of the cell, the major histocompatibility complex (MHC), or human leukocyte antigen (HLA) in human (Neefjes *et al.*, 2011). We can further differentiate T cells, based on the coreceptor they use to recognize the MHCs and peptides, into helper $CD4^+$ and cytotoxic $CD8^+$ T cells (Bonilla and Oettgen, 2010).

MHCs are heterodimeric protein complexes which can retain peptides of certain characteristics inside the cell and present them on the surface. There are two classes of MHC, depending on whether they are co-recognized by CD8 or CD4, termed MHC-I and MHC-II, respectively (Neefjes *et al.*, 2011; Wieczorek *et al.*, 2017). Both complexes are encoded in large loci in the genome, composed by highly polymorphic genes that provide flexibility to antigen binding and presentation and therefore, to adaptive immunity (Kumánovics, Takada and Lindahl, 2003).

Structurally, MHC-I is composed of a common monomer (β-2 microglobulin) and a variable α-chain that generates the peptide binding groove, the structure where peptides can bind, on its own (Neefjes *et al.*, 2011; Wieczorek *et al.*, 2017). MHC-II is composed by two variable α- and β-chains, that together form the peptide groove (Godkin *et al.*, 2001). This makes MHC-I-presented peptides more rigid in size and aminoacidic composition than the MHC-II ones (Godkin *et al.*, 2001; Wieczorek *et al.*, 2017).

Moreover, MHC-I is usually associated with intracellular antigens, since it loads peptides from the cytoplasm inside the endoplasmic reticulum (Neefjes *et al.*, 2011; Kobayashi and van den Elsen, 2012). On the contrary, MHC-II is classically related to extracellular antigens due to a vesicle-associated loading mechanism (Hiltbold and Roche, 2002; Lennon-Duménil *et al.*, 2002; McCormick, Martina and Bonifacino, 2005; ten Broeke, Wubbolts and Stoorvogel, 2013). However, both MHCs can present intra- and extracellular antigens, provided their loading mechanisms are respected (Neefjes *et al.*, 2011; Roche and Furuta, 2015; Rock, Reits and Neefjes, 2016; Wieczorek *et al.*, 2017).

Lastly, MHC-I and thus, the ability to present peptides to cytotoxic $CD8^+$ T cells, is expressed in every nucleated cell in the organism. On the contrary, MHC-II expression and helper T cell

activation capacity are restricted to antigen presenting cells (APCs) (Neefjes *et al.*, 2011; Kobayashi and van den Elsen, 2012; Roche and Furuta, 2015; Wieczorek *et al.*, 2017).

Antigen presenting cells and MHC-II machinery

The cell types in which MHC-II and its associated machinery are expressed are called APCs. Depending on the MHC-II expression level under homeostasis or upon infection, and their antigen presenting capacities, among other differences, APCs can be categorized into professional or non-professional APCs (Kambayashi and Laufer, 2014). Professional APCs, such as DCs, B cells and pro-inflammatory macrophages, express MHC-II during homeostasis (Steinman, 2007; Merad *et al.*, 2013); whereas non-professional APCs, like innate lymphoid cells, neutrophils, monocytes or megakaryocyte progenitors, only upregulate MHC-II expression under certain stress situations (Hepworth *et al.*, 2013; Oliphant *et al.*, 2014; Finkielsztein *et al.*, 2015; Jakubzick, Randolph and Henson, 2017; Vono *et al.*, 2017).

Nonetheless, not only the expression levels of the different α- and β-chains from MHC-II are relevant for antigen presentation to $CD4^+$ T cells. Many other molecules are involved and required in the process (Figure 4). For instance, CD74 is a molecule that mediates dimerization of the complex (Su *et al.*, 2017). Once CD74 is cleaved in the endosomal compartment, a small fragment, called class II invariant chain-associated peptide (CLIP), remains bound to and stabilizes the peptide groove until an antigen is bound (Neefjes *et al.*, 2011; Su *et al.*, 2017). The exchange of CLIP for an antigen is mediated by a MHC-II-resembling dimeric chaperone encoded by the genes *H2-DMa* and *H2-DMb1/2* in mice and *HLA-DMA* and *HLA-DMB* in human (Mellins and Stern, 2014). Additionally, there is a similar dimer that inhibits this process encoded by the genes *H2-DOa* and *H2-DOb* in mice and *HLA-DOA* and *HLA-DOB* in human (Mellins and Stern, 2014).

All these genes are in the same genetic locus under the control of class II major histocompatibility complex transactivator (CIITA) a transcription factor that acts a master regulator (Steimle *et al.*, 1993). CIITA expression and function and thus, the entire locus, can be additionally regulated by stress and interferon signaling (Steimle *et al.*, 1994). This means, that the antigen presenting machinery gets upregulated upon inflammation to ensure adequate antigen presentation of a potential threat, establishing a bridge between the innate and adaptive immune systems (Kambayashi and Laufer, 2014; Jurewicz and Stern, 2019).

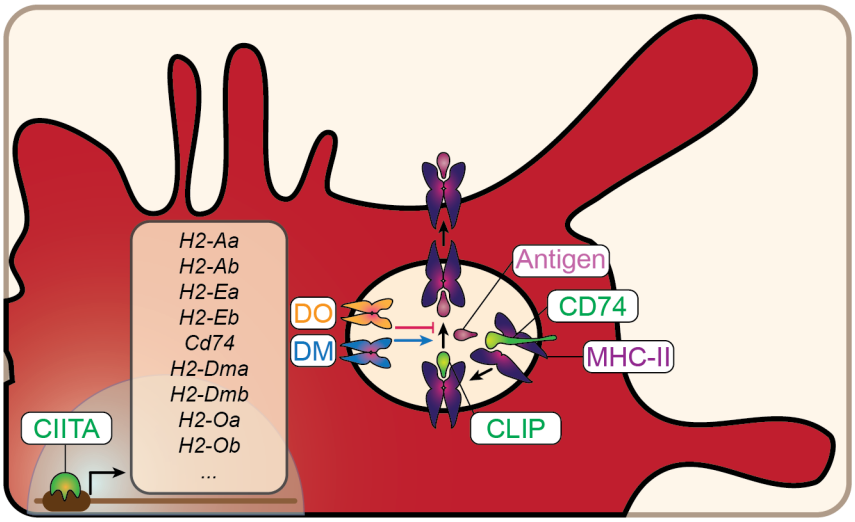

Figure 4. MHC-II antigen presenting machinery.
Scheme depicting different MHC-II-related genes regulated in mouse by CIITA (left) and their function in antigen presentation within the endosomal compartment of APCs (right).

T cell function and activation

As the nomenclature suggests, $CD4^+$ helper and $CD8^+$ cytotoxic T cell types have fundamental differences in their functions. Cytotoxic T cells, once activated through MHC-I, kill the cell presenting the antigen through the secretion of granzyme and perforin and the expression of cell death ligands. They are crucial for viral clearance and cancer control, since they can directly eliminate infected or transformed cells (Zhang and Bevan, 2011). On the other hand, upon activation, helper T cells secrete a broad array of cytokines and modulate the surrounding immune system and its response (Zhu and Paul, 2008).

Notably, not only antigen presentation is important for T cell activation (Figure 5). Accordingly, when only receiving MHC-TCR stimuli, T cells become anergic or dysfunctional (Fathman and Lineberry, 2007). Therefore, there is a need for other signaling cues that promote survival, cell cycle induction and activation. The responsible molecules expressed by APCs can either promote activation (co-stimulatory), or inhibition (co-inhibitory) on T cells (Driessens, Kline and Gajewski, 2009; Chen and Flies, 2013; Hilligan and Ronchese, 2020).

In addition, another signaling layer, provided by the cytokines from the microenvironment and the APC, fine tunes the immune response (Curtsinger and Mescher, 2010). Altogether, this “three signal” model accounts for the definitive activation and function of T cells (Corthay, 2006; Hilligan and Ronchese, 2020).

Importantly, these interactions are not always unidirectional and APCs also receive signals from T cells. For example, in DCs, innate immune and adaptive feedback signaling, such as CD40-CD40L binding, activate them to upregulate MHCs and co-stimulatory molecule

expression (Steinman, 2007; Merad *et al.*, 2013). Thus, the adaptive immune system not only receives reinforcement from innate immunity, but also from this feedback loop.

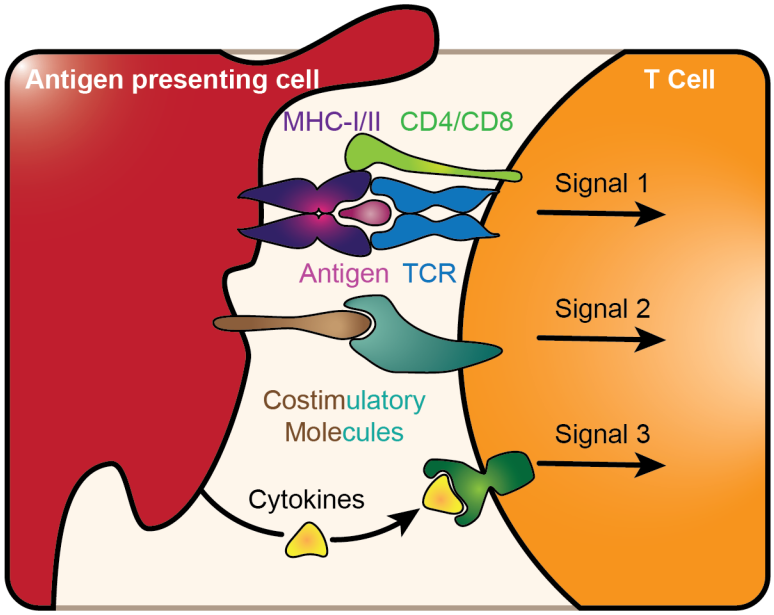

Figure 5. The "three signal" model of T cell activation.
Model for T cell (on the right) activation by APCs (on the left). On top, first signal, antigen specific, mediated by MHC and TCR molecules. In the middle, second signal composed by co-stimulatory or co-inhibitory ligands present on the APCs and receptors on T cells. On the bottom, cytokines from either the APC or the microenvironment provide the third signal in order to shape the T cell response.

Helper T cell subsets

The integration of the three signals in the cytoplasm and nucleus of $CD4^+$ T cells promotes the transcription of different genes in a process called T cell education or polarization (Zhu and Paul, 2008). Amongst the first response genes, there are survival and proliferative genes (Chen and Flies, 2013), but also few defined master transcription factors that dictate the secondary transcriptional wave and thus, the definitive T cell function (Zhu and Paul, 2010).

This polarization results in functionally distinct subsets of $CD4^+$ helper T cells (Figure 6), that secrete different cytokines, modulating the surrounding immune system in distinct ways (Wilson, Rowell and Sekimata, 2009; Zhu and Paul, 2010). Of note, helper T cells are not only carrying proinflammatory and immune activatory roles, but also restricting and inhibiting the immune system when the encountered antigen does not suppose a threat or when an immune reaction is no longer required (Sakaguchi *et al.*, 2008; Zhu and Paul, 2010).

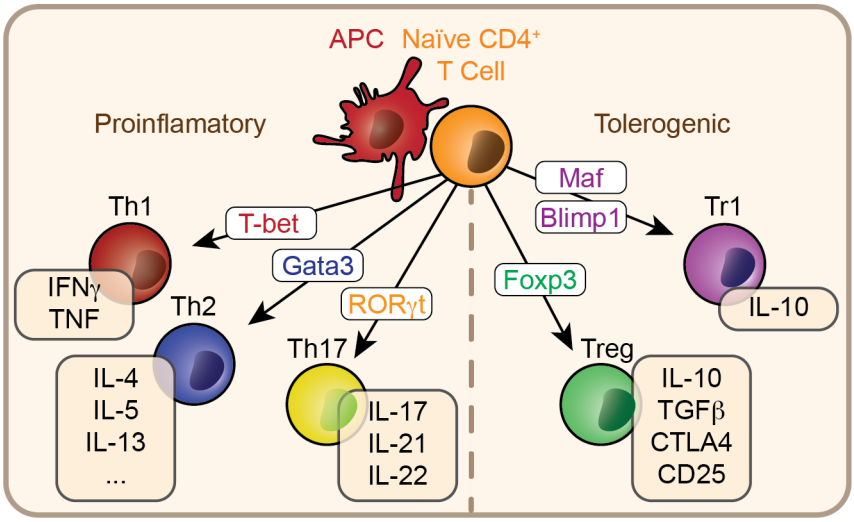

Figure 6. Helper T cell subsets.
Main polarization alternatives that a naïve helper T cell can undergo after encountering its cognate antigen (top), the master regulators (middle) and the main effector molecules (bottom) for each helper T cell subset.

The main proinflammatory helper T cell subtypes, Th1, Th2 and Th17, are controlled by the master transcription factors T-bet, Gata3 and RORγt, respectively (Zhu and Paul, 2010). Th1 cells promote antiviral immunity via IFNγ secretion. Th2 cells enhance the humoral immune response enhancing antibody production in B cells through the secretion of several cytokines, such as IL-4, IL-5, IL-13 and others. Lastly, Th17 cells mainly secrete IL-17 and IL-21 and are thought to maintain immunity active in mucosal barriers (Wilson, Rowell and Sekimata, 2009; Zhu and Paul, 2010).

In contrast, the main regulatory/tolerogenic helper T cell subtypes are Tregs and type 1 regulatory T cells (Tr1), transcriptionally regulated by Foxp3, Maf and Blimp1, respectively (Zeng *et al.*, 2015). Both have similar functional effects, reflected in their ability to suppress immune responses in their surroundings (Sakaguchi *et al.*, 2008; Roncarolo *et al.*, 2018). Nonetheless, their origin and mechanisms of immune suppressions differ. While Tr1 cells mostly use IL-10 to promote immune inhibition, Tregs use a wide range of strategies (Zeng *et al.*, 2015; Roncarolo *et al.*, 2018). For instance, Tregs secrete immunoregulatory cytokines like TGFβ or IL-10, express co-inhibitory receptors like CTLA-4 and upregulate surface levels of IL-2 receptor (IL2R or CD25) (Sakaguchi *et al.*, 2008; Tang and Bluestone, 2008). However, regardless of whether it is via inhibitory signaling, or buffering of activatory mechanisms, the end product of all mechanisms is the suppression of immune reactions.

Tolerance, autoimmunity and cancer

The avoidance of an immune response towards an antigen is termed tolerance. There are many ways in which tolerance is established, but all these processes can be clustered in central and peripheral tolerance (Goodnow *et al.*, 2005; Xing and Hogquist, 2012).

Central tolerance is a consequence of T cell development and TCR repertoire formation (Cheng and Anderson, 2018; Klein, Robey and Hsieh, 2019). While T cells develop and rearrange their TCRs in the thymus, they are exposed to a large number of peptides, encoded in the organism's genome, that can bind MHC complexes (Brennecke *et al.*, 2015; Meredith *et al.*, 2015). When a T cell recognizes any of those self-peptides, the TCR signaling triggers pro-apoptotic signals, a process named negative selection, depleting self-reacting T cells (Cheng and Anderson, 2018; Klein, Robey and Hsieh, 2019). Moreover, if the TCR affinity is high, but not sufficient to drive apoptosis, these T cells are immediately polarized to $Foxp3^+$ natural Tregs (nTregs) (Cheng and Anderson, 2018; Klein, Robey and Hsieh, 2019). In this way, the organism ensures the lack of either self-reactive T cells or immune reactions against the organism, i.e. autoimmunity.

Despite the strict selective process in the thymus, it does not account for external innocuous antigens. Thus, peripheral tolerance ensures lack of unwanted immune reactions outside the thymus (Goodnow *et al.*, 2005; Xing and Hogquist, 2012). Peripheral tolerance relies mostly on the "three signal" model (Figure 5). In this line, when the innate immune system and the APCs have not been activated and upregulated costimulatory molecules (i.e., when there is no inflammation), they cannot provide T cells with the necessary activation signals and T cells become anergic (Fathman and Lineberry, 2007; Chen and Flies, 2013). Moreover, the balance between co-stimulatory and co-inhibitory molecules, together with the cytokine microenvironment, can not only promote anergy, but also T cell polarization to $Foxp3^+$ induced Tregs (iTregs) and Tr1 cells (Chen and Flies, 2013; Hilligan and Ronchese, 2020).

When the tight equilibrium between immunity and tolerance is disrupted, the health status is deeply affected. If tolerance is lost, the organism can develop allergies towards external harmless antigens, or autoimmune diseases towards self-antigens (Goodnow *et al.*, 2005; Cheng and Anderson, 2018). This is the case of aplastic anemia (AA), a rare disease where the immune system depletes the bone marrow of HSCs and thus, hematopoietic cells (Young, 2018). This disease is associated with a loss of Tregs, specific MHC-II allele variants and a loss of heterozygosity in the MHC-II locus (Nakao *et al.*, 1994; Nimer *et al.*, 1994; Saunthararajah *et al.*, 2002; Rehman *et al.*, 2009; Dhaliwal *et al.*, 2011; Katagiri *et al.*, 2011; Liu *et al.*, 2016).

Conversely, if tolerance mechanisms overpower immunity, pathogens avoid the immune system and diseases can become chronic. In the case of cancer, since it originates from within

the organism, they passively make use of the central tolerance preestablished and actively use peripheral tolerance mechanisms in its favor (Dunn *et al.*, 2002; Hanahan and Weinberg, 2011; Beatty and Gladney, 2015; Spranger and Gajewski, 2018). In fact, many co-inhibitory molecules (i.e. immune checkpoints) are being targeted by immune checkpoint inhibition, a powerful therapy for many different malignancies (Sharma and Allison, 2015).

Interplay between stem and helper T cells

Somatic stem cells

During the last years, stem cell research has acknowledged the importance of the immune system in tissue homeostasis and stem cell function (Naik *et al.*, 2018). In this line, many have indicated the importance of an immune privileged niche to ensure a lower stress for stem cells. Notably, Tregs have been placed in the center of such niches throughout the organism (Fujisaki *et al.*, 2011; Burzyn *et al.*, 2013; Arpaia *et al.*, 2015; Kuswanto *et al.*, 2016; Ali *et al.*, 2017; Biton *et al.*, 2018; Hirata *et al.*, 2018).

Furthermore, $CD4^+$ T cells have not only been highlighted as crucial for immune suppression but key in directly modulating stem cell function (Naik *et al.*, 2018). In this line, they are fundamental for maintaining lung homeostasis and repair (Arpaia *et al.*, 2015), but also for muscle, intestinal and hair follicle skin stem cell functions (Burzyn *et al.*, 2013; Kuswanto *et al.*, 2016; Ali *et al.*, 2017; Biton *et al.*, 2018). Of note, Biton and colleagues recently revealed expression of MHC-II in intestinal stem cells, suggesting a recruiting and scaffolding role to facilitate this interplay (Biton *et al.*, 2018). However, these key functions for all mentioned stem cells are attributed to helper T cell-secreted cytokines and not to direct interactions with the stem cells.

Hematopoietic stem cells

As previously mentioned, the HSC niche is believed to be rich in helper T cells. In fact, the bone marrow is the main reservoir for both, memory and regulatory T cells in mammals (Price and Cerny, 1999; Zou *et al.*, 2004; Tokoyoda *et al.*, 2009; Di Rosa and Gebhardt, 2016). These cells are functionally active and capable of being activated within the bone marrow (Feuerer *et al.*, 2003; Siracusa *et al.*, 2017). Thus, the bone marrow is a prime site of T cell activation, but also of immune regulation and maintenance of tolerance (Mercier, Ragu and Scadden, 2012).

Interestingly, broad stimulation of T cells strongly modulates hematopoiesis, suggesting an important role of T cells besides classical immune functions (Hirsch *et al.*, 1989; Schneider *et al.*, 1997; Monteiro *et al.*, 2005). In more in detail, many different T cell subsets are linked to

HSC functions. When depleting key transcription factors for specific T cell subsets, hematopoiesis suffers alterations in a T cell-dependent manner (Broxmeyer *et al.*, 2002; Kaplan *et al.*, 2011). Moreover, many CD4+ T cell-secreted cytokines have been linked to variations in hematopoietic output (Ogawa and Matsunaga, 1999; Dent and Kaplan, 2008; Li *et al.*, 2014; Mojsilovic *et al.*, 2015; Giampaolo *et al.*, 2017). Of note, other cells whose function is modulated by T cell secretions, such as macrophages, can also alter hematopoiesis (Luo *et al.*, 2018).

Importantly, Tregs surround HSCs in the bone marrow (Fujisaki *et al.*, 2011). In fact, they have been shown to coordinate hematopoiesis by several means. First of all, by modulating other cells in the microenvironment, thereby generating an immune privileged niche (Lee, Wang and Kim, 2009; Giampaolo *et al.*, 2017; Pierini *et al.*, 2017). Secondly, by direct hematopoietic modulation through secreted factors (Urbieta *et al.*, 2010; Hirata *et al.*, 2018).

Healthy and malignant HSCs and MHC-II

Previous studies showed that hematopoietic progenitor cells expressed MHC-II molecules (Fitchen, Foon and Cline, 1981; Robinson *et al.*, 1981; Sieff *et al.*, 1982; Falkenburg *et al.*, 1984, 1985; Okumura, Tsuji and Nakahata, 1992). Moreover, depleting MHC-II-expressing cells in different bone marrow cell populations, also depleted stem cell function *in vitro* in mouse (Russell and Engh, 1979) and human (Falkenburg *et al.*, 1984, 1985; Broudy and Fitchen, 1986). Interestingly, when enriching for MHC-II an enhanced hematopoiesis was shown (Janossy *et al.*, 1978). In addition, bone marrow transplants in dogs failed to restore blood when depleting MHC-II$^+$ cells (Szer *et al.*, 1985). Lastly, mass-spectrometry following MHC-II pull-down showed functional peptides being presented by human hematopoietic progenitors (Nowak *et al.*, 2013; Berlin *et al.*, 2015). Altogether, historic evidence suggests a potential function of MHC-II in HSPCs. However, a detailed understanding of the exact role and functionality of MHC-II in HSPCs is still missing.

In acute myeloid leukemia (AML), an aggressive hematological cancer characterized by the accumulation of immature blasts that originate from HSCs or myeloid progenitors, MHC-II is expressed in a heterogenous manner between different patients, but also within the same malignant entities (Miale *et al.*, 1982; Newman and Greaves, 1982; Newman *et al.*, 1983; Yunis *et al.*, 1989). In fact, in acute promyelocytic leukemia (APL), a disease were blasts have a more differentiated state, MHC-II is not expressed (Griffin *et al.*, 1983). Lastly, MHC-II dysregulation and T cell exhaustion have been linked to immune escape upon relapse after allogenic stem cell transplantation (Christopher *et al.*, 2018; Toffalori *et al.*, 2019). However, neither a rationale for MHC-II expression heterogeneity, nor a link to APC capacity and clinical or

biological features of AMLs have been established yet (Miale *et al.*, 1982; Mutis *et al.*, 1997, 1998; Costello *et al.*, 1999; Berlin *et al.*, 2015)

Malignant hematopoiesis

Premalignant HSCs

Throughout the lifespan of an organism, HSPCs accumulate mutations, despite various intracellular and extracellular protection mechanisms. The accumulation of mutations is linked with cell cycle entrance (Walter *et al.*, 2015) and thus, with age (Adams, Jasper and Rudolph, 2015). In fact, a vast majority of the population displays mutations in their hematopoietic cells upon ageing (Young *et al.*, 2016). These mutations frequently occur in genes such as DNA (cytosine-5)-methyltransferase 3A (*DNMT3A*), isocitrate dehydrogenase 1/2 (*IDH1/2*), Fms-related receptor tyrosine kinase 3 (*FLT3)*, nucleophosmin (*NPM1)* and others (Genovese *et al.*, 2014; Xie *et al.*, 2014). However, mutational burden in HSCs does not necessary translate into malignant transformation and these pre-malignant (or pre-leukemic) HSCs are able to give rise to all mature hematopoietic cells (Shlush *et al.*, 2014; Zink *et al.*, 2017).

A noteworthy proportion of individuals carrying mutations in HSCs exhibit clonal expansion of that mutated HSC and its progeny (Zink *et al.*, 2017). This non-malignant phenomenon is termed clonal hematopoiesis of indeterminate potential (CHIP). Although CHIP does not imply by itself any malignancy, it increases the chances for leukemia development (Genovese *et al.*, 2014; Steensma *et al.*, 2015).

Acute myeloid leukemia

CHIP can further evolve to diverse hematopoietic malignancies if other driver mutations occur (Jaiswal *et al.*, 2014; Sperling, Gibson and Ebert, 2016; Bowman, Busque and Levine, 2018). In the case of AML, mutations enhance HSPCs cycling activity while blocking their differentiation capacity (Welch *et al.*, 2012). The overpopulation of blasts not only decreases the amount of functional hematopoietic cells, but avoids the generation of new ones in favor of more blasts, with a proliferative advantage (Miraki-Moud *et al.*, 2013).

Unlike in other hematopoietic malignancies, HSCs and myeloid-committed progenitors are the cell of origin in AML (Krivtsov *et al.*, 2006, 2013; Shlush *et al.*, 2014; Ye *et al.*, 2015; Liran I Shlush *et al.*, 2017). Therefore, only mutations in these specific immature cells can drive the malignant transformation. In addition, not all mutations have the same potential in all cells. Some genomic aberrations, like *FLT3* internal tandem duplication (*FLT3*-ITD) or Casitas B-

lineage Lymphoma (*CBL*) mutation, in combination with *DNMT3A* mutation, can only transform HSCs (Rathinam *et al.*, 2010; Ebrahim *et al.*, 2016; Yang *et al.*, 2016). Others, like histone-lysine N-methyltransferase 2A (*KMT2A*, better known as *MLL*) rearrangements or NPM1 can transform both, HSCs and myeloid-committed progenitors (Krivtsov *et al.*, 2006, 2013; de la Guardia *et al.*, 2020; Uckelmann *et al.*, 2020). Thus, the mutational profile can, in some cases, indicate what the cell of origin might be in AML.

Leukemic stem cells and clonality in AML

Similar to the healthy hematopoietic system, AML maintains a hierarchical organization, with leukemic stem cells (LSCs) maintaining the disease (Meacham and Morrison, 2013; Kreso and Dick, 2014; Greaves, 2016). These LSCs, like healthy HSCs, remain quiescent and are difficult to target by conventional therapies (i.e., radio/chemotherapy) (Corces-Zimmerman *et al.*, 2014; Liran I Shlush *et al.*, 2017). These characteristic features in combination with their potential to regenerate the disease and promote relapse, makes LSCs harmful cells whose depletion would enhance treatment options for AML patients.

LSCs have classically been studied by HSC-like surface phenotype (Hosen *et al.*, 2007; Majeti, Becker, *et al.*, 2009; Majeti, Chao, *et al.*, 2009; Jan *et al.*, 2011) or by functional xenograft assays (Eppert *et al.*, 2011; Ng *et al.*, 2016; Pabst *et al.*, 2016; Raffel *et al.*, 2017). However, identifying and targeting them *in vivo* has remained elusive due to their low abundance and high resemblance to healthy and pre-leukemic HSCs or blast populations (Trumpp and Wiestler, 2008; Essers and Trumpp, 2010; Pollyea and Jordan, 2017).

In addition, once established, AML cells keep acquiring mutations, driving the disease to change and evolve (Welch *et al.*, 2012; Sperling, Gibson and Ebert, 2016). Thus, at some point within the same disease, cells with different sets of mutations can co-exist (Chen, Hu and Wang, 2019). This high mutational plasticity, makes of AML a highly clonal disease yet to be fully understood.

AIMS OF THE THESIS

Since the discovery and characterization of HSCs, their role regarding hematopoiesis has been studied in great detail. In addition, the immune system surrounding HSCs, has been thoroughly studied in context of immunity and hematopoiesis. However, alternative functions of HSCs remain poorly understood. Thus, this thesis aims to investigate direct immunological properties of healthy and leukemic HSCs. Moreover, it attempts to unravel the effects of these properties in immunology, stem cell biology and hematopoiesis. These findings are presented and discussed under the section titled "**Healthy and malignant hematopoietic stem cells are immunoregulatory antigen presenting cells**".

During the last years, the study of AML and the enhancement of therapeutic options have tried to deplete all leukemic cells, including LSCs, while sparing healthy HSCs. However, the abundant similarities between the mentioned cells have made it extremely challenging. In the section titled "**Identification of leukemic and pre-leukemic stem cells by clonal tracking from single-cell transcriptomics**" we aim to tackle this major medical concern by tracking transcriptomic and mutational single cell profiles of healthy and diseased hematopoietic systems.

RESULTS

Healthy and malignant hematopoietic stem cells are immunoregulatory antigen presenting cells

Most of the results shown in this section of the thesis are part of the manuscript with the same provisional title currently submitted for publication. Some parts of the text, figures and figure legends have been taken and/or adapted from the aforementioned manuscript, originally co-written by myself (see author contributions for more details).

Hematopoietic stem cells express the MHC-II antigen presenting machinery

Previous studies have pointed out the presence of MHC-II in cells involved in hematopoietic cell production (Janossy *et al.*, 1978; Russell and Engh, 1979; Fitchen, Foon and Cline, 1981; Robinson *et al.*, 1981; Sieff *et al.*, 1982; Falkenburg *et al.*, 1984, 1985; Szer *et al.*, 1985; Broudy and Fitchen, 1986; Okumura, Tsuji and Nakahata, 1992; Berlin *et al.*, 2015). Nonetheless, the expression of MHC-II and more importantly, its functionality, have not been tested under the umbrella of the knowledge acquired on HSCs ever since.

Under this light, we made use of previously generated RNA-Seq data of murine HSPCs, characterized by the lack of mature lineage markers and the presence of Sca-1 and cKit on the cell surface (LSK) and committed progenitors, characterized by the lack of mature lineage markers and Sca-1 and the presence of cKit on the cell surface (LS^-K) under homeostatic conditions (Klimmeck *et al.*, 2014). HSPCs showed increased expression of MHC-II and related genes when compared to committed progenitors (Figure 7A). Among the observed genes, we found different α and β chains belonging to MHC-II (*H2-Aa*, *H2-Ab* and *H2-Eb1*), its chaperone for peptide exchange (*H2-Dma*, *H2-Dmb2*) or its inhibitor (*H2-Oa*, *H2-Ob*), its stabilizing molecule (*Cd74*) or its main transcription factor (*Ciita*).

This observation was ratified by qPCR on FACS-sorted cells and flow cytometric analyses on more thoroughly characterized hematopoietic immature and mature cell populations (Figure 7B, D and E and Supplementary Figure 1A and B). Under homeostatic conditions, HSCs and MPPs displayed similar levels of MHC-II genes and proteins. Interestingly, MHC-II expression in HSPCs was only slightly lower than known APCs, such as DCs or macrophages, and significantly higher than further committed progenitors and non-APC mature cells, such as T cells. Moreover, upon exposure to different stress-like stimuli, HSCs further upregulated MHC-II and other related genes (Figure 7C). This translated into higher surface expression of the complex, to similar levels as in professional APCs (Figure 7D and E and Supplementary Figure 1A and B).

To ultimately determine whether all HSCs express MHC-II, all immature cells in the bone marrow were sorted and transplanted into primary and secondary lethally irradiated mice, solely based on the presence or absence of MHC-II expression (Supplementary Figure 1C). While MHC-II-negative bone marrow cells were not capable of reconstituting hematopoiesis long-term, MHC-II-positive bone marrow cells repopulated all hematopoietic lineages efficiently, demonstrating that long-term self-renewal capacity is restricted to MHC-II expressing bone marrow cells (Figure 1F and Supplementary Figure 1D).

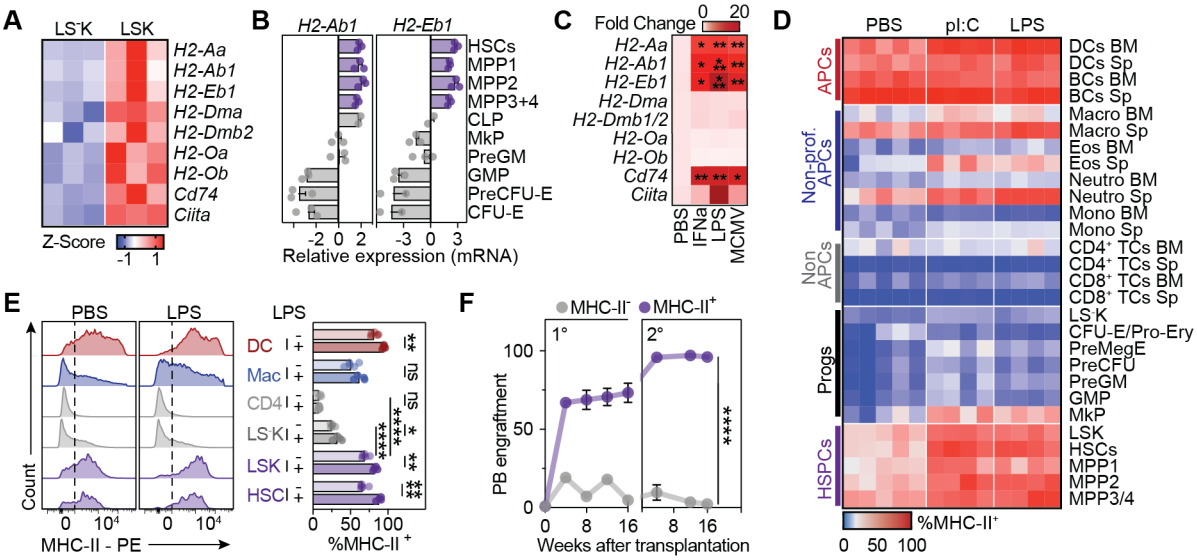

Figure 7. MHC-II expression in mouse HSPCs.

(**A**) z-scores of genes encoding components of the MHC-II antigen presentation machinery in mouse HSCs and MPPs (LSK) and committed progenitors (LS⁻K) inferred from genome-wide RNA-Seq data (Klimmeck *et al.*, 2014), *n=3*. (**B**) Relative gene expression of MHC-II genes across bone marrow populations measured by qPCR, *n=2-3*. (**C**) Relative gene expression of MHC-II genes across sorted bone marrow HSCs (Lin⁻cKit⁺CD150+CD48⁻) measured by qPCR. Mice were treated with indicated agents 24 hours prior to the sort. Gene expression is displayed relative to PBS treatment, *n=3*. (**D**) Heatmap summarizing MHC-II surface measurements by flow cytometry for bone marrow (BM) and spleen (Sp) populations. (**E**) MHC-II surface measurements by flow cytometry of indicated populations at homeostasis or 24 hours post LPS treatment. Representative histograms (left panels) and quantification (right panels), *n=4-5*. Dashed lines indicate thresholds for gating. (**F**) Transplantation experiments of MHC-II bone marrow populations. Lineage-negative bone marrow cells were sorted according to MHC-II expression and transplanted into lethally irradiated mice together with rescue bone marrow. Four months post transplantation, total bone marrow cells were transplanted into secondary recipients, *n=4-6*. See also Supplementary Figure 1. Individual values are shown in **A** and **D**, means in **C** and means and SEM are depicted otherwise. No significance = ns, P<0.05 *, P<0.01 **, P<0.001 ***, P<0.0001 ****. One- or two-way ANOVA were performed in C and E as discovery test, respectively. If not stated otherwise, unpaired two-tailed t-tests were performed as post-hoc tests. When comparing paired cell populations within the same animal (E), paired two-tailed t-tests were performed. Two-way ANOVA was performed in F. In case of multiple comparisons, p-values were corrected according to Benjamini-Hochberg.

Lack of MHC-II in HSPCs impairs hematopoiesis

MHC-II expression on HSCs inevitably prompted us to better understand the effect that such molecule could elicit on HSC biology and hematopoiesis. To address this question, we generated a mouse model comprising three different genetic alterations (Figure 8A):

A) The *CreERT2* fusion gene, encoding for a Cre protein only transported to the nucleus after tamoxifen binding, under the *Scl* promoter, active in HSPCs.
B) The first exon of the *H2-Ab* gene floxed in order to generate a knock-out (KO) of the gene and of functional MHC-II upon Cre nuclease function.
C) The enhanced yellow fluorescent protein (EYFP) preceded by a floxed STOP codon into the *Gt(ROSA)26Sor* locus, to induce its expression upon Cre nuclease function.

Indeed, tamoxifen injection in these mice triggered the expression of YFP and the downregulation of MHC-II in different hematopoietic cells, including HSCs (Figure 8B and C). Notably, MHC-II downregulation was more efficiently achieved than YFP expression (Figure 8C). Thus, for the experiments performed in this mouse model, YFP^+ cells from $CreERT2^+$ were compared to total $CreERT2^-$ cells from tamoxifen-treated mice as explained in the "Methods" section.

To functionally evaluate the effect of the MHC-II loss, MHC-II^- and MHC-II^+ HSPCs were transplanted separately (Figure 8D-F) or jointly (Figure 8G-J) into lethally irradiated mice (Figure 8A). In both the settings, MHC-II levels were maintained over time (Figure 8D and H). Moreover, MHC-II^- HSCs seemed to have a reduced capacity to generate lymphoid, mainly T cells; and an enhanced myeloid bias (Figure 8E-F and I-J). Lastly, in a chimeric setting, MHC-II^- HSCs produce a significant higher amount of progeny in primary recipients (Figure 8G). Even though not definitive, this results pinpoint to a role of MHC-II in HSC biology and functionality and thus, in hematopoiesis.

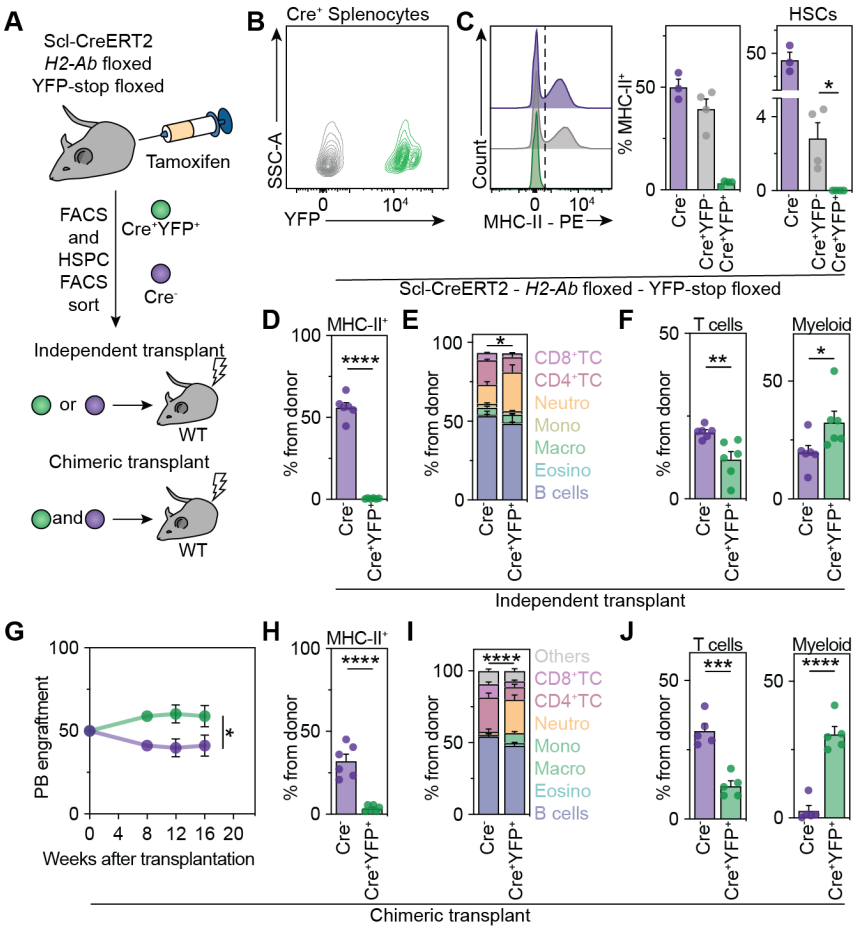

Figure 8. Effects on hematopoiesis of MHC-II KO in HSPCs.

(**A**) Experimental scheme. Scl-CreERT2 (+ or -) *H2-Ab* floxed YFP-stop floxed mice were injected daily with tamoxifen during five days and three weeks afterwards the bone marrow and spleen was analyzed by flow cytometry (B and C). Moreover, the same number of total HSPCs (MHC-II^{+}) from Cre^{-} mice and YFP^{+} (MHC-II^{-}) from Cre^{+} mice were isolated and transplanted either into independent (D-F), or the same (G-J) lethally irradiated recipients. (**B**) YFP upregulation upon tamoxifen treatment. Representative flow cytometry plot of total spleen from a Cre^{+} mouse treated with tamoxifen. (**C**) MHC-II downregulation upon tamoxifen treatment. Left, representative MHC-II plot of total spleen from a Cre^{-} mouse (purple), and YFP- (gray) or YFP+ (green) from a Cre^{+} mouse, all treated with tamoxifen. Dashed line depicts quantification threshold for positivity. Quantification of MHC-II^{+} cells from the populations mentioned before (middle) or HSCs from bone marrow (right), *n=3-4*. (**D-F**) MHC-II^{-} or MHC-II^{+} were transplanted into different lethally irradiated mice and 8 weeks afterwards were bled and analyzed, *n=6*. (**G-J**) MHC-II^{-} and MHC-II^{+} were transplanted together into the same lethally irradiated mice and were bled monthly, week 16 bleeding data is depicted in H-J, *n=5*. (**D** and **H**) MHC-II expression pattern is maintained upon transplantation. Percentage of MHC-II^{+} cells in peripheral blood. (**E** and **I**) Hematopoietic output of MHC-II$^{+/-}$ HSPCs. Percentage of all hematopoietic progeny generated by the different HSPCs according to their genotype-phenotype. (**F** and **J**) Myeloid and lymphoid bias of MHC-II$^{+/-}$ HSPCs. Percentage of progeny corresponding to T (left) or myeloid (right) cells generated by the different HSPCs according to their genotype-phenotype. (**G**) Total peripheral blood engraftment in the chimeric transplantation. Means are depicted in E and I and means and SEM are depicted otherwise. No significance = ns, P<0.05 *, P<0.01 **, P<0.001 ***, P<0.0001 ****. Two-way ANOVA was performed in E, G and I. When comparing paired cell populations within the same animal (C, H and J), paired two-tailed t-tests were performed. If not stated otherwise, unpaired two-tailed t-tests were performed as post-hoc tests. In case of multiple comparisons, p-values were corrected according to Benjamini-Hochberg.

HSPCs intake and present antigens in MHC-II

The canonical role of MHC-II is the presentation of peptides to $CD4^+$ T cells. Therefore, our next goal was to assess whether HSCs would also be capable of MHC-II mediated antigen presentation. The classical view of antigen presentation establishes exogenous antigens as mainly presented via MHC-II. Thus, to understand whether HSPCs can uptake and cleave extracellular antigens into peptides, DQ-Ovalbumin was used. DQ is a fluorophore quenched by a protein (ovalbumin), that once cleaved by cellular proteases, releases DQ, which can be detected by flow cytometry. DCs or HSPCs were cultured *in vitro* (Figure 9A) or mice were administered (Figure 9B) with DQ-Ovalbumin and cells were analyzed by flow cytometry as a proxy for antigen uptake and processing capacity. Both, *in vitro* and *in vivo*, HSPCs showed comparable capacity to DCs to cleave external molecules intracellularly.

To assess the capacity of HSC to integrate peptides onto MHC-II and present them on the cell surface, we made use of a monoclonal antibody Y-Ae. This antibody binds specifically to the MHC-II-derived Eα peptide (52-68) when presented in the context of MHC-II $I\text{-}A^b$ haplotype (Murphy *et al.*, 1989; Rudensky *et al.*, 1991). Accordingly, in C57BL/6 mice, that display the $I\text{-}A^b$ haplotype but lack expression of Eα, exogenous Eα peptide can be used as foreign antigen to characterize antigen presentation capacities of cell populations *ex vivo*. As expected, professional APCs efficiently presented the Eα peptide via MHC-II, whereas non-APCs failed to do so (Figure 9C). Importantly, multipotent HSPCs also presented Eα efficiently via MHC-II, suggesting that HSPCs can present exogenous peptides.

To investigate presentation of self-antigens via MHC-II *in vivo*, we crossed BALB/C mice, which express Eα but exhibit the $I\text{-}A^d$ haplotype, to C57BL/6 mice ($I\text{-}A^b$, Eα-negative). In mice of the F1 generation, MHC-II mediated antigen presentation can be assessed by the Y-Ae antibody *in vivo*, due to the expression of Eα in the presence of MHC-II molecules with $I\text{-}A^b$ haplotype (Henri *et al.*, 2010) (Supplementary Figure 2A). As expected, professional APCs showed high MHC-II mediated presentation of Eα during homeostasis and upon LPS treatment *in vivo* (Figure 9D and E and Supplementary Figure 2B). Interestingly, macrophages did not present Eα at homeostasis, but acquired strong antigen presentation capacity upon LPS treatment, in line with previous studies (Kambayashi and Laufer, 2014; Jakubzick, Randolph and Henson, 2017). In contrast, non-professional APCs and non-APCs showed no or very limited antigen presenting activity during homeostasis or upon LPS treatment. Importantly, HSCs and MPPs exhibited low, but significant antigen presentation at homeostasis, and efficiently increased antigen presenting capacity upon LPS treatment in an MHC-II restricted manner (Figure 9D and E and Supplementary Figure 2B). To further characterize antigen presentation by HSPCs, we performed immunoprecipitation of MHC-II molecules, followed by peptide elution and mass spectrometry from lysates of HSPCs (Figure 9F). We also included T cells and splenocytes, serving as negative and positive control of APCs, respectively. Enumeration and characterization of eluted peptides revealed that peptides from HSPCs resembled those from

splenocytes in number and length distribution, and considerably outnumbered peptides eluted from non-APCs. Together, these data suggest that HSCs and MPPs present antigens via MHC-II at homeostasis and further increase antigen presentation activity upon inflammation.

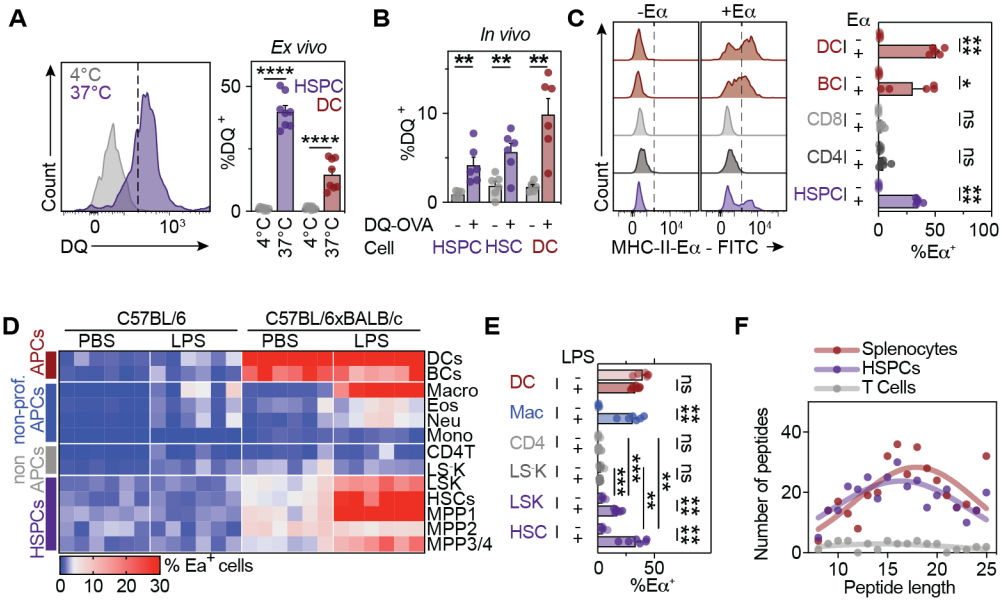

Figure 9. Mouse HSPC intake present antigens via MHC-II.

(**A**) Flow cytometry analyses of HSPCs and DCs *ex vivo* cultured in the presence of DQ-OVA. Cells were cultured for three hours at 4°C or 37°C and analyzed for intake and processing. Dashed lines indicate thresholds for gating. Representative HSPC plots (left panel) and quantification (right panel) are depicted, *n=8*. (**B**) Antigen intake and processing *in vivo*. DQ-positive cells were measured 2 hours after DQ-OVA injection, *n=6*. (**C**) Ex vivo antigen presentation assay of the indicated populations. Cells were cultured in the presence or absence of Eα peptide for three hours. The Y-Ae antibody was used to measure presentation of Eα via MHC-II. Representative histograms (left panels) and quantification (right panels), *n=4*. Dashed lines indicate thresholds for gating. (**D**) In vivo antigen presentation assay. The Y-Ae antibody was used to measure presentation of Ea via MHC-II in C57BL/6xBALB/c mice and control C57BL/6 mice 24 hours post PBS or LPS injection. Percentage of Y-Ae$^+$ cells is depicted, *n=6*. (**E**) Quantification of selected population from D. Only data for C57BL/6xBALB/c mice are depicted, *n=6*. (**F**) Mass spectrometry analyses of peptides recovered from MHC-II of cKit$^+$ HSPCs and control populations. See also Supplementary Figure 2. Individual values are shown in **D**, means and SEM are depicted otherwise. No significance = ns, P<0.05 *, P<0.01 **, P<0.001 ***, P<0.0001 ****. One- (B and C) or two-way ANOVA (E) were performed as discovery tests. If not stated otherwise, unpaired two-tailed t-tests were performed as post-hoc tests. When comparing paired cell populations within the same animal (E), paired two-tailed t-tests were performed. In case of multiple comparisons, p-values were corrected according to Benjamini-Hochberg.

HSPCs express T cell costimulatory and polarizing molecules

As previously explained. APCs require to provide T cells with additional stimulation other than MHC-II peptide presentation in order to activate them. Therefore, unveiling whether HSPCs are capable of providing T cells with a second and third signal (see Figure 5) was crucial to elucidate further immunogenic mechanisms. To that end, we further explored the previously used publicly available RNA-Seq dataset (Klimmeck *et al.*, 2014). A systematical exploration of different co-stimulatory and co-inhibitory molecules revealed the expression of molecules capable of providing the second T cell activation signal on HSPCs, such as the CD28 ligand CD86 (Figure 10A). Interestingly, *Cd274* (PD-L1) a powerful co-inhibitory molecule responsible for tolerance induction in health and disease displayed the highest expression (Keir *et al.*, 2008; Francisco *et al.*, 2009; Sharpe and Pauken, 2018). Furthermore, the presence of different cytokine transcripts on HSPCs was confirmed and thus, the "three signals" required by T cells in order to get activated (Figure 10B). Remarkably, the top expressed cytokine transcripts were *Ebi3* and *Il12a*, which encode proteins that together form IL-35, shown to promote peripheral tolerance (Collison *et al.*, 2007, 2010).

Next, we validated that our top transcriptomic hits are also expressed on protein level by different means. In this context, CD86 and PDL1 were previously described to be expressed on HSPCs (Shimazu *et al.*, 2012; Tober *et al.*, 2018; Ali and Park, 2020). We further confirmed the expression of these costimulatory/inhibitory ligands on the surface of HSPCs and purified HSCs (Figure 10C-E). Interestingly, upon LPS treatment, the costimulatory molecule CD86 was downregulated, especially in percentage of expressing cells. On the contrary, the coinhibitory molecule PD-L1 was highly upregulated. Taken together, these findings set evidence of T cell activation capacity by HSCs. Moreover, they hint towards a tolerogenic T cell education being a plausible pathway for such process.

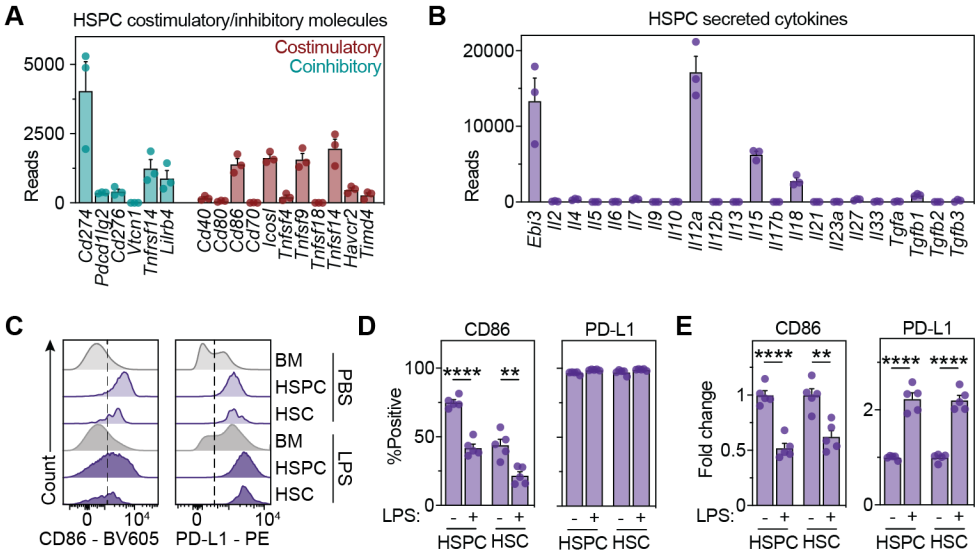

Figure 10. T cell costimulatory and polarizing cues in mouse HSPCs.
(**A**) Reads of genes encoding the main T cell costimulatory/inhibitory molecules in mouse HSPCs taken from genome-wide RNA-Seq data (Klimmeck *et al.*, 2014), *n=3*. (**B**) Reads of genes encoding the main T cell instructing/polarizing cytokines in mouse HSPCs inferred from genome-wide RNA-Seq data (Klimmeck *et al.*, 2014), *n=3.* (**C-E**) CD86 (left) and PD-L1 (right) surface measurements by flow cytometry of total bone marrow (BM), HSPCs and HSCs at homeostasis or 24 hours post LPS treatment. Representative histograms (**C**) and quantification of positive cells (**D**) and fluorescence intensity relative to PBS of each population (**E**), *n=5*. Dashed lines indicate thresholds for gating. Means and SEM are depicted. No significance = ns, P<0.05 *, P<0.01 **, P<0.001 ***, P<0.0001 ****. One-way ANOVA was performed in D and E as discovery test, followed by unpaired two-tailed t-tests as post-hoc tests. In case of multiple comparisons, p-values were corrected according to Benjamini-Hochberg.

HSPCs can activate CD4$^+$ T cells

In order to investigate whether the antigen presenting machinery present in HSPCs translates into efficient T cell activation, OT-II and 2D2 mouse models were used (Barnden *et al.*, 1998; Bettelli *et al.*, 2003). In this mice, transgenic TCR genes are introduced so that TCRs are clonal. This translates to all T cells having the same affinity for specific and known antigens, ovalbumin (OVA 323-339) and myelin oligodendrocyte glycoprotein (MOG 35-55) for OT-II and 2D2, respectively. The co-culture of CD4$^+$ T cells isolated from these mice with specified peptides and DCs, as an APC control, resulted in T cell activation and proliferation *in vitro* (Figure 11A). Such effect could not be seen when the co-cultured cells were not APCs, such as CD8$^+$ T cells. Notably, when HSPCs were cultured with CD4$^+$ T cells from either mouse model, T cell activation could also be seen (Figure 11A and B). Moreover, HSPC-mediated T cell activation was accompanied by T cell proliferation (Figure 11D) and was peptide- and MHC-II-dependent (Figure 11D and E). Importantly, all different HSC and MPP subpopulations comprised within the HSPC compartment were capable of triggering antigen-specific CD4$^+$ T cell activation (Figure 11F).

To simultaneously investigate all hallmarks of antigen internalization, cleavage and presentation and T cell activation, OT-II CD4+ T cells were cocultured as before with the OVA peptide or in the presence of the whole ovalbumin protein (Figure 11G). As expected, DCs were extremely efficient in executing all aspects of antigen presentation, whereas CD8$^+$ T cells were incapable of doing so. Importantly, HSPCs significantly activated antigen-specific CD4$^+$ T cells, although to a lesser degree than DCs. In addition, antigen internalization, cleavage and presentation could be enhanced by LPS. To gain a more comprehensive view of the process of antigen presentation, CD8$^+$ T cells from OT-I mice, analogous to OT-II but with a MHC-I-restricted TCR, were subject to the same experimental outline (Figure 11H). Indeed, the results were similar, with DCs being equally efficient in activating T cells, regardless of the antigen original form, and with HSPCs less efficiently activating them with the full protein but displaying enhancing antigen presenting capability upon LPS treatment.

Next, to confirm these findings in different *in vivo* settings, we first administered PBS or ovalbumin in mice, and co-cultured isolated DCs, CD8$^+$ T cells, and HSPCs from these mice with OT-II CD4$^+$ T cells (Figure 11I). Alternatively, these cell types isolated from wild type (WT) or mice endogenously expressing ovalbumin (CAG-OVA) and co-cultured with OT-II T cells (Figure 11J). Both setups recapitulated the *in vitro* setting, DCs were extremely efficient in intaking, processing and presenting antigens, whereas CD8$^+$ T cell were incapable of doing so. Notably, HSPCs significantly activated T cells, though less efficiently than DCs. Altogether, these results demonstrate that HSCs and HSPCs are antigen presenting cells capable of effectively activating T cells.

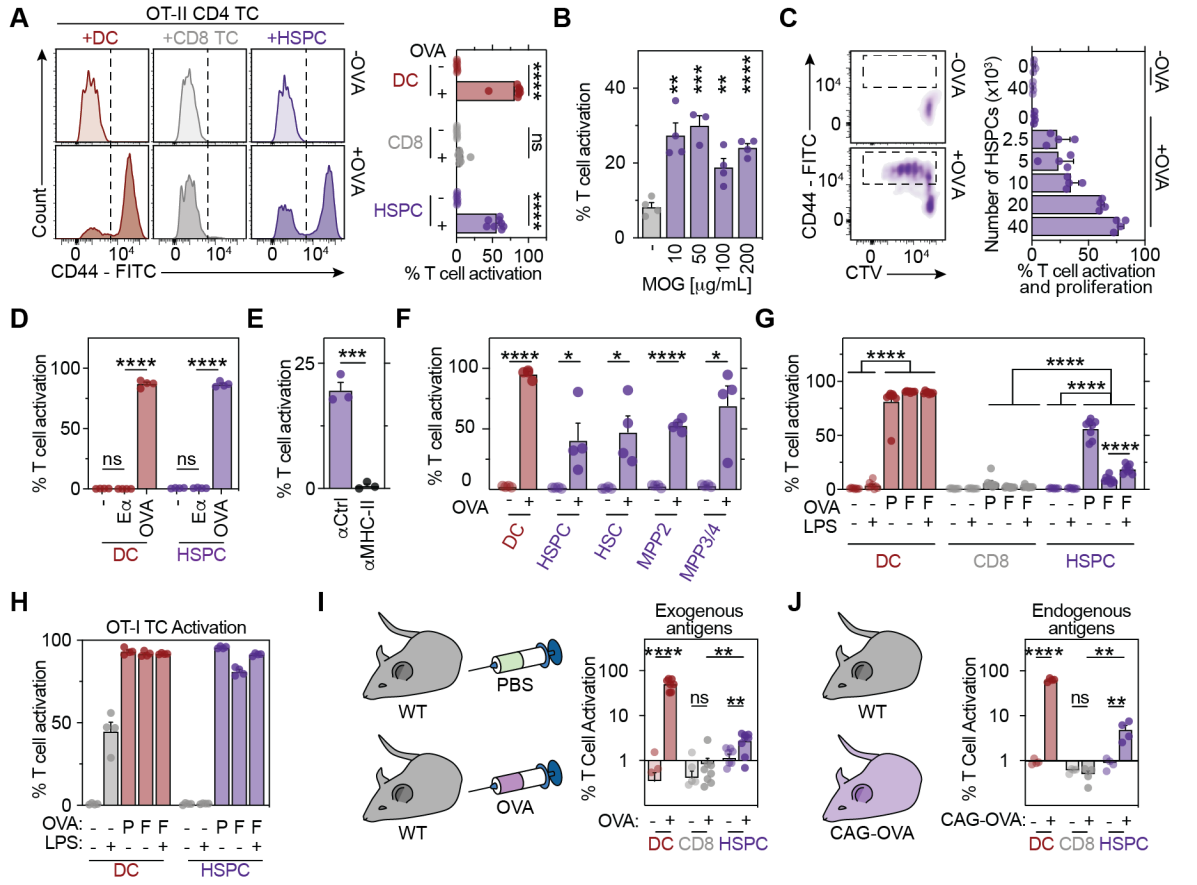

Figure 11. Mouse HSPCs activate CD4⁺ T cells via MHC-II.

Evaluation of antigen presentation capacity by co-cultures of naïve T cells with HSPCs (LSKs) and selected control populations in the presence or absence of MHC-restricted peptides after 72h of co-culture. MHC-I-restricted OVA and OT-I CD8⁺ T cells were used in H, MHC-II-restricted MOG and 2d2 CD4⁺ T cells in B and MHC-II-restricted OVA and OT-II CD4⁺ T cells in the remaining. (**A**) Representative histograms of CD44 expression (left panels) and quantification (right panel), *n=8*. Dashed lines indicate thresholds for gating. (**B**) Evaluation of antigen presentation capacity after 72h of co-cultures of 2D2 CD4⁺ T cells with HSPCs (LSKs) in the presence or absence of different concentrations of MOG MHC-II-restricted peptide, *n=4*. (**C**) Proliferation and activation assays of OT-II CD4⁺ T cells upon co-culture with different numbers of HSPCs. Proliferation was read out by CellTrace Violet (CTV) labelling dilution and activation by CD44 staining. Representative plots (left panels) and quantification for different ratios of HSPCs and OT-II CD4+ T cells (right panel), *n=4*. Dashed boxes represent quantified population. (**D**) Activation assays of OT-II CD4⁺ T cells upon co-culture with HSPCs and DCs, in the absence of peptide, in the presence of OT-II-non-specific Eα peptide or in the presence of the OT-II-specific OVA peptide, *n=4*. (**E**) T cell activation upon culture with a MHC-II-blocking antibody or isotype control, *n=3*. (**F**) T cell activation assays for different HSPC subpopulations (2.5x10³ cells), *n=4*. (**G**) Quantification of T cell activation in co-cultures in the absence (-) or presence of OVA peptide (P) or full OVA protein (F) with (+) or without (-) LPS, *n=8*. (H) (**G**) Quantification of T cell activation in co-cultures in the absence (-) or presence of OVA peptide (P) or full OVA protein (F) with (+) or without (-) LPS, *n=4*. (**I**) In vivo antigen presentation assay for exogenous antigens. One hour post administration of PBS or OVA protein to mice, 4x10⁴ CD8⁺ T cells, DCs or LSKs were isolated and co-cultured with naïve OT-II CD4⁺ T cells in the absence of exogenous OVA peptide. Left, scheme of used mice and treatments. Right, T cell activation quantification, *n=8*. (**J**) In vivo antigen presentation assay for endogenous antigens. HSPCs were isolated from CAG-OVA mice, endogenously expressing membrane-bound OVA, and from control mice. Antigen presenting capacity was read out by co-culture with OT-II CD4⁺ T cells in the absence of exogenous OVA peptide. Left, scheme of used mice and treatments. Right, T cell activation quantification, *n=4*. Means and SEM are depicted. No significance = ns, P<0.05 *, P<0.01 **, P<0.001

, P<0.0001 *. One- (A, B, D, E and F) or two-way ANOVA (C, I and J) were performed as discovery tests. If not stated otherwise, unpaired two-tailed t-tests were performed as post-hoc tests. In case of multiple comparisons, p-values were corrected according to Benjamini-Hochberg.

HSPC-mediated T cell activation promotes HSPC proliferation and differentiation

$CD4^+$ T cells are highly secretive cells, whereas HSPCs act as integrative cellular hubs that swiftly adapt differentiation upon cytokine sensing. Thus, we wondered whether the activation of $CD4^+$ T cells upon contact with HSPCs would have an effect on hematopoiesis. To that end, we made use of our co-culture system, focusing now on investigating HSPCs instead of $CD4^+$ T cells. While no T cell interaction was established, HSPCs remained relatively quiescent *in vitro* (Figure 12A). In contrast, upon antigen- and MHC-II-dependent interaction, a drastic and rapid cell cycle induction was observed. In fact, the proliferation of HSPCs was directly proportional to the degree of $CD4^+$ T cell activation (Figure 12B).

Next, we analyzed the transcriptomic changes between HSPCs that did or did not serve as APCs. Interestingly, the upregulation of differentiation programs could be observed alongside the proliferative effect (Figure 12C). To understand the functional meaning underlying the transcriptomic alterations, we analyzed differentiation markers of HSPCs upon co-culture or transplanted them into lethally irradiated mice (Figure 12D). Antigen presenting HSPCs downregulated stem cell markers and upregulated myeloid markers *ex vivo*, acquiring a granulocyte-monocyte progenitor (GMP) or mature myeloid immunophenotype (Figure 12E). This *ex vivo* differentiation translated into a reduced, albeit not lost, *in vivo* long-term repopulating capacities (Figure 12 F and G). To understand whether our findings could be recapitulated *in vivo*, we loaded HSPCs with the $CD4^+$ T cell-specific OVA peptide and transferred them together with OT-II T cells into untouched mice (Figure 12H). According to previous results, the ability to interact with antigen-specific T cells triggered HSPCs to lose stem cell markers while acquiring a more myeloid or differentiated state (Figure 12I).

In order to further characterize this bidirectional interaction and how it affects surrounding HSPCs not directly interacting with T cells, we made use of a transwell system. HSPCs and antigen-specific $CD4^+$ T cells were cultured together, and other HSPCs were placed sharing the same media, but not in close proximity to T cells (Figure 12J). Again, comparing HSPCs in contact with OT-II T cells in the presence or absence of the MHC-II-specific OVA peptide showed enhanced proliferation upon antigen presentation (Figure 12K). In addition, HSPCs separated from OT-II T cells but sharing the well with ongoing HSPC-mediated T cell activation also proliferated more than their inactivated counterparts. However, this cell cycle induction was significantly lower if compared to HSPCs directly interacting with T cells. Moreover, isolated HSPCs differentiated alongside the myeloid lineage only when T cells were being activated in their proximity (Figure 12L). However, the observed differentiation and loss of stem cell markers was drastically lower if compared to HSPC being directly involved in the antigen presentation process.

To validate this finding *in vivo*, we made use of our conditional MHC-II KO mouse model (see Figure 8). Due to the knock-out efficiency, we could separate MHC-II KO or expressing cells by YFP expression alone or in combination with MHC-II surface levels. After KO induction, OT-II T cells were intravenously (IV) transferred and ovalbumin intraperitoneally (IP) injected three days prior to the analysis (Figure 12M). Without ovalbumin and thus, without the ability to form antigen-specific interactions, no difference in cell cycle induction could be seen on YFP-positive or negative HSCs (Figure 12N). Interestingly, upon ovalbumin injection, only YFP^- HSCs, enriched for MHC-II expression, significantly increased their cell cycle entry. Strikingly, when adding MHC-II expression for qualifying cells as $YFP^-MHC\text{-}II^+$ (WT) or $YFP^+MHC\text{-}II^-$ (KO), only WT HSPCs displayed a massive increase in cell cycle induction and progression (Figure 12O). Altogether, these results indicate that antigen- and MHC-II-specific interactions between HSPCs and helper T cells activate HSPCs to cycle and differentiate to myeloid cells upon antigen presentation *in vivo*.

Continuous antigen-specific HSC-T cell interactions trigger HSC exhaustion

While the effects of an acute and short bidirectional interaction on HSCs were deeply characterized, the consequences of chronic antigen-specific stimulation remained unexplored. To that end, the same amount of WT and CAG-OVA HSPCs were transplanted into lethally irradiated mice. This, resulted in a chimera with HSPCs, and their offspring, constantly presenting (CAG-OVA) or not presenting (WT) the OT-II specific antigen. Moreover, OT-II T cells were co-transferred into these mice at the same time or two months after the transplantation (Figure 12P). On the one hand, $CD4^+$ T cell interactions did not affect peripheral blood chimerism when transferred after hematopoietic reconstitution (Figure 12Q). On the other hand, when OT-II T cells were transferred at the same time as the HSPCs, no reconstituting stem cell capacity was seen in CAG-OVA cells. Importantly, this effect was not due to antigen-specific CD8+ T cells (Figure 12R).

Furthermore, CAG-OVA HSPCs significantly altered their lineage output in the presence of OT-II T cells (Figure 12S). More specifically, myeloid and $CD8^+$ T cell production were incremented at the expense of B cell development. Then, we further analyzed the differences in the less represented lineages produced by antigen presenting HSCs. To that end, rather than seeing the progeny spectrum as a whole, we analyzed the fold change produced by antigen presentation in all different lineages individually (Figure 12T). In line with previous results, the highest fold change in any lineage production was seen in myeloid subtypes. Thus, the bidirectional communication between HSCs and antigen-specific T cells promotes proliferation and myeloid differentiation of HSCs, while in the context of transplantation it results in HSC exhaustion.

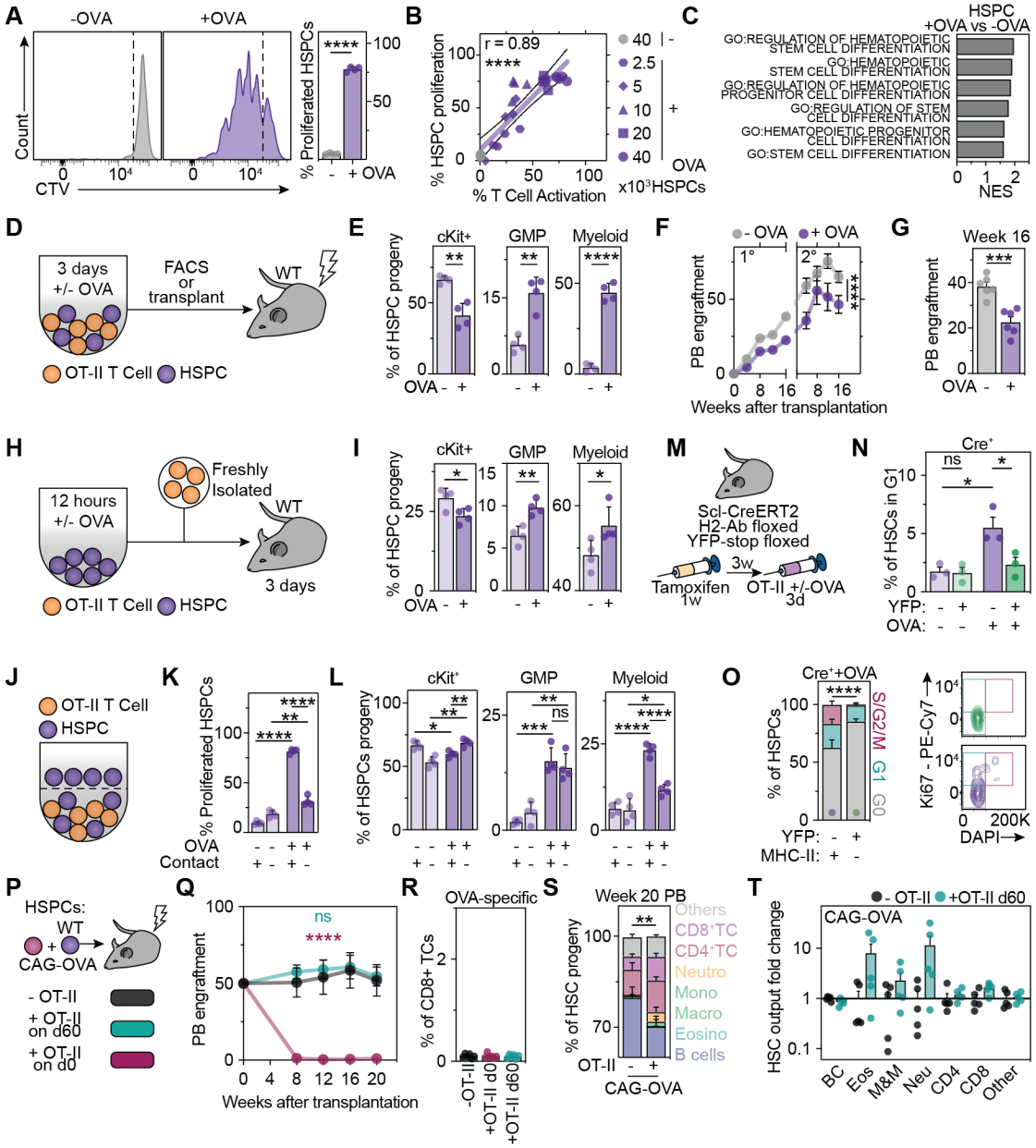

Figure 12. MHC-II mediates an antigen-specific bidirectional interaction between HSPCs and CD4⁺ T cells.

(**A**) Impact of antigen presentation on HSPC proliferation. Co-cultures with OT-II CD4+ T cells were performed as previously. Proliferation of HSPCs was read out by CellTrace Violet (CTV) dilution 72 hours post co-culture. Dashed lines represent the limits between divided and undivided cells. Representative plots (left panels) and quantification (right panel), *n=4*. (**B**) Correlation of T cell activation with HSPC proliferation. Different numbers of HSPCs were co-cultured with naïve OT-II T cells in the presence or absence of OVA for three days. Linear regression with 95% CI, *n=4*. (**C**) HSC differentiation genes are upregulated upon antigen presentation. Bulk RNA-Seq of HSPCs co-cultured with OT-II T cells for 72h in the presence or absence of OVA peptide, *n=3-4*. GSEA was performed in the RNA-Seq data, and normalized enrichment score (NES) of HSC-related gene sets are represented. (**D-G**) Impact of antigen presentation on HSPC differentiation. (**D**) Experimental scheme. Co-cultures were performed as previously, and analyzed by flow cytometry (E) or transplanted into lethally irradiated mice (F and G). (**E**) Numbers of cKit+, GMP (cKit+CD16/32+) or myeloid (cKit-CD16/32+ and CD11b+) populations were quantified from the HSPC progeny, *n=4*. (**F**) Peripheral blood engraftment over time of primary and secondary transplantation, *n=6*. (**G**) Peripheral blood engraftment at week 16, *n=6*. (**H** and **I**) *In vivo* impact of antigen presentation on HSPCs. (**H**) Experimental scheme. Sorted

HSPCs (LSKs) were cultured in the presence or absence of OVA peptide for 12 hours and adoptively co-transferred with freshly sorted naïve OT-II CD4$^+$ T cells in untouched WT mice. (**I**) 3 days post transfer, numbers of cKit$^+$, GMP (cKit$^+$CD16/32$^+$) or myeloid (cKit$^-$CD16/32$^+$ and CD11b$^+$) populations were quantified of the HSPC progeny. (**J**-**L**) Contact-dependent assessment of HSPC proliferation and differentiation. (**J**) Experimental scheme. Co-cultures were performed in a transwell plate with HSPCs in contact with T cells in the lower well and the same amount of HSPCs in the upper insert without contact to OT-II CD4$^+$ T cells. Proliferation (K) and differentiation (L) were quantified previously, *n*=4. (**M**-**O**) Native antigen-specific HSPC-T cell interaction promotes HSPCs to cycle. (**M**) Experimental scheme. Scl-CreERT2 *H2-Ab* floxed YFP-stop floxed mice were injected daily with tamoxifen during five days and three weeks, OT-II CD4$^+$ T cells and OVA were injected three days prior to readout. Afterwards, HSPC cell cycle status was analyzed by flow cytometry as follows, G0, Ki67$^-$DAPI^{low}; G1, Ki67$^+$ DAPI^{low}, S/G2/M, Ki67$^+$DAPI$^{mid/high}$. (**N**) Comparison of YFP$^+$ and YFP$^-$ HSCs from Cre+ mice treated or not with ovalbumin, *n=3*. (**O**) Quantification (left) and representative plots (right) of YFP$^+$MHC-II$^-$ and YFP$^-$MHC-II$^+$ HSPCs from Cre+ mice treated with ovalbumin, *n=5*. (**P-T**) Sustained native bone marrow antigen-specific HSPC-T cell interactions trigger HSPC differentiation and exhaustion. (**P**) Experimental scheme. WT or CAG-OVA FACS sorted HSPCs were sorted and co-transplanted in equal ration into irradiated WT recipients with or without OT-II T cells at the same time or 2 months after bone marrow reconstitution. (**Q**) Recipient mice were bled monthly and percentage of CAG-OVA progeny in peripheral blood is depicted, *n=6*. (**R**) Percentage of OVA-specific CD8$^+$ T cells in bone marrow after 20 weeks, *n=6*. (**S**) Lineage-bias changes upon HSPC-T cell interactions. Percentage of each of the represented lineages generated by CAG-OVA cells in mice with no OT-II T cells or with OT-II T cell injected after 2 months, *n=6*. (**T**) Fold change of all the studied lineages produced by T cell interactions when compared to no-interacting T cell condition, *n=6*. Individual values are depicted in B and C. Means and SEM are depicted otherwise. No significance = ns, P<0.05 *, P<0.01 **, P<0.001 ***, P<0.0001 ****. One- (E, I and N) or two-way ANOVA (F, K, L, O, Q and S) were performed as discovery tests. Paired two-tailed t-tests were performed as post-hoc tests in N. If not stated otherwise, unpaired two-tailed t-tests were performed as post-hoc tests. Linear regression analysis was performed in B. In case of multiple comparisons, p-values were corrected according to Benjamini-Hochberg.

HSPC-activated T cells acquire a stable immunoregulatory phenotype

To further understand the effects of the HSPC-T cell interaction we then decided to characterize the T cells derived from such contacts. Firstly, we co-cultured naïve OT-II $CD4^+$ T cells with different hematopoietic cell types from spleen or bone marrow in the presence or absence of OVA (Figure 13A). As expected, regardless of the tissue of origin, APCs such as DCs, monocytes, macrophages and HSPCs were capable of efficient T cell activation, while non-APCs such as neutrophils or $CD8^+$ T cells were not. Interestingly, eosinophils a non-professional APC subtype were also able to do so, though to a lesser extent. Next, we analyzed the surface immunophenotype of the activated T cells co-cultured with the different APCs and performed principal component analysis (PCA) to address their differences in an unbiased manner. Interestingly, all T cells showed variability according to the APC and organ of origin (Figure 13B), with the HSPC-activated T cells (T_{HSCs}) clustering away from other T cells, mostly based on a PD-L1 upregulation. To better understand in which way T_{HSCs} were different to T cells activated by other APCs, we decided to systematically compare them to canonical DC-activated T cells (T_{DCs}). Targeted (Nanostring) or whole transcriptomic analysis (RNA-Seq) proved T_{HSCs} to be different from T_{DCs} (Figure 13C).

To unveil the differences induced on antigen-specific $CD4^+$ T cells by HSPCs, we performed unbiased gene set enrichment analysis (GSEA) on the RNA-Seq data comparing T_{HSCs} to T_{DCs}. Strikingly, the significant top hits of enrichment scores were all related to negative regulation of the immune response and tolerance (Figure 13D). Noteworthy, T_{HSCs} also displayed an enormous enrichment for a co-regulated transcriptional module of coinhibitory molecules highly tied to immune tolerance and a Tr1 T cell phenotype (Chihara *et al.*, 2018) (Figure 13D and E). Some of the main transcription factors and effector molecules were further validated by qPCR (Figure 13F). As expected, all checkpoint molecule transcripts were upregulated in T_{HSCs}. Interestingly , *Foxp3*, the main regulator of Treg fate, was not expressed, while *Maf*, the key transcription factor of the Tr1 subtype, was highly expressed in T_{HSCs}.

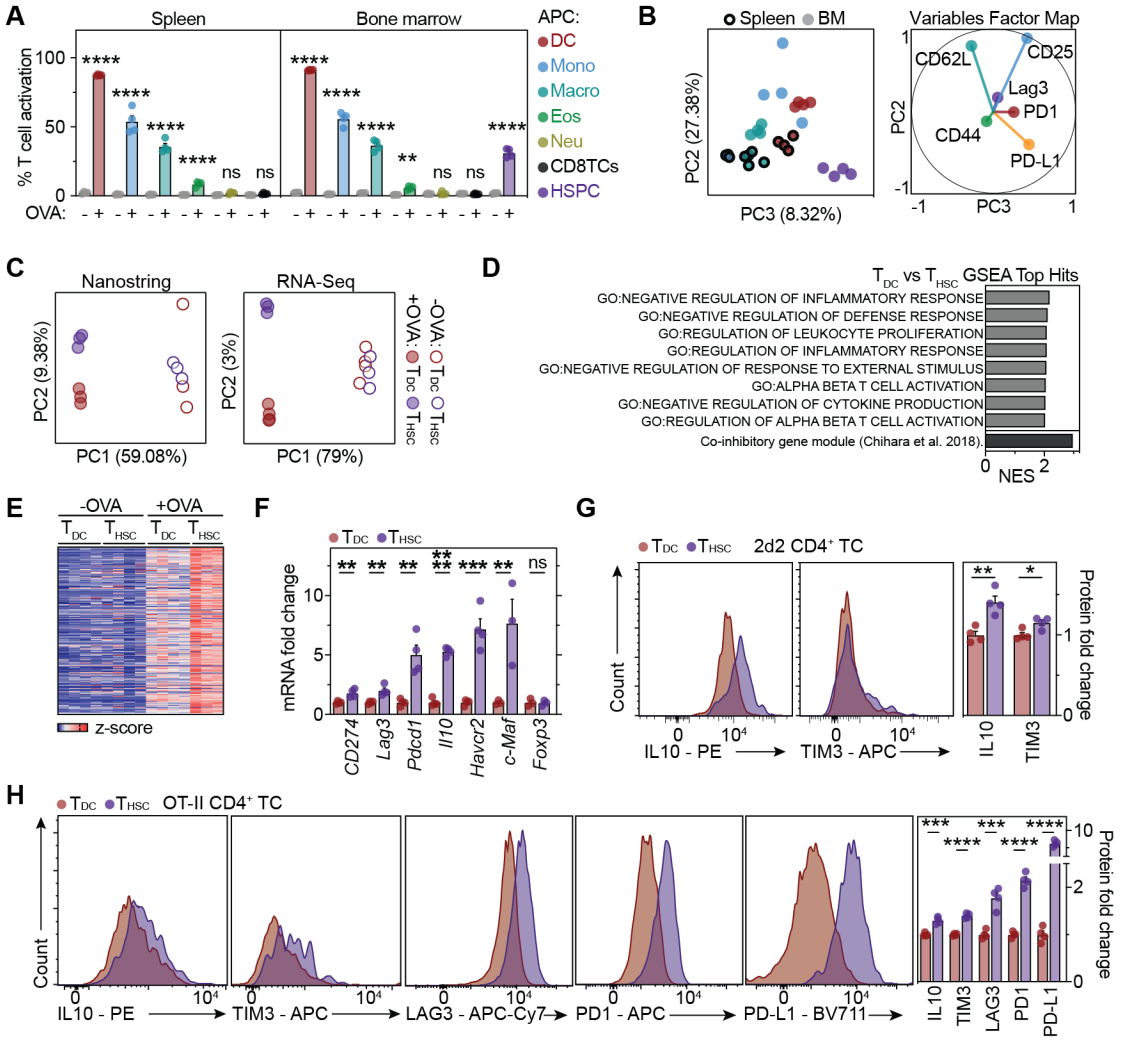

Figure 13. T_{HSC} immunophenotype characterization.

(**A** and **B**) 5x10^4 naïve OT-II T cells were cultured in the presence of 2x10^4 APCs from spleen or bone marrow in the presence or absence of OVA. (**A**) Percentage of T cell activation was quantified as previously and is represented for all the different APCs tested. (**B**) Principal component analysis (PCA) was performed in the activated T cells (left), considering the expression of several T cell activation surface markers represented in the variables factor map(right). (**C**) Nanostring (left) and RNA-Seq (right) gene expression profiling of OT-II CD4$^+$ T cells activated by HSPCs (T_{HSCs}) or dendritic cells (DCs) (T_{DCs}) for 72h in the presence or absence of OVA peptide. Principle component analyses (PCA) was performed, *n=3-4*. (**D**) GSEA was performed in the RNA-Seq data from C, comparing T_{HSCs} and T_{DCs}. Normalized enrichment score (NES) of the top T_{HSC}-enriched gene sets are represented. (**E**) Heatmap representing normalized RNA-Seq gene expression from C of the co-inhibitory gene module (Chihara *et al.*, 2018). (**F**) qPCR analyses of T_{HSCs} and T_{DCs}. T_{HSCs} and T_{DCs} were generated as previously. Gene expression is presented relative to T_{DCs}, *n=4*. (**G** and **H**) Flow cytometric analyses of T_{HSCs} and T_{DCs} from 2d2 (**G**) or OT-II (**H**) T cells. Representative plots (left panels) and quantification relative to T_{DCs} (right panel), *n*=4. Individual values are depicted in B, C and E and means and SEM otherwise. No significance = ns, P<0.05 *, P<0.01 **, P<0.001 ***, P<0.0001 ****. One-way ANOVA (A, F, G and H) was performed as discovery test. Unpaired two-tailed t-tests were performed as post-hoc tests. In case of multiple comparisons, p-values were corrected according to Benjamini-Hochberg.

Next, we aimed to understand whether the immunoregulatory phenotype was stable over time and under different circumstances. To this end, after the T cell being educated, their cognate antigen was withdrawn from the culture and qPCRs were performed before and after withdrawal (Figure 14A). All studied checkpoint molecules remained significantly higher in T_{HSCs} than in T_{DCs}. Of note, some of them, either associated to T cell activation status (*Pdcd1* or *Lag3*) or with T cell functionality (*Il10*), were downregulated, but still higher in T_{HSCs}. Importantly, the Tr1 master regulators (*Prdm1* and *Maf*) not only remained expressed, but were even further upregulated. After the antigen-rest, we provided the T cells with non-specific restimulation and measured PD-L1 and PD1 surface expression as a proxy of the immunosuppressive phenotype (Figure 14B). Both surface markers were more expressed also after reactivation in T_{HSCs}, suggesting a stable phenotype maintained over time. To further validate the stability of the T cell phenotype, we restimulated T_{DCs} and T_{HSCs} with freshly isolated DCs or HSCs (Figure 14C). In line with the aforementioned results, T_{HSCs} activated by either of the cell types maintained higher surface levels of PD1 when compared to T_{DCs} reactivated by DCs. Strikingly, T_{DCs} reactivated by HSPCs upregulated PD1 expression when compared to their DC-activated counterparts.

Lastly, to address whether additional proinflammatory stimuli would modify checkpoint molecule expression, we repeated the co-culture in presence of LPS. Interestingly, not only T_{DCs}, but also T_{HSCs}, remained unaffected by the additional proinflammatory cues (Figure 14D). All in all, HSPCs were capable of imprinting a unique, pronounced and stable immunoregulatory phenotype on naïve or previously activated T cells.

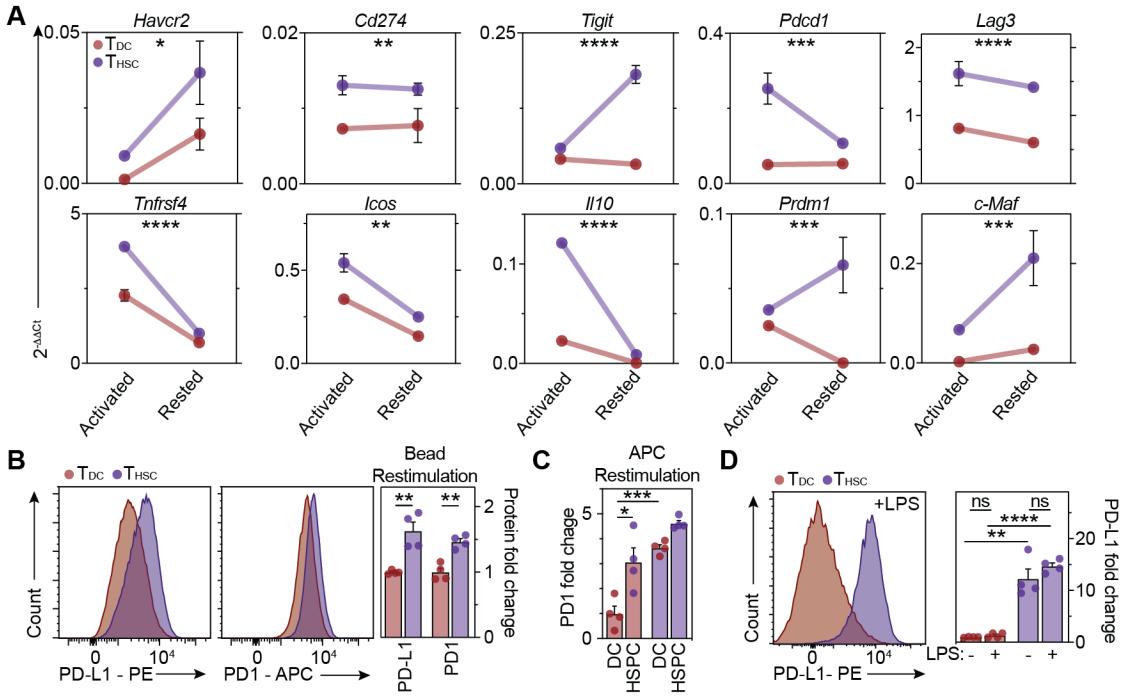

Figure 14. T_{HSCs} maintain a stable phenotype upon different challenges.
(**A**) qPCR analyses of T_{HSCs} and T_{DCs}. T_{HSCs} and T_{DCs} were generated as previously and rested for 2 days without peptide. *n*=4. (**B**) The immune suppressive phenotype of T_{HSCs} is maintained upon antigen-unspecific re-activation of T_{HSCs}. T_{HSCs} and T_{DCs} were generated as previously, followed by 2 days of rest without peptide and 2 days of culture with αCD3/αCD28 beads. PD-L1 and PD1 flow cytometry representative histograms are depicted (left). Protein expression is presented relative to T_{DCs} (right), *n*=4. (**C**) The immune suppressive phenotype of T_{HSCs} is maintained upon antigen-specific re-activation of T_{HSCs} and induced in HSPC-activated T_{DCs}. T_{HSCs} and T_{DCs} were generated as previously, followed by 2 days of rest without peptide and 2 days of culture with DCs or HSPCs. T_{DCs} and T_{HSCs} are displayed with red or purple bars, respectively. PD1 expression is presented relative to DC-restimulated T_{DCs}, *n*=4. (**D**) The immune suppressive phenotype of T_{HSCs} is maintained upon inflammation. T_{HSCs} and T_{DCs} were generated as in Fig. 2A in the presence or absence of LPS ($2.5x10^3$ HSPCs). PD-L1 flow cytometry representative histograms are depicted (left), and quantified (right), *n*=4. Means and SEM are depicted. No significance = ns, P<0.05 *, P<0.01 **, P<0.001 ***, P<0.0001 ****. One- (B) or two-way ANOVA (C and D) were performed as discovery tests. If not stated otherwise, unpaired two-tailed t-tests were performed as post-hoc tests. Two way ANOVA was performed in A. In case of multiple comparisons, p-values were corrected according to Benjamini-Hochberg.

T_{HSCs} are IL-10 dependent immunoregulatory T cells

The next step was to move from phenotype to function and thus, to confirm that T_{HSCs} are functionally immunosuppressive and if so, to determine the underlying mechanism. To that end, we designed an array of experiments spanning diverse responder/bystander immune cells in various *in vivo* and *ex vivo* settings. First, we co-cultured naïve bystander $CD4^+$ T cells with activatory antibodies in the presence of other T cells, including T_{HSCs}, to address their immunosuppressive capacity. As expected, bystander T cells activated and proliferated based on the presence of the activating antibodies (Figure 15A-B). The presence of Tregs significantly suppressed this activation. Importantly, T_{HSCs} suppressed bystander T cell activation more effectively than T_{DCs} (Figure 15B and C). Concomitantly, bystander $CD8^+$ T cell activation and proliferation were also suppressed by T_{HSCs} in an analogous setting (Figure 15D). Strikingly, this T cell immunosuppressive capacity was depleted when the bystander T cells did not express the IL-10 receptor (Figure 15E). To further validate both, the immunosuppressive functionality and its IL-10 dependency, we co-cultured WT and IL-10 receptor KO bone marrow monocytes and macrophages with T_{DCs} or T_{HSCs} (Figure 15F). In line with their immunosuppressive capacity, T_{HSCs} primed significantly less proinflammatory (M1) and more immunosuppressive (M2) macrophages when compared to the canonical T cell control. Again, this priming capacity was eliminated in the absence IL-10 signaling.

Next, to validate the immunosuppressive capacities of T_{HSCs} in an antigen-specific manner *in vivo*, we co-transferred them with responder OT-II T cells and subsequently treated the mice with ovalbumin (Figure 15G). Both, in the absence of other OT-II-derived T cells or with T_{DCs}, the responder T cells were strongly activated (Figure 15H). However, this activation was significantly dampened in the presence of T_{HSCs}, confirming the immunosuppressive role of these cells *in vivo*. Next, we extracted T_{HSCs} generated *in vivo* (see Figure 12P), and co-cultured them *ex vivo* in different cell ratios with bystander T cells, bone marrow mononuclear cells (as a source of APCs) and OVA peptide (Figure 15I). Importantly, bystander T cell activation was suppressed in the presence of one *in vivo*-generated T_{HSCs} for every 25 bystander T cells (Figure 15J). This inhibitory effect was strongly increased when augmenting the proportional number of T_{HSCs} relative to bystander cells. Therefore, HSPC-educated T cells are primed in the bone marrow and are functionally immunosuppressive in an IL-10-dependent manner.

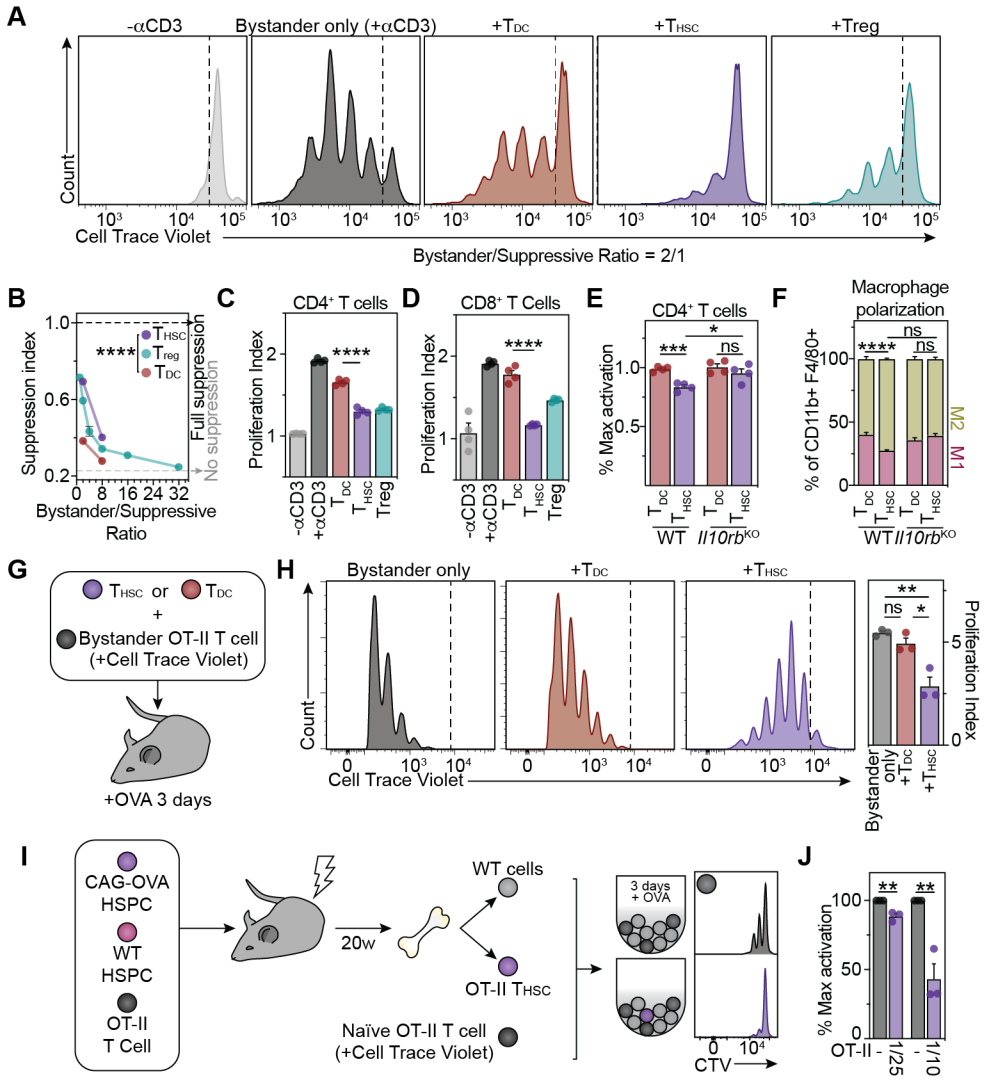

Figure 15. T_{HSC} immunoregulatory effect on different immune cells.

(**A-C** and **E**) *Ex vivo* CD4$^+$ T cell suppression assay. T_{HSCs} and T_{DCs} were generated as previously, followed by 2 days rest without peptide. T_{HSCs}, T_{DCs} and freshly isolated T_{regs} were then co-cultured in different ratios with CTV-stained bystander/responder WT (**A-C** and **F**) or *Il10rb*$^{-/-}$ (**F**) naïve CD4$^+$ T cells and supporting CD3$^-$CD19$^-$ splenocytes in the presence or absence of activator αCD3 antibody for 72h. (**A**) Representative plots from the 1:2 suppressive/bystander naïve CD4$^+$ T cells condition. Dashed line indicates non-proliferated bystander T cells. (**B**) Suppression index was calculated as explained in the "Methods" section and depicted for all performed ratios, *n=4*. (**C**) Proliferation index of responder CD4$^+$ T cells are depicted for the 1:2 ratio, *n=4*. (**D**) *Ex vivo* CD8$^+$ T cell suppression assay. T_{HSCs} and T_{DCs} were generated as previously, followed by 2 days rest without peptide. T_{HSCs}, T_{DCs} and freshly isolated T_{regs} were then co-cultured in a 1:2 ratio with CTV-stained bystander/responder naïve CD8$^+$ T cells and supporting CD3$^-$CD19$^-$ splenocytes in the presence or absence of activator αCD3 antibody for 72h. Quantification of the proliferation of responder CD8$^+$ T cells is depicted, *n=4*. (**E**) Effect of IL-10 in the CD4$^+$ T cell suppressive effect of T_{HSCs}. Ratio of activation of WT (left) or *Il10rb*$^{-/-}$ (right) bystander T cells in the presence of T_{HSCs} relative to the presence of T_{DCs}, *n=4*. (**F**) E*x vivo* macrophage polarization assay. T_{HSCs} and T_{DCs} were generated as previously, followed by 2 days rest without peptide. They were then co-cultured with CD11b$^+$SSC^{low} WT (left) or *Il10rb*$^{-/-}$ (right) monocytes/macrophages and activator αCD3/αCD28 beads for 24h. Quantification of F4/80+MHC-II+ (M1) and F4/80+CD206+ (M2) macrophages is depicted, *n=4*. (**G** and **H**) In vivo suppression assay. THSCs and TDCs were generated as before and adoptively co-transferred with CTV-labelled bystander naïve OT-II CD4+ T cells in a ratio of 1:8 into wild type (wt) mice. Bystander T cells were analyzed 3 days post OVA administration to

mice. (**G**) Experimental scheme. (**H**) Representative flow cytometry plots (left) and quantification of bystander T cell proliferation (right), *n=3*. (**I** and **J**) T_{HSCs} generated in vivo are immunoregulatory. (**I**) Experimental scheme. WT and CAG-OVA FACS sorted HSPCs were sorted and co-transplanted in equal ration into irradiated WT recipients together with OT-II T cells. After 20 weeks, WT-derived bone marrow cells and OT-II T cells were isolated from the bone marrow and cultured with CTV-stained naïve OT-II cells. Three days after, naïve OT-II cell proliferation was measured (right) and quantified (**J**). Means and SEM are depicted. No significance = ns, P<0.05 *, P<0.01 **, P<0.001 ***, P<0.0001 ****. One- (C, D, H and I) or two-way ANOVA (E) were performed as discovery tests. If not stated otherwise, unpaired two-tailed t-tests were performed as post-hoc tests. Two-way ANOVA was performed in B and F. In case of multiple comparisons, p-values were corrected according to Benjamini-Hochberg.

T_{HSCs} promote a MDSC-like phenotype in HSPCs upon antigen presentation

Next, we aimed to understand whether the T_{HSC} immunoregulatory phenotype had an impact on the concomitant HSPC differentiation. To that end, we made use of the previously generated RNA-Seq dataset comprising HSPCs that activated or did not activate antigen specific T cells. Interestingly, GSEA analyses revealed a significant enrichment in genes signatures related to immune inhibition in antigen presenting HSPCs (Figure 16A). Enriched gene sets included different ones involved in immunoregulatory cytokine production and reactive oxygen species (ROS) response. Additionally, immunoregulatory cytokines, such as *Ebi3*, *Il10* and *Il27,* and checkpoint molecules, such as *Cd274*, were upregulated following antigen presentation (Figure 16B-D). Therefore, the tolerogenic induction triggered by HSPCs in T cells, seemed to feedback on the HSPCs, promoting a doubled-sided tolerance induction.

Considering the myeloid differentiation that HSPCs undergo following T cell activation, we hypothesized that HSPC-derived cells might resemble myeloid-derived suppressive cells (MDSCs). Indeed, antigen presenting HSPCs upregulated a wide array of MDSC-specific genes recently described (Alshetaiwi *et al.*, 2020) (Figure 16E). To ultimately link differentiation to a tolerogenic immunophenotype, we screened the most important surface and functional MDSC markers on T cell co-cultured HSPCs. We then compared quiescent HSPC-like against divided and differentiated cells (Figure 16F). As expected, the differentiated cells displayed an MDSC-like immunophenotype when compared to the quiescent HSPC-like cells (Figure 16G). This includes MHC-II downregulation, CD84 and CD206 upregulation and increased ROS production.

All in all, HSCs and helper T cells interact in an MHC-II- and antigen-dependent manner. This interaction has bidirectional consequences. On the one hand, T cells acquire an immunosuppressive Tr1-like phenotype and suppress the immune system in their surroundings. On the other hand, HSCs proliferate and differentiate towards the myeloid lineage. Ultimately, this interaction drives antigen-presenting HSCs to exhaustion, while generating an immunosuppressive environment for the non-antigen presenting HSCs.

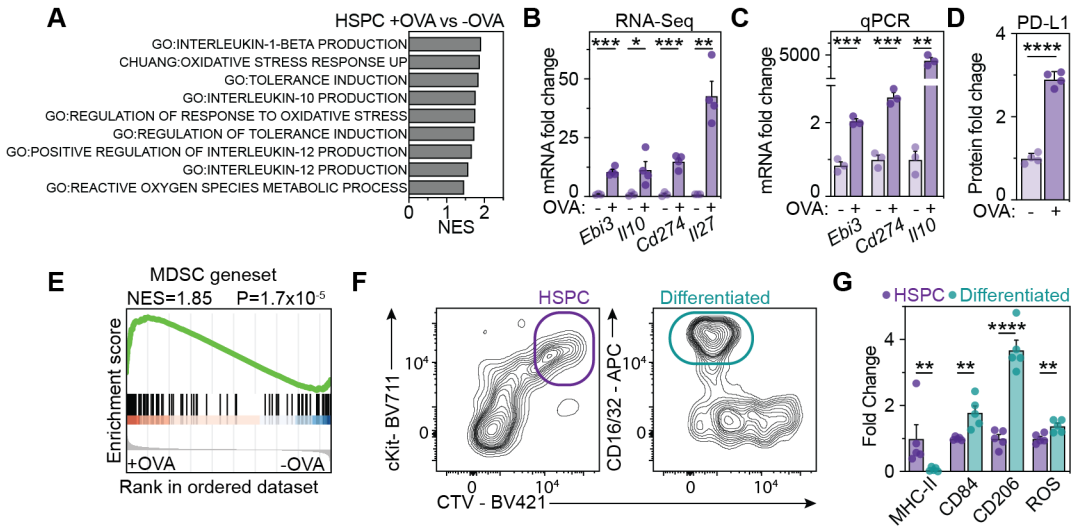

Figure 16. T_{HSC}-induced HSPC progeny displays an MDSC-like phenotype.
(**A-E**) Tolerogenic genes are upregulated upon antigen presentation in HSPCs. HSPCs were co-cultured, as previously, with OT-II T cells for 72h in the presence or absence of OVA peptide, *n=3-4*. (**A**) GSEA was performed in the RNA-Seq data, and normalized enrichment score (NES) of tolerance-related gene sets are represented. (**B** and **C**) Individual and crucial tolerogenic genes from RNA-Seq (B) are plotted and reconfirmed by qPCR (C) of OVA-incubated HSPCs relative to -OVA condition, *n=3-4*. (**D**) PD-L1 surface expression on HSPCs of OVA-incubated HSPCs relative to -OVA condition, *n=4*. (**E**) GSEA for a myeloid derived suppressive cell (MDSC) comprehensive geneset (Alshetaiwi *et al.*, 2020). (**F** and **G**) The MDSC phenotype is displayed on the cells that proliferate and differentiate. (**F**) Representative flow cytometry plot from HSPC-OT-II co-cultures + OVA, with gating strategies to distinguish quiescent HSPC-like cells from proliferated MDSC-like cells. (**G**) MDSC-related hallmarks measured by flow cytometry. Expression is presented relative to the HSPC population, *n=5*. Means and SEM are depicted. No significance = ns, P<0.05 *, P<0.01 **, P<0.001 ***, P<0.0001 ****. One-way ANOVA was performed as discovery test. If not stated otherwise, unpaired two-tailed t-tests were performed as post-hoc tests. In case of multiple comparisons, p-values were corrected according to Benjamini-Hochberg.

Human HSPCs express the MHC-II machinery

In order to investigate whether our findings obtained in the mouse system can be translated to humans, we first analyzed bulk and single-cell transcriptome datasets of human HSPCs (Novershtern *et al.*, 2011; Hay *et al.*, 2018; Pellin *et al.*, 2019). These analyses revealed high expression of genes encoding MHC-II (e.g. HLA-DRA, HLA-DRB) and the machinery related to antigen presentation via MHC-II (e.g. HLA-DMA, HLA-DMB, CD74) in HSCs and MPPs (Figure 17A-C). Of note, while the expression of the MHC-II antigen presenting machinery was maintained throughout commitment of HSCs to lineages with APC function (DC, B cell and monocyte/macrophage lineages), it was gradually downregulated upon commitment to all other lineages (neutrophil, eosinophil/basophil/mast cell, erythroid, megakaryocytic lineages).

We next performed a cell surface flow cytometric characterization of the MHC-II molecule HLA-DR across hematopoietic compartments of the bone marrow from healthy donors. The results accurately recapitulated our findings from the different aforementioned datasets and the mouse system, with no expression of HLA-DR in non-APCs, such as T and NK cells, high expression in professional APCs, like BCs and DCs, and robust, albeit slightly lower expression in HSCs and early progenitors of the $CD34^+$ compartment (Figures 17D and E).

To confirm that MHC-II marks human HSCs with long-term self-renewal and multilineage differentiation capacity, we transplanted human bone marrow, separated based solely on HLA-DR expression, into immunodeficient sublethally irradiated mice (Figure 17F). At 16 weeks post-transplant, HLA-DR-positive bone marrow cells gave rise to significantly higher levels of human engraftment compared to $HLA\text{-}DR^-$ bone marrow (Figure 17G). Crucially, all lineages were generated by $HLA\text{-}DR^+$ bone marrow, implying that human HSC activity is associated with HLA-DR expression.

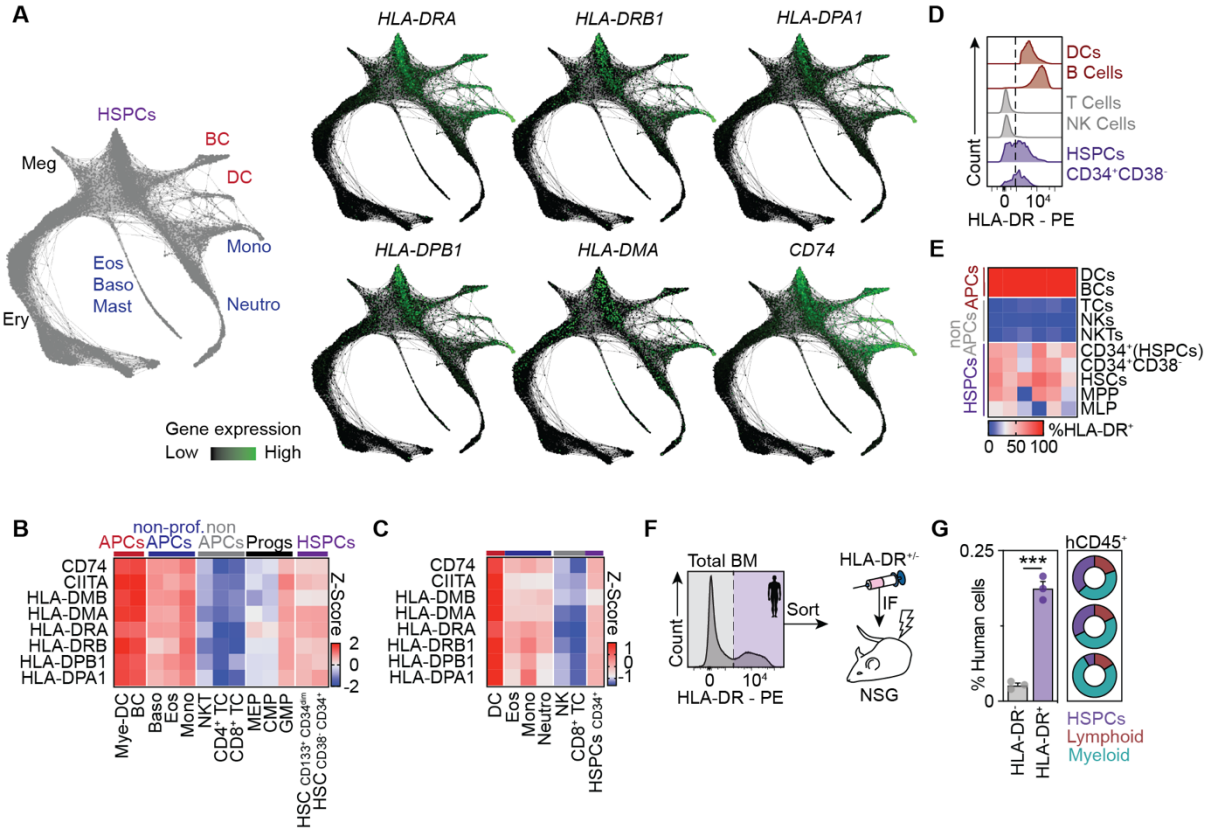

Figure 17. MHC-II expression in human HSPCs.

(**A**) scRNA-seq across human HSPC differentiation trajectories (Pellin *et al.*, 2019). Lineage annotation (left) and MHC-II and related gene expression (right) are depicted. (**B** and **C**), z-scores of genes encoding the MHC-II antigen presentation machinery in different human populations, inferred from microarray (Novershtern *et al.*, 2011) (**B**) or RNA-Seq (Hay *et al.*, 2018) (**C**) data. (**D**) HLA-DR (MHC-II) surface measurements by flow cytometry of selected populations. Representative plots, *n=6*. Dashed lines indicate thresholds for gating. (**E**) Heatmap representing HLA-DR (MHC-II) surface measurements by flow cytometry of selected populations from bone marrow aspirates of healthy donors, *n=6*. (**F** and **G**) Xenotransplantation experiments of HLA-DR bone marrow populations. (**F**) Total human bone marrow from 3 healthy donors was sorted based on HLA-DR expression and transplanted into sub-lethally irradiated NSG mice. (**G**) Four months post transplantation, human $CD45^+$ cells in the bone marrow (left) and multilineage engraftment (right) were quantified. Each dot/donut plot represents average engraftment per donor. Individual values are depicted in E, means in B and C, and mean and SEM in G. No significance = ns, P<0.05 *, P<0.01 **, P<0.001 ***, P<0.0001 ****. Unpaired two-tailed t-tests were performed in G.

Human HSPCs can activate CD4$^+$ T cells in an immunoregulatory manner

Next, we aimed to test whether the MHC-II expression in human HSPCs translated into antigen presenting and T cell activating capacities. To that end naïve CD4$^+$ T cells from peripheral blood of healthy donors were co-cultured with DCs, TCs and CD34$^+$ HSPCs in the presence or absence of Cytostim (CS). This antibody-based reagent crosslinks MHC molecules to TCRs in a non-antigen-specific manner. Moreover, unlike superantigens, the crosslinking does not involve any other co-stimulatory molecule, enabling a bigger influence of the APC in the T cell priming and education (Bourdely *et al.*, 2020). Similar to the murine system, DCs efficiently activated CD4$^+$ T cells and other T cells only did so residually (Figure 18A and B). Importantly, HSPCs activated T cells to a similar extent as the positive control.

Furthermore, when investigating the immunophenotype of the DC or HSPC activated T cells, both cell states differed in a similar trend as in mouse. Checkpoint molecules, related to a tolerogenic cell state, were more expressed on T_{HSCs} surface and transcriptionally (Figure 18C and D). Moreover, there was a significant upregulation of the Tr1 master regulator *MAF* and effector cytokine *IL10*, while *FOXP3* was unaltered in CD4$^+$ T cells activated by HSPCs, recapitulating our findings in the murine system (Figure 18D).

To confirm the previous results in an antigen-specific manner, the same cells and setup were repeated without CS, but with an MHC-II-restricted peptide pool (PP) from common human pathogens. Under this conditions, DCs and HSPCs equally activated T cells (Figure 18E) while the tolerogenic immunophenotype was recapitulated, as seen by PD-L1 upregulation (Figure 18F). All in all, human HSPCs are also capable of antigen presentation and T cell activation with tolerogenic priming.

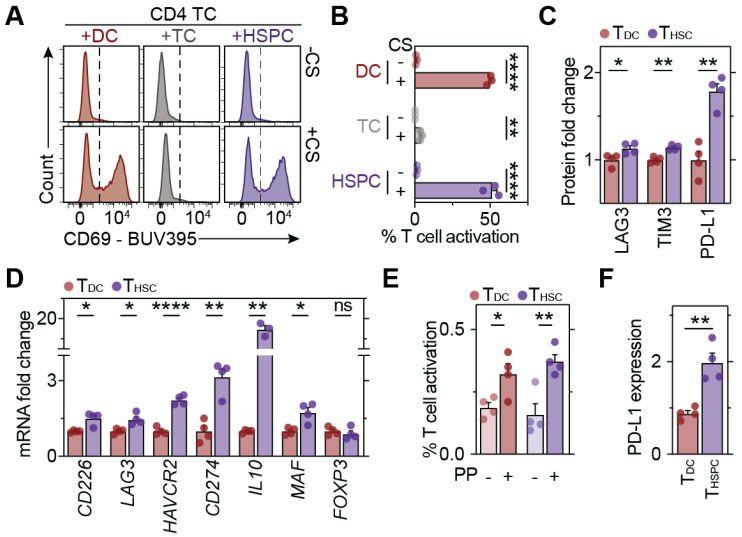

Figure 18. Human HSPCs can activate TCs in a tolerogenic manner.
Human bone marrow HSPCs (Lin^-CD34^+), DCs ($CD11c^+HLA\text{-}DR^+$) or T cells from peripheral blood (PB) were co-cultured with CTV-labelled naïve $CD4^+$ T cells in the presence or absence of CytoStim (CS) (**A-D**) or a MHC-II-restricted peptide pool (PP) (**E** and **F**) for 72 hours. Representative T cell activation plots (**A**) and quantification (**B** and **E**), *n=3-4*. Dashed lines indicate thresholds for gating. (**C** and **D**) Surface (**C** and **F**) and qPCR (**D**) analyses of human T_{HSCs} and T_{DCs}. T_{HSCs} and T_{DCs} were generated as in A. Gene expression is presented relative to T_{DCs}, *n=4*. Means and SEM are depicted in all bar-plots. No significance = ns, P<0.05 *, P<0.01 **, P<0.001 ***, P<0.0001 ****. One-way ANOVA was performed as discovery tests. Unpaired two-tailed t-tests were performed as post-hoc tests. In case of multiple comparisons, p-values were corrected according to Benjamini-Hochberg.

MHC-II expression correlates with stemness in AML

AML is a disease with an HSC or a progenitor origin that generates a block in differentiation of those cells (Papaemmanuil *et al.*, 2016). Therefore, immature cells called blasts overpopulate the bone marrow and blood of patients. Taking this into account, we aimed to understand whether MHC-II expression in healthy HSPCs was maintained upon malignant transformation. To that end, we obtained surface expression of different standardized markers used in AML research for over 60 AML patients at diagnosis (Figure 19A-F). Of note, among the used markers, HLA-DR can be found (van Dongen *et al.*, 2012).

A comparison of HLA-DR surface expression with all other studied surface markers revealed significant positive correlation with stem cell molecules, such as CD34 or CD117 (Figure 18A). On the contrary, a negative correlation was observed for many different maturation markers. Therefore, we wanted to understand whether intrapatient heterogeneity for MHC-II expression could be seen as in the healthy hematopoietic system. Hence, we segregated all different cells within individual AMLs based on surface positivity of representative stem or mature cell markers (Figure 19B and C). Indeed, more stem-like cells expressed more MHC-II, while more mature-like cells expressed significantly less MHC-II. Furthermore, to test interpatient heterogeneity, we performed unsupervised clustering of the patients only based on the average surface expression of all studied molecules (Figure 19D and E). This approach found four clearly distinguishable groups of patients based on their immunophenotype

resembling stem cells, monocytes, granulocytes or intermediate undifferentiated progenitors. Interestingly, MHC-II surface expression differed between the different clusters (Figure 19F). As in the healthy hematopoietic system, intermediate and granulocytic-like AMLs displayed the lowest expression of MHC-II. In contrast, patients with monocytic and stem-like AMLs portrayed the highest MHC-II expression values. Altogether, these results suggest that MHC-II expression of AML cells resembles that of the original healthy hematopoietic system.

Furthermore, we made use of a publicly available dataset comparing transcriptomic data from a wide array of patients with different mutational backgrounds and states of the disease (Pölönen *et al.*, 2019). When excluding monocytic AMLs, these patients had a high correlation between the expression of MHC-II and related genes with hematopoietic stem cell genes (Figure 19G). Such correlation could be a reflection of AMLs originating from more immature MHC-II-expressing HSCs versus more differentiated MHC-II-negative progenitors. To test this, we analyzed the transcriptomes of normal karyotype, genetically defined AML subsets. On the one hand, FLT3-ITD, in combination with other driver mutations, can only transform HSCs (Rathinam *et al.*, 2010; Yang *et al.*, 2016). On the other hand, NPM1 mutations can generate AML from HSCs and other committed progenitors (de la Guardia *et al.*, 2020; Uckelmann *et al.*, 2020). Thus, we compared MHC-II and associated gene expression patterns on FLT3-ITD/NPM1^{wt} and FLT3^{wt}/NPM1^{mut} AMLs (Kohlmann *et al.*, 2010). Firstly, we confirmed that, as expected, FLT3-ITD AMLs had higher expression of stem cell and leukemic stem cell genes when compared to NPM1^{mut} diseases (Ng *et al.*, 2016) (Figure 19H). No difference could be observed between the two groups when comparing MHC-I genes. However, MHC-II and related machinery expression was highly enriched in HSC-derived AMLs. These data suggest that the cell of origin might determine MHC-II expression on the derived disease. This can potentially affect its ability to interact with and modulate the adaptive immune system.

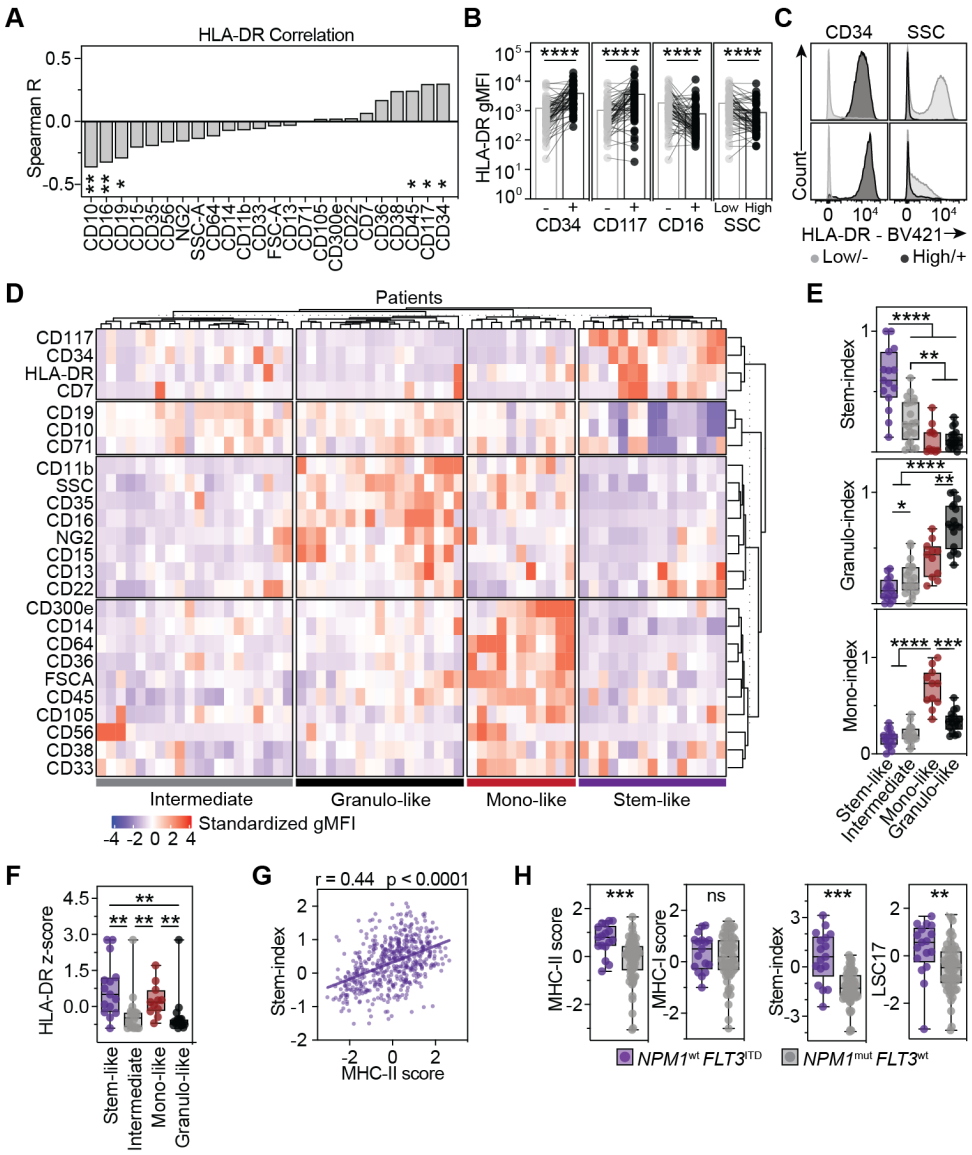

Figure 19. MHC-II expression correlates with stem-like phenotype in AML.

(**A**) Spearman correlation of HLA-DR expression in the blast compartment of AML patients at diagnosis with other markers of the Euroflow panel (van Dongen et al., 2012), *n=63*. (**B** and **C**) Intra-patient heterogeneity of HLA-DR in leukemic cells of 63 AML patients at diagnosis. BM aspirates were stained with EuroFlow panels. (**B**) HLA-DR geometric mean fluorescence intensity within blast sub-compartments positive or negative for representative stem (CD34 and CD117) or mature (CD16 and SSC) markers, *n=63*. (**C**) Representative flow cytometry histograms of $CD34^{+/-}$ (left) or $SSC^{high/low}$ (right) populations from different AML patients. (**D**) Heatmap showing standardized gMFIs of the EuroFlow flow cytometry markers across AML patients at diagnosis. Patients and markers were partitioned by PAM clustering. Dendrograms depict within- and between-partition similarities based on hierarchical clustering using Spearman distances, *n=63*. (**E**) EuroFlow patients were stratified into the indicated groups based on clustering and corresponding indices summarizing expression of stem cell, granulocyte or monocyte marker expression across patient clusters (see Methods). (**F**) HLA-DR expression in different AML groups, *n=63*. (**G**) AMLs from (Pölönen *et al.*, 2019) depicted for the sum of scaled MHC-II gene expression and stem cell scores (see Methods). (**H**) Sum of scaled MHC-II or MHC-I related genes (left) or stem cell scores (Ng et al., 2016) (right, see Methods), in AML patients segregated based on NPM1 and FLT3 mutational state (Kohlmann et al., 2010), *n=78*. Means and SEM are depicted in all bar-plots. No significance = ns, P<0.05 *, P<0.01 **, P<0.001 ***, P<0.0001 ****. Kruskal-Wallis (E and F) were performed as discovery tests. Spearman correlation coefficients were

performed in A. Paired Mann-Whitney test was performed in B. Unpaired Mann-Whitney was test performed in E, F and H. In case of multiple comparisons, p-values were corrected according to Benjamini-Hochberg.

High MHC-II expression correlates with poor prognosis in AML

Once established that stem-like AMLs express higher levels of MHC-II, we wanted to investigate whether this was of prognostic value. Hence, we took advantage of a transcriptomic dataset of different non-complex karyotype DNMT3A^{mut} AMLs at diagnosis for which the exact outcome of the disease after treatment has been documented (Figure 20A-D). We quantified all individual MHC-I and MHC-II and related genes from patients that suffered from early relapse (ER) or long term remission (LTR) (Figure 20A). GSEA and normalization of all studied genes revealed that while no difference in MHC-I genes was observed between both patient groups, MHC-II genes were highly enriched in poor prognosis, early relapse patients (Figure 20B and D). Moreover, when not considering the relapse-free time and separating the patients only based on MHC-I expression, no difference was observed (Figure 20D). In contrast, Patients with high MHC-II expression had a worse relapse free survival outcome. Thus, MHC-II expression in AML not only correlates with a more stem-like state of the disease, but also with worse prognosis.

To further validate this finding, we made use of "The Cancer Genome Atlas" (TCGA) dataset for AML (Ley *et al.*, 2013). To avoid severe mutational effects on prognosis, normal karyotype NPM1^{mut} patients were used as a genetically homogenous subset. Additionally and as previously explained, while NPM1^{mut} patients have a defined mutational profile, their cell of origin might vary and thus, so will their MHC-II expression. In this cohort, the differences in MHC-I expression could not predict any differences in the outcome of the patients (Figure 20E). On the contrary, patients with higher MHC-II expression suffered from an adverse prognosis. As a matter of fact, this worse prognosis, was not significantly different from the FLT3-ITD/NPM1^{wt} stem-like AML (Figure 20F). Therefore, high MHC-II expression not only enriches for HSC-derived malignancies, but also for adverse prognosis in AML.

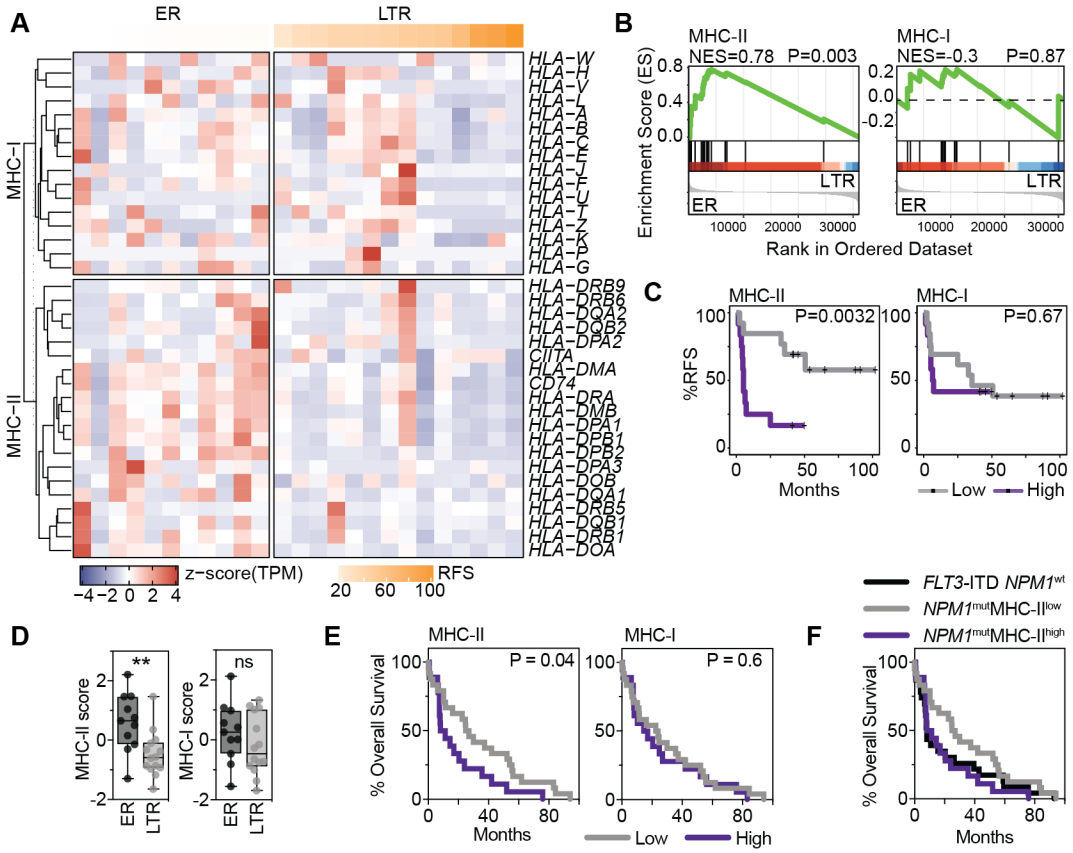

Figure 20. MHC-II expression correlates with worse prognosis in AML.

(**A**) Heatmap depicting standardized transcripts per million (TPMs) values for all MHC-I (top) or MHC-II (bottom) related genes in DNMT3A^{mut}NPM1^{mut} AML patients. RNA-Seq was performed in AML blasts at diagnosis from patients stratified according to disease outcome after treatment early relapse (ER, relapse <6 months post treatment) and long-term remission (LTR, relapse >6 months post treatment) AML patients, *n=25*. Relapse free survival time in months is indicated in the upper part of the panel. (**B**) Gene set enrichment analyses (GSEA) for MHC-II (left) or MHC-I (right) related genes in early relapse and long-term remission AML patients from A. (**C**) Analyses of relapse free survival (RFS), stratified by high (above median) or low (below median) expression of MHC-II (left) or MHC-I (right) related genes. (**D**) Sum of scaled MHC-II (left) or MHC-I (right) related genes in ER and LTR AML patients, *n=25*. (**E**) Analyses of overall survival, stratified by high (above median) or low (below median) expression of MHC-II (left) or MHC-I (right) related genes in NPM1^{mut} AML patients (Ley *et al.*, 2013), *n=42*. (**E**) Analyses of overall survival in NPM1^{mut} AML patients stratified according to MHC-II as in E compared to NPM1^{wt}FLT3^{ITD} AML patients, *n=65*. No significance = ns, P<0.05 *, P<0.01 **, P<0.001 ***, P<0.0001 ****. Unpaired Mann-Whitney was test performed in D. Log-rank (Mantel-Cox) test was performed in C, E and F.

HSC-initiated AML maintains the healthy HSC immunogenic capacities

To functionally address the differences observed in patient data and ultimately, the role of MHC-II in AML onset and progression, we made use of different mouse models. Firstly, we took into account the differences in MHC-II expression on stem-like or more differentiated AML (see Figure 19). Then, we generated AML from HSPCs or GMPs as previously described (Krivtsov *et al.*, 2006, 2013). In line with our previous observations, HSPC-derived AML maintained a higher capacity to interact with helper T cells than its GMP-counterpart (Figure 21A).

We then analysed how healthy aging and preleukemic mutations alter MHC-II expression, antigen presentation and tolerogenic induction of T cells (Figure 21B and C). Aged HSPCs showed a trend towards higher expression of MHC-II, but high variations in combination with a low sample size impedes a definitive conclusion. (Figure 21B). This trend did not translate into an enhanced T cell activation capacity, nor in a different type of T cell education. On the other hand, in mice with the genetic insertion of human FLT3-ITD that develop preleukemic myeloproliferative neoplasm (Chu *et al.*, 2012), no MHC-II expression differences were seen (Figure 21C). Nonetheless, they displayed an enhanced immunogenic potential, while the activated T cell phenotype was unperturbed. These results, suggest that the HSC-T cell immunosuppressive interaction is only modestly affected by aging and pre/malignant transformation.

MHC-II-mediated interactions between HSC-like AML and T cells prevent leukemia onset

To address the relevance of this antigen-dependent AML-T cell interaction, we continued using HSPC-derived AML cells. We injected mice with AML generated from CAG-OVA HSPCs, able of presenting the OT-II $CD4^+$ T cell cognate antigen constantly, functionally resembling a leukemic neoantigen. Moreover, OT-II T cells were injected at the same time or two weeks after the injection of the malignant cells, resembling an AML-T cell interaction at the onset leukemogenesis or at a fully established AML state (Figure 21D).

First, if T cells did not interact with the AML cells during onset, the leukemia populated peripheral blood exponentially over time (Figure 21E). On the contrary, upon T cell interaction, resembling the healthy HSC T cell-driven exhaustion, AML was not seen in peripheral blood. In addition, both these findings were perfectly recapitulated within the bone marrow, with massive AML expansion not being established in the presence of antigen-specific T cell (Figure 21F). Of note, an expansion of OT-II T cells was observed in the bone marrow, suggesting an antigen-specific expansion *in vivo* (Figure 21F). Moreover, these T cells activated by HSPC-derived AML cells displayed an extraordinary upregulation of PD-L1, resembling healthy T_{HSCs}

(Figure 21G). Strikingly, this translated into a more quiescent and suppressed state of the bystander immune system when T cells interacted with the AML, as seen the distribution of the T cell subpopulations (Figure 21H). More naïve and less effector host $CD4^+$ and $CD8^+$ T cells were present when OT-II T cells were injected. All in all, the MHC-II-dependent interaction between HSPC-derived AML and antigen-specific helper T cells effectively protect the hematopoietic system from AML onset, while simultaneously preventing an overactivation of the bystander immune system. While difficult to prove with the current methodology, this might be due to the immunosuppressive capacities of educated T_{HSCs}.

Lastly, if T cells were only able to interact with the AML cells after leukemia onset, the disease continued to overpopulate blood over time without significant differences (Figure 21I). Importantly, in this experimental setup mice injected with T cells unexpectedly suffered from worse health status (Figure 21J). This could potentially be explained by OT-II T cell derived immune suppression, leading to uncontrolled AML growth and ultimately, death. A reflection of this inability to control the disease, could also be seen in the lack of development of $CD8^+$ OVA-specific T cells when comparing the late-recognized to early-recognized leukemia (Figure 21K). Thus, while the thoroughly characterized antigen-specific bidirectional interaction would serve as a first line of defense against leukemia onset and a driver of an immune-privileged niche for healthy HSCs, it might also be hijacked by AML in order to avoid its immune clearance.

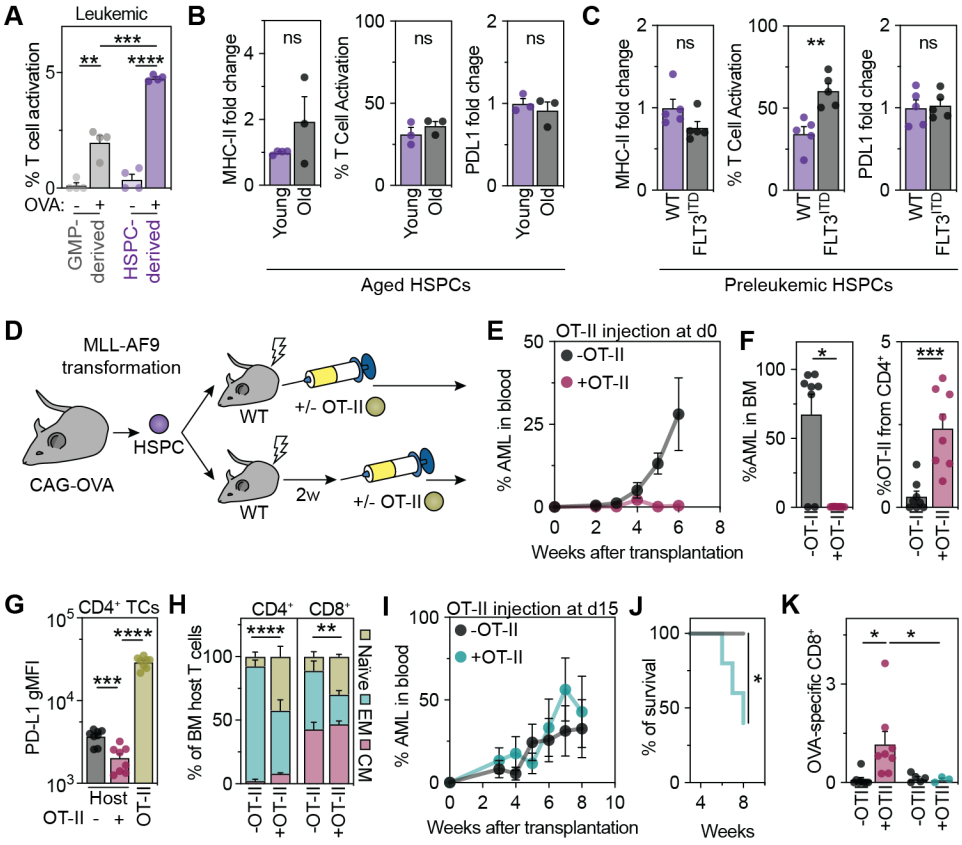

Figure 21. HSPC-derived AML maintains antigen presenting properties.
(**A**) Antigen presentation assays of HSC- and GMP-derived MLL-AF9 leukemia. Leukemias were induced by transduction of mouse LSK and GMP populations and transplantation into mice. Antigen presentation capacity was assessed by co-culture of leukemic cells with naïve CD4 OT-II T cells for 72 hours in the presence or absence of OVA peptide, *n=4*. (**B** and **C**) *Ex vivo* antigen-specific mouse T cell activation. HSPCs from old (A) or preleukemic (B) MHC-II expression (left), T cell activation capacity (middle) and T cell PD-L1 upregulation (right) were quantified and compared to young healthy mice, *n=3-4*. (**D-K**) Stem cell-derived leukemia antigen presentation impact on disease onset and development. (**D**) Experimental scheme. MLL-AF9 AML was induced in CAG-OVA HSPCs as previously (see Methods section) and injected in sublethally irradiated mice with or without OT-II T cells at the same time (E-H) or 2 weeks afterwards (I-J). (**E** and **I**) Percentage of AML cell in blood over time, *n=5-8*. (**F**) Percentage of AML (left) or OT-II T cells (right) in bone marrow after 7 weeks, *n=8*. (**G**) PD-L1 surface expression on host and OT-II CD4$^+$ T cells, *n=8*. (**H**) CD4$^+$ (left) and CD8$^+$ (right) host naïve (CD44$^-$ CD62L$^+$), effector memory (EM, CD44$^+$CD62L$^-$) and central memory (CM, CD44$^+$CD62L$^+$) quantification, *n=8*. (**J**) Kaplan Meier curve displaying survival of OT-II un/treated mice, *n=5*. (**K**) Percentage of OVA-specific CD8+ T cells in blood 5 weeks after AML transfer at the same time (left) or later (right), *n=3-8*. Means and SEM are depicted. No significance = ns, P<0.05 *, P<0.01 **, P<0.001 ***, P<0.0001 ****. Two-way ANOVA (A and H) or Kruskal-Wallis (G and K) were performed as discovery tests. If not stated otherwise, unpaired two-tailed t-tests were performed as post-hoc tests. Unpaired Mann-Whitney test was performed in F, G and K. Log-rank (Mantel-Cox) test was performed in J. In case of multiple comparisons, p-values were corrected according to Benjamini-Hochberg.

Identification of leukemic and pre-leukemic stem cells by clonal tracking from single-cell transcriptomics

The results shown in this section of the thesis are part of the manuscript with the same title published in 2021 in "Nature Communications" (Velten *et al.*, 2021). Some parts of the text, figures and figure legends have been taken and/or adapted from the aforementioned manuscript, originally co-written by myself (see author contributions for more details).

Capturing mutational and transcriptomic status from AML single cells

AML is a malignancy that can originate from HSCs or myeloid committed progenitors. As the hematopoietic system, it has a hierarchical organization with HSC-like quiescent leukemic stem cells (LSCs) generating highly proliferative blasts (Wang and Dick, 2005; Kreso and Dick, 2014). LSCs can survive conventional therapies and trigger relapse (Liran I Shlush *et al.*, 2017). Thus, in order to enhance current AML treatment approaches and avoid relapse, targeting LSCs is a major objective to achieve (Trumpp and Wiestler, 2008; Essers and Trumpp, 2010; Pollyea and Jordan, 2017). However, healthy, preleukemic and leukemic HSCs display highly overlapping phenotypes, making the specific targeting of LSCs difficult. Therefore, methods that permit the identification of differences between healthy and pre/leukemic HSCs bear the potential to unravel effective treatment options that specifically eradicate malignant cells.

Similar to healthy HSCs, LSCs have been historically identified based on their phenotype and function. The former, has exploited expression levels of molecules present on healthy HSCs, such as CD34 (Hosen *et al.*, 2007; Majeti, Becker, *et al.*, 2009; Majeti, Chao, *et al.*, 2009). The latter, relies on the capacity to regenerate the disease in mice (Eppert *et al.*, 2011; Ng *et al.*, 2016; Pabst *et al.*, 2016; Raffel *et al.*, 2017). Both these approaches have exploited big subgroups of cells within each patient and analyzed them as a whole or bulk. However, AML is a highly heterogeneous disease both, intra- and interpatient. This means that bulk experiments have the potential to ignore sparse cells, such as LSCs, in the disease. Additionally, the findings extracted from bulk analyses cannot be applied to other AMLs, since they strongly vary in origin and immunophenotype.

To overcome the aforementioned limitations, single cell studies have been aiming to better find and characterize LSCs within the disease and compared to healthy HSCs. Of note, HSCs and LSCs mostly vary genotypically. Therefore, mutational profiling of single cells is the most reliable approach to distinguish them to date. However, functional data has to be extracted at the same time to better compare healthy versus malignant cells. Previous studies have achieved mutational calling of single cells from or together with RNA-Seq using diverse methods (Dey *et al.*, 2015; Macaulay *et al.*, 2015; Giustacchini *et al.*, 2017; Filbin *et al.*, 2018; Nam *et al.*, 2019; Petti *et al.*, 2019; Rodriguez-Meira *et al.*, 2019; van Galen *et al.*, 2019). However, the efficacy in identifying the clonality of each single cell by these methods was not

unequivocal and they suffered from a high drop-out rate. This translates in not a clear comparison between clones and loss of valuable information.

Taking this into account, we developed MutaSeq. MutaSeq is an adaptation of SmartSeq2, in which mutation-spanning primers are added to the obtained cDNA to amplify mutation-specific reads for each single cell (Figure 22A). In combination with a computational pipeline, developed by our collaborators, MutaSeq makes use of the mitochondrial genetic variations that provide an additional layer of genetic variability (Ludwig *et al.*, 2019; Xu *et al.*, 2019). Therefore, we combined previous methods aiming at defined nuclear and general mitochondrial mutations in order to better classify clones and thus, healthy or pre/malignant origin of individual cells within AML samples.

To this end, we obtained and sequenced bulk AML blasts and healthy tissue from four AML patients at diagnosis (P1-4) and included a healthy control (H1) (Figure 22C). This allowed us to know the mutations and design specific primers for each of the screened samples. Then, we index-sorted different compartments of all samples based on the surface expression of lineage markers and CD34 (Figure 22D). Finally, by using the recorded surface molecule expression we could characterize stem-like ($CD34^+$) and mature cells ($CD34^-$) at the same time.

In addition, to confirm the clonal output of MutaSeq, we performed single-cell cultures, followed by DNA sequencing to directly target genomic mutations with high efficiency and accuracy. Hence, we aimed to generate a comprehensive atlas of clonal origin and transcriptomic state for different AML samples with the goal of identifying a) healthy, pre-malignant and malignant HSCs and b) molecular consequences of each of the former cellular states (Figure 22B).

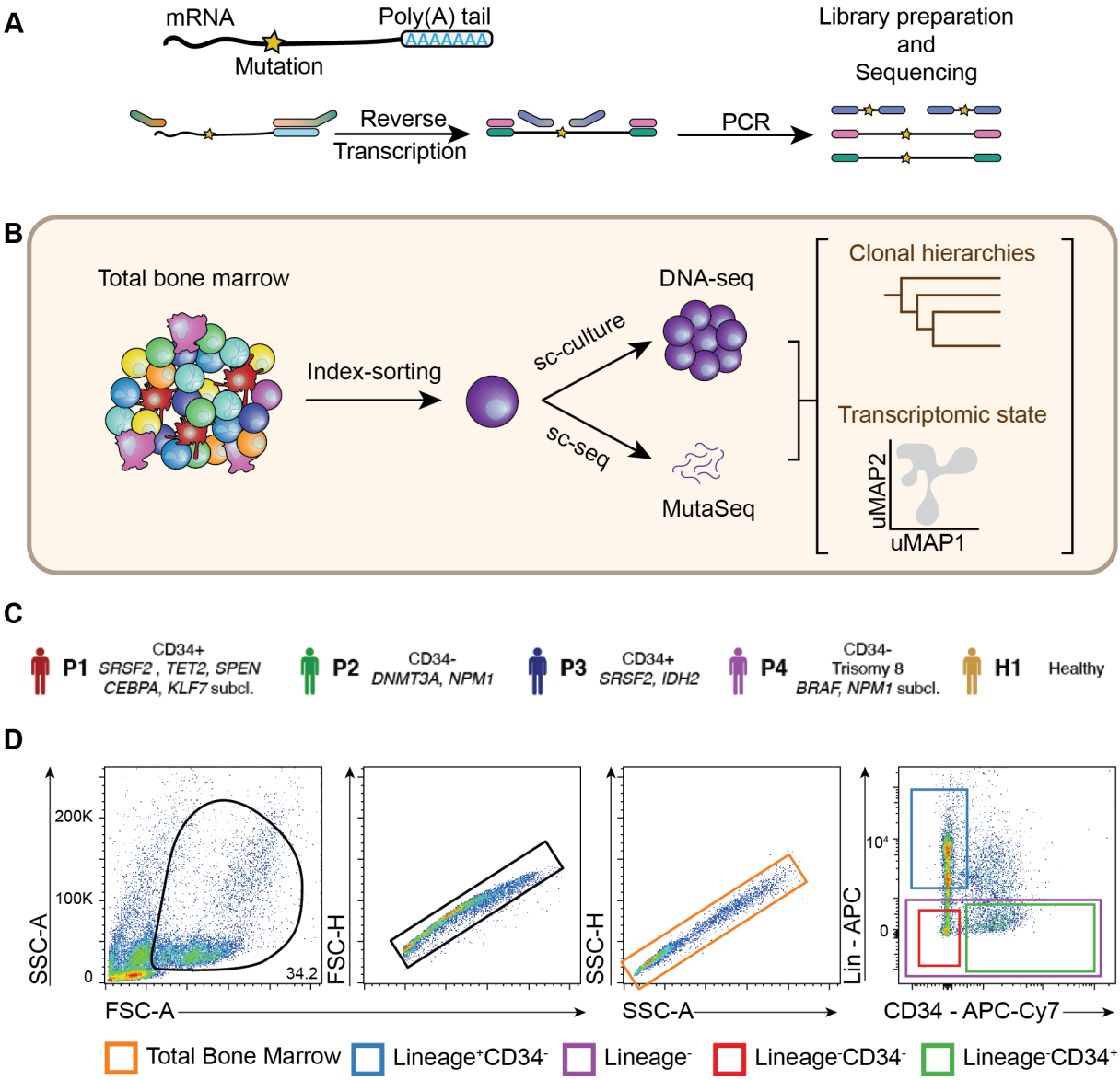

Figure 22. MutaSeq experimental design.

(**A**) Scheme of the sequencing steps following single cell mRNA purification with special importance given to modifications if compared with SMART-Seq2. On top, mutated mRNA and on the bottom, targeted mutation amplification procedure. (**B**) Scheme of the experimental approach, from bone marrow single cell suspension (left) to the final desired analyzed outcome (right). (**C**) Surface CD34 of most blasts, mutational profile and color code for the patients (P1-4) and healthy donor (H1) that underwent MutaSeq analysis. (**D**) Scheme for P1 of the different single cells sorted in each sample for further analysis.

Simultaneous mapping of mitochondrial and genomic mutations permits high-confidence tracking of leukemic, pre-leukemic and healthy clones

Tracking mutations transcribed to mRNA in addition to mitochondrial genetic variations allowed us to assign unique genetic signatures to each single cell of P1 and P2 (Figure 23A and B). Subsequently, each signature was clustered by similarities to others, thereby, reconstructing clonal hierarchies. In addition to unveiling clonal origin, knowing the mutational history for each single cell, as well as the genotype of the AML, allowed us to classify all cells as healthy, preleukemic or leukemic. Therefore, for each patient, clonal identities underlying healthy and pre-leukemic hematopoiesis, but also AML were reconstructed.

To validate the clonality attributed by MutaSeq, single cells of P1 were cultured and DNA was extracted from the derived colonies. DNA sequencing of these single cell-derived colonies confirmed all leukemic and pre-leukemic clones discovered by MutaSeq (Figure 23C). Altogether, this strategy allowed us to find somatic mutations and mitochondrial genetic variations, reconstruct clonal hierarchies and qualify each cell as healthy, pre-/leukemic from single cell RNA sequencing data in AML (Figure 23D and E).

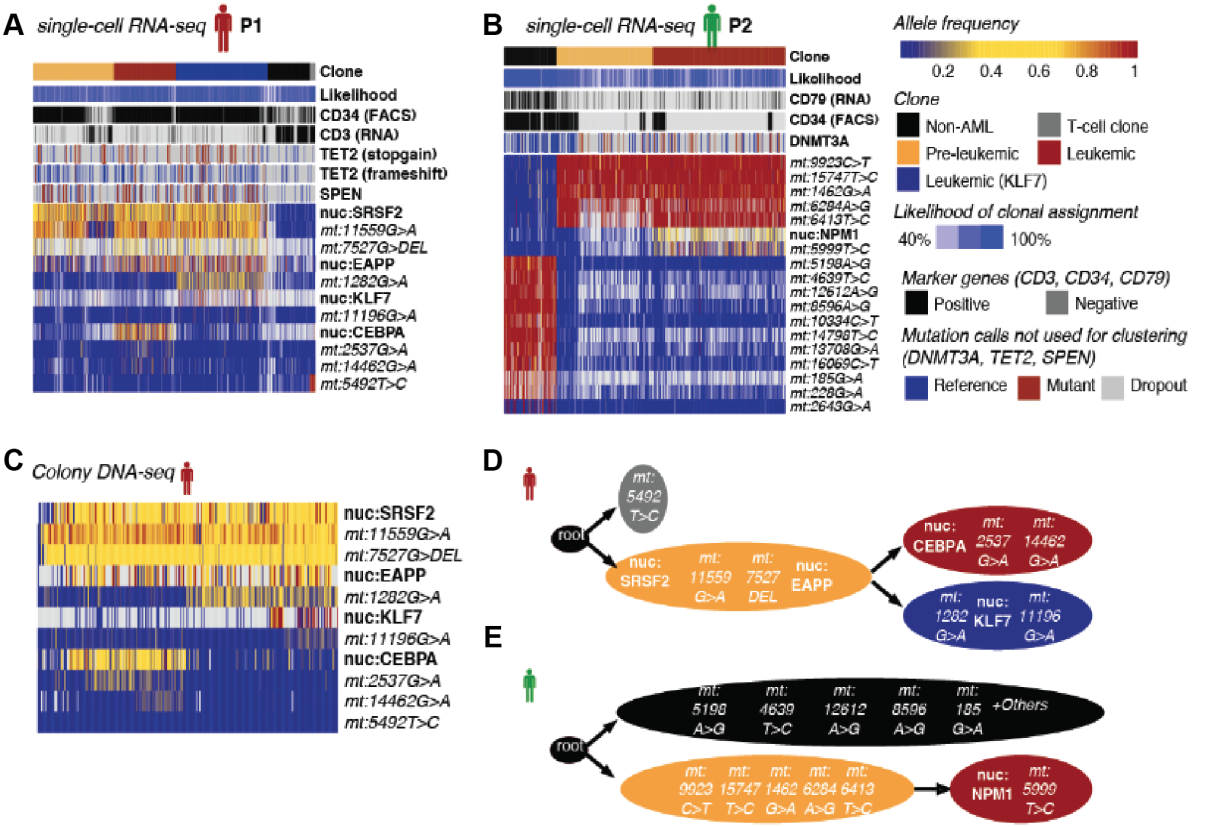

Figure 23. Clonal hierarchy reconstitution using genetic and mitochondrial variations.
(**A and B**) Heatmap depicting variant allele frequencies (color coded, see right of the figure) observed in scRNA-seq data of *n=1430* cells from P1 (**A**) and *n=1066* cells from P2 (**B**). Grey indicates missing values. Cells and mutations are arranged according to the clustering result obtained by PhISCS (Malikic *et al.*, 2019) as described in the Methods, section Analysis of mitochondrial mutations and reconstruction of clonal hierarchies. Calculation of the likelihood is described in the same section. Mutations with low coverage (in *DNMT3A*, *TET2*, and *SPEN*) were not included in the clustering and are depicted in the heatmaps as metadata. For reproducing the computations, see the vignettes accompanying the mitoClone package. For mutations, nuc is nuclear genome; mt is mitochondrial genome. (**C**) Heatmap depicting variant allele frequencies observed in targeted DNA-seq data from *n=288* single-cell derived colonies from P1. (**D and E**) PhISCS (Malikic *et al.*, 2019) was run on the mutational data from P1 (**D**) to reconstruct an 855 clonal hierarchy and P2 (**E**), see Methods section "Analysis of mitochondrial mutations and reconstruction of clonal hierarchies".

MutaSeq allows to explore molecular consequences associated with malignant transformation

Based on their transcriptomes, all malignant and healthy sequenced cells clustered separately as immature progenitors, T/NK cells or leukemic blasts of different nature and differentiation state (Figure 24A). All sequenced samples contained blasts with very diverse phenotype, based on the subset of disease (Figure 24B). In addition, not only healthy mature cells could also be found, but also variable numbers of HSPCs.

Combining the transcriptomic classification of cell types (Figure 24A) with the clonal information of each cell (see Figure 23), molecular consequences associated to each mutational step could be explored. For instance, by comparing immature $CD34^+$ blasts to healthy HSPCs in P1, several MHC-II genes were found to be enriched in healthy HSPCs (Figure 24C). Moreover, transcription factors known to trigger cell proliferation, such as *EGR1*, *FOS*, *FOSB*, *JUN* or *JUNB*, were enriched in the leukemic blasts. These findings are in line with AML having a greater proliferative advantage when compared to healthy hematopoiesis.

Furthermore, in the complex clonal structure of P2 permitted comparisons between healthy, pre-leukemic and leukemic HSPCs (Figure 24D and E). Interestingly, and in line with other studies, leukemic HSPCs showed upregulation of *HOXB3* and *CD96* (Hosen *et al.*, 2007). On the other hand, pre-leukemic cells upregulated *MLLT3* if compared with their healthy and malignant counterparts. Lastly, healthy HSPCs displayed increased MHC-I genes and decreased FOS expression. These data open the possibility of further exploring candidate therapeutic options to target LSCs (e.g. *CD96*) , pre-LSCs (e.g. *MLLT3*), or both (e.g. *FOS*), while leaving HSPCs unaffected.

Altogether, MutaSeq allowed us to confidently assign clonal origins to single cells of four different AML patients. At the same time, transcriptomic data allowed to distinguish all studied single cells molecularly and thus, to understand the cellular compartment to which they belonged. This dual characterization, genetic and phenotypic, permitted us to classify HSPCs as healthy or pre/leukemic. Importantly, this enabled to explore transcriptomic differences derived from mutational steps from healthy to malignant HSCs.

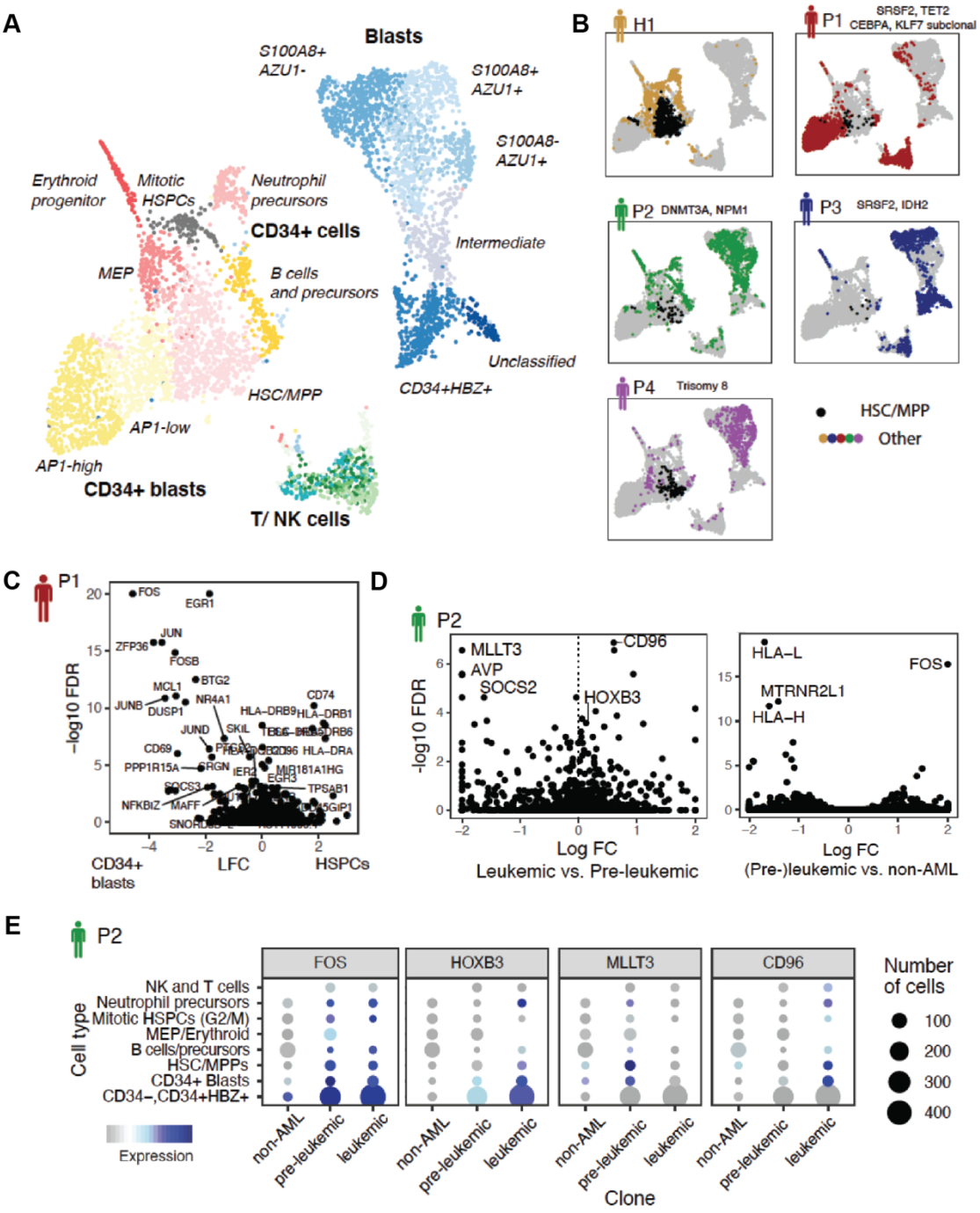

Figure 24. Molecular consequences of pre- and malignant transformations.

(**A**) Data from the five individuals (Figure 22C) were integrated using Scanorama (Hie, Bryson and Berger, 2019) and visualized in two dimensions using uMAP (Becht *et al.*, 2019). Clusters are color-coded, *n* = 5228 cells. (**B**) Cells corresponding to each of the samples included. Cells in black are grouped in the HSC/MPP cluster according to their transcriptomic profile. (**C**) Volcano plot of the log10 expression change in *n* = 569 *AP1*-high CD34+ blasts vs. *n* = 667 HSC/MPP-like cells, plotted against corrected p-values from MAST, using a model that accounts for differences in library quality and patient identity / batch (see Methods, section "Single-cell gene expression data analysis" for detail). *AP1*-high CD34+ blasts were chosen for this comparison since *AP1*-low blasts, in terms of all marker genes, appear to constitute an intermediate state between Healthy-like HSC/MPPs and *AP1*-high blasts. (**D**) Volcano plots of the log10 expression change in pre-leukemic (*n* = 55) vs. leukemic (*n* = 50) $CD34^+$ cells of P2 (left), or pre-leukemic (*n* = 105) vs. non-leukemic (*n* = 41) $CD34^+$ cells of P2 (right),

plotted against p-values from MAST, using a model that accounts for differences in cell type and library quality (see Methods for detail). Only the following $CD34^+$ cell types from Figure 24A were included in the test: HSC/MPP, $CD34^+$ Blasts (both subsets), Neutrophil precursors, and MEPs (megakaryocyte erythroid progenitors). (**E**) Dot plot comparing the expression of relevant genes across non-leukemic, pre-leukemic and leukemic cells in the different cell types. Symbol size scales with the number of cells.

DISCUSSION

Healthy and malignant hematopoietic stem cells are immunoregulatory antigen presenting cells

HSCs, more than "just stem cells"

"Hematopoietic stem cells are responsible for lifelong production of all different hematopoietic cells" is a standardized sentence in scientific literature in the fields of hematopoiesis and stem cell biology (Eaves, 2015; Liggett and Sankaran, 2020). Since hematopoiesis is of such vital importance in the organism, it is plausible that these cells are physically and biologically protected. Indeed, they are located inside the bone marrow, isolated by the most solid barrier in the organism, bones. In addition, they are considered to be surrounded by a protective and supportive microenvironment that would defend them and free them from threats (Pinho and Frenette, 2019).

Nonetheless, considering HSCs isolated from local and systemic pressure is a naïve point of view. In fact, they are known responders to stress cytokines and other inflammatory and infectious stimuli (King and Goodell, 2011; Pietras, 2017; Chavakis, Mitroulis and Hajishengallis, 2019). The so-called stress hematopoiesis involves the modulation of the HSC cellular output to match and deal with the potential threat. Recently, the concept of stress hematopoiesis has further evolved with the discovery of HSC memory for these stress signals (Chavakis, Mitroulis and Hajishengallis, 2019; Netea *et al.*, 2020). Trained immunity places HSCs as more efficient responders upon secondary stimulations through diverse epigenetic modifications. This ability to specifically and efficiently respond to external cues and reinforce the immune system has added a role as "integrative hubs for hematopoietic and immune fine-tuning" (Chavakis, Mitroulis and Hajishengallis, 2019).

Even though stress hematopoiesis and trained immunity only slightly amend the functional definition of HSC, they challenge the to-date isolated and naïve attributed roles. In other words, HSC function remains unaltered as offspring producer. Along these lines, the data presented in this thesis challenge the idea of HSCs being mere integration hubs and offspring producers. Here, we demonstrate that HSCs can actively present antigens and activate $CD4^+$ helper T cells. For the first time, this provides evidence for HSCs being actively involved in adaptive immunity.

Not only this alternative function as antigen presenting cells provides novelty to the classical view of HSC functionality. As previously discussed, stress hematopoiesis and trained immunity placed HSCs as integrative hubs for external cues. Moreover, the view of how HSCs were interacting with the cellular components of the niche also placed them as passive receivers of instructive cytokines (Pinho and Frenette, 2019) (Figure 25A). In this study, we show that HSCs are able to not only activate helper T cells, but also to instruct them with a unique and stable

phenotype. Therefore, HSCs can be considered instructive cells for other niche component and thus, more than mere responders, but active modulators of their microenvironment.

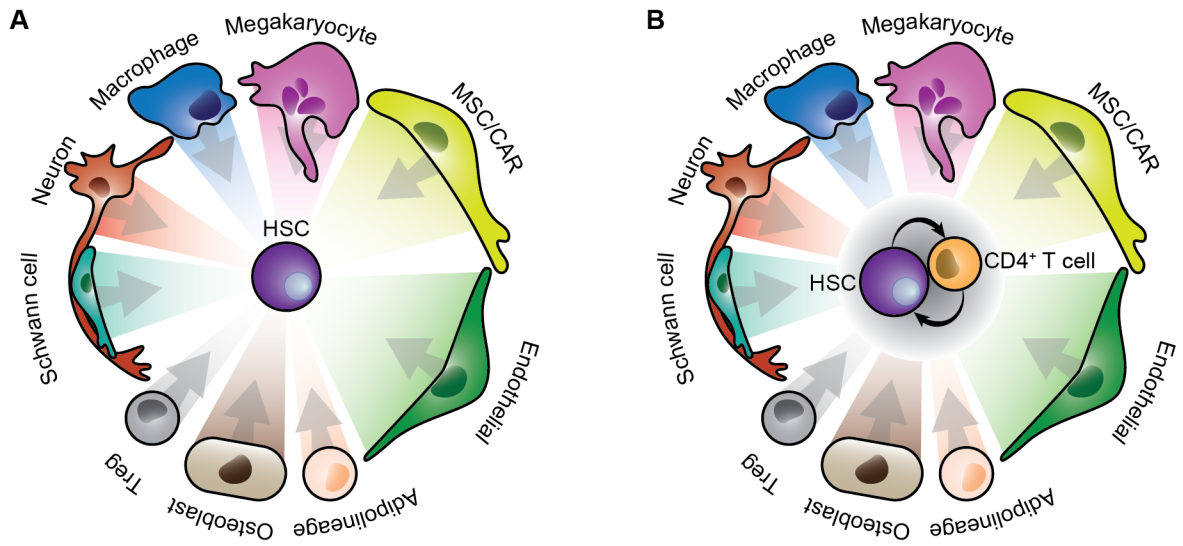

Figure 25. Interactions between niche cell types and HSCs.
(**A**) Classical view of functional/instructive interactions between HSCs and the different cellular components of its niche. (**B**) Additional interactions discovered in this thesis, highlighted in grey. Adapted from (Pinho and Frenette, 2019). Arrows go from the signal submitter to the receiver cell type.

HSCs as active modulators of their immune microenvironment

Strong adaptive immune responses occur in the bone marrow (Feuerer *et al.*, 2003; Siracusa *et al.*, 2017), Nonetheless the HSC niche is considered an immune privileged site (Fujisaki *et al.*, 2011; Hirata *et al.*, 2018). This means that immune reactions are dampened. However, only co-localization of Tregs with HSCs has been provided as evidence for this hypothesis.

In this thesis, we showed that upon antigen-specific activation by HSCs, T cells (T_{HSCs}) adapted a stable Tr1-like phenotype. T_{HSCs} suppressed other immune cells in an antigen- and IL-10 dependent manner. They also instructed other cells, such as macrophages towards an immunoregulatory phenotype. Lastly, the differentiated progeny from the antigen presenting HSCs also upregulated immunosuppressive molecules. Thus, this bidirectional interaction triggers a cascade of tolerogenic events not limited to HSCs and T_{HSCs}. We here provide compelling evidence to confirm that not only the HSC niche is an immune privileged site, but that the HSCs contribute as an active and central part in establishing this immune-regulatory environment.

Supporting this hypothesis, upon allotransplantation, immune tolerance is crucial for avoiding graft versus host disease (GVHD) (Gupta *et al.*, 2019). In fact, enhanced survival is seen when tolerogenic APCs are co-transplanted (Sato *et al.*, 2003). Notably, and of most relevance, the ultimate protection against GVHD is linked to the appearance of Tr1-like cells (Zhang *et al.*, 2018). Importantly, these cells show a high degree of similarity with T_{HSCs}. In line, in a model of experimental autoimmune encephalomyelitis (EAE), an autoimmune pre-clinical model for multiple sclerosis, HSPC injection ameliorated the disease in a T cell-dependent manner (Korniotis *et al.*, 2020). Altogether, data from us and others merge into the idea that HSCs actively modulate T cells, in order to induce an immune privileged site in their surroundings.

Mechanistic insights into the bidirectional interaction of HSCs and T cells in health and disease

Remaining open questions that might affect the understanding of the HSC-T cell interactions are the instructive mechanisms behind the HSC cell cycle induction followed by differentiation and T_{HSC} polarization. The former, might be mediated by a combination of T_{HSC}-secreted cytokines known to drive HSC activation and myelopoiesis, such as IFNs or TNF (Essers *et al.*, 2009; Matatall *et al.*, 2014; Hérault *et al.*, 2017). Additionally, the tolerogenic molecule upregulation on HSC-derived cells, could be a consequence of the T_{HSCs} immunosuppressive phenotype.

The tolerogenic polarization of $CD4^+$ T cells upon antigen-specific interactions with HSCs, could be mediated by different mechanisms. A wide variety of candidates arise from both, unperturbed, but antigen presenting HSCs. Freshly isolated stem cells express limited amounts of co-stimulatory molecules, which could lead to a less activatory T cell phenotype (Chen and Flies, 2013). In addition, the high presence of PD-L1 on the cell surface and its further upregulation upon inflammation could be an additional factor to drive the observed tolerogenic phenotype (Francisco *et al.*, 2009). Notably, the highest expressed T cell instructive cytokine genes in HSCs are *Ebi3* and *Il12*, that, together, form the heterodimeric IL-35, a potent instructor of immunosuppressive helper T cells (Collison *et al.*, 2007, 2010). Additionally, upon T cell activation, T_{HSCs} maintain high PD-L1 expression levels and upregulate *Il27*, a key cytokine in regulating the co-inhibitory gene module (Hirahara *et al.*, 2012; Chihara *et al.*, 2018). While all these polarizing mechanisms might play a role, it is likely that a temporal combination of them drives the unique and stable T_{HSC} phenotype.

Antigen-specific exhaustion of HSCs - A sacrifice for the greater good

Antigen-specific HSC-T cell interactions trigger HSC proliferation and differentiation. While transient presentation of the antigen results in reduced stem cell capacity, chronic antigen presentation leads to absolute exhaustion of the antigen presenting HSCs. In contrast, non-antigen expressing HSCs in the bone marrow remain largely unaffected (Figure 26). This observation, opens up the idea that under homeostasis, HSC-mediated antigen presentation might serve as a peripheral tolerance mechanism. This would be in line with the concept of HSCs in the need of protection against excessive replicative stress, associated to inflammation (King and Goodell, 2011; Walter *et al.*, 2015; Chavakis, Mitroulis and Hajishengallis, 2019). In this scenario, the antigen presenting HSC would lose its stemness but the immune tolerance mechanisms triggered in parallel, would protect other HSCs against excessive replicative stress (Figure 26).

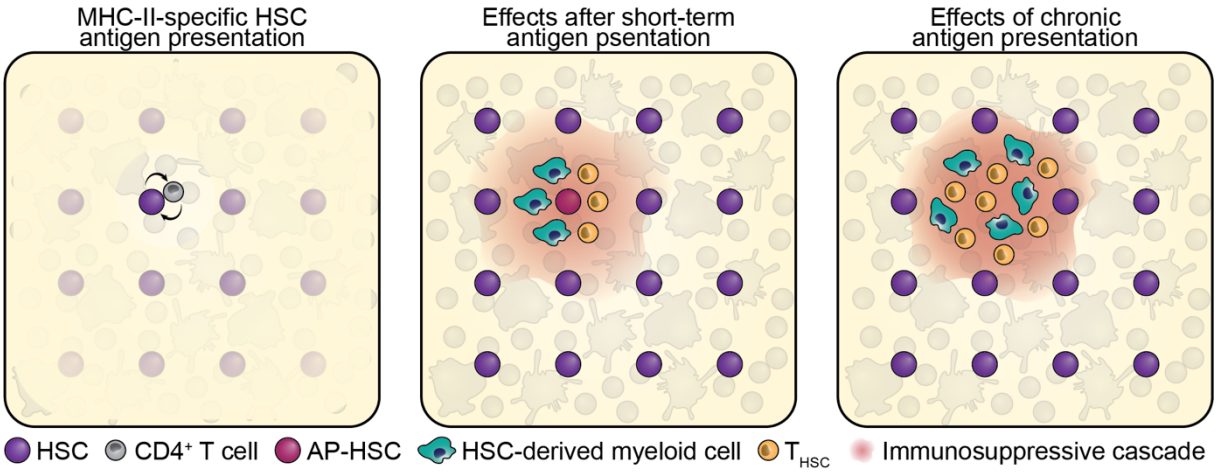

Figure 26. Consequences of short- and long-term HSC antigen presentation.
(Left) HSC-mediated antigen presentation within the bone marrow. Highlights of the functional consequences suffered by antigen presenting (AP) and non-presenting HSCs, activated T cells and the immune microenvironment after sporadic (middle) or chronic antigen presentation (right).

Aplastic anemia, less of an idiopathic disease?

Aplastic anemia (AA) is a heterogeneous group of disorders with different origin and common symptoms (Young, 2018). Patients suffering from AA progressively lose hematopoietic cellularity until they reach an "empty" bone marrow. Importantly, this is associated to a specific decrease in HSC numbers (Maciejewski *et al.*, 1996). AA can originate from a direct physical/chemical damage, as a secondary effect of other diseases or with an idiopathic origin (Young, 2018). Interestingly, the last subset of unknown origin is characterized by an autoimmune-like phenotype of the T cell compartment in the bone marrow. This is characterized by an increased number of effector and reduced number immunosuppressive T cells (Solomou, Keyvanfar and Young, 2006; Kordasti *et al.*, 2016). In fact, the most frequently used therapeutic strategies against this disease are immunosuppressive treatments (Scheinberg and Young, 2012).

While an immune attack against HSCs seems to cause idiopathic AA, little is known about the underlying cellular and molecular causes. Notably, polymorphisms in different MHC-I and -II genes are associated with idiopathic AA development and response to immunosuppressive treatment (Nakao *et al.*, 1994; Nimer *et al.*, 1994; Sauntharajah *et al.*, 2002; Rehman *et al.*, 2009; Dhaliwal *et al.*, 2011; Liu *et al.*, 2016; Deng *et al.*, 2018). Moreover, the deletion of MHC-I and -II alleles by loss of heterozygosity (LOH) was also associated to its appearance (Katagiri *et al.*, 2011). Importantly, different MHC-II alleles can alter the way in which APCs activate T cells and impact on their phenotype (Gebe *et al.*, 2001).Thus, MHC-II seem to play a crucial role in idiopathic AA onset.

Observations made in this thesis provide new angles and hypotheses that might help understanding the underlying cause of idiopathic AA. On the one hand, a decreased ability of HSCs to generate immune tolerance, either by decreased ability to present antigens or to induce the T_{HSC} phenotype, could result in the hyperactivated T cell phenotype observed in idiopathic AA. This would lead to high replicative stress on HSCs and adaptive immune attack against either self or foreign antigens presented by HSCs. In line with this, self-peptides are highly presented in AA, while several infections can promote AA development (Katagiri *et al.*, 2011; Nowak *et al.*, 2013; Young, 2018). On the other hand, an altered MHC-TCR binding, associated to specific polymorphisms, could enhance and reinforce HSC-T cell interactions. As previously observed, this might lead to a T cell-mediated HSC exhaustion. Even though no information in this thesis unequivocally points at any of these hypotheses, our findings provide missing information on the bidirectional immune interactions of T cells and HSCs that might help explaining the pathophysiological basis of idiopathic aplastic anemia.

A double-edged sword against AML

MHC-II expression in AML resembles the expression patterns of the healthy hematopoietic system. Accordingly AMLs with an immature, HSC-like phenotype, express high levels of MHC-II. On the contrary, AMLs derived from committed myeloid progenitors lack MHC-II expression, as shown by us and others (Griffin *et al.*, 1983). In addition and in line with the healthy scenario, HSC-derived AMLs chronically presenting an antigen are subject to antigen- and $CD4^+$ T cell-specific clearance. Together, these data point towards an immune surveillance mechanism protecting the hematopoietic system against AML onset. This "tumor suppressing" mechanism would be dependent on MHC-II expression and neoantigen formation.

While the existence of MHC-I-presented neoantigens in AML is well-known, their MHC-II-presented counterparts are partially unexplored (Berlin *et al.*, 2015; Roerden, Nelde and Walz, 2019). However, there is major evidence on the importance of MHC-II-mediated neoantigen presentation to inhibit tumor growth and improve survival (Alspach *et al.*, 2019). In fact, in glioblastoma, a nervous system malignancy, the *IDH1-R132H* mutation has been shown to generate an MHC-II-presented neoantigen with targetable therapeutic effect (Schumacher *et al.*, 2014; Platten *et al.*, 2021). Interestingly, some AML subtypes and glioblastoma have this immunogenic *IDH1* mutation in common (Dang, Jin and Su, 2010). Of note, other *IDH1* mutations that do not generate immunogenic neoantigens are also present in AML (Mardis *et al.*, 2009).

When analyzing co-occurring genetic alterations with the different *IDH1* mutations, *IDH1-R132H* AMLs were usually found to also be $NPM1^{mut}$ (Falini *et al.*, 2019). This particular mutation was not found in *RUNX1*- or *ASLX1*-mutated AMLs. Strikingly, all other *IDH1* mutations, that do not generate neoantigens could be found in these AMLs. As previously mentioned, *NPM1* mutations can induce AML from MHC-II-expressing HSCs, but also from MHC-II-negative committed progenitors (de la Guardia *et al.*, 2020; Uckelmann *et al.*, 2020). On the contrary, *RUNX1* or *ASLX1* mutations are associated with stem-like AMLs (Gerritsen *et al.*, 2019; Bill *et al.*, 2020). Therefore, while mutations that result in the generation of immunogenic neoantigens are present on mature-like AMLs, they are frequently absent in stem-like AMLs.

In addition, recent studies have shown the importance of MHC-II downregulation for AML relapse after allogenic transplantation (Christopher *et al.*, 2018; Toffalori *et al.*, 2019). This becomes more important when considering that one of the desired effects of allogenic transplantation is the graft-versus-leukemia (GVL) effect (Sweeney and Vyas, 2019). This is the T cell mediated-attack of chemo/radiotherapy-surviving AML cells. In fact, it has been shown that the MHC-II mismatch can activate the graft $CD4^+$ T cells in an MHC-II-dependent manner, similarly to an antigen-dependent activation against the leukemic cells (Rutten *et al.*, 2013; Klobuch *et al.*, 2020). Therefore, relapse and disease onset have in common that they can be restrained by MHC-II-mediated GVL or antigen-specific $CD4^+$ T cell activation, respectively.

On the other hand, high MHC-II expression is also associated with an adverse prognosis in the AML cohorts tested in this thesis. When allowing full-grown HSC-derived AML cells to interact with $CD4^+$ T cells in mice, the survival dropped dramatically. Interestingly, immunosuppressive T cell polarization was observed in these mice, similar to our observations in the healthy system. This could be explained by a direct hijack of a stem cell mechanism by tumors in order to fulfill one of the hallmarks of cancer, avoiding the immune system surveillance (Hanahan and Weinberg, 2011; Yamashita *et al.*, 2020). The consequence would be the suppression of any adaptive or innate immune response and thus, the lack of any growth restrain for AML, that would potentially lead to a worse prognosis.

However, in the case of our mouse experimental setup (Figure 21J) we cannot exclude an excessive T cell reaction due to an overwhelming antigen stimulation as cause of death. If this held true, a massive immune response might also lead to a sepsis-like response, that could be responsible for the observed premature decease. In addition, MHC-II expression could be not necessarily directly linked to a worse prognosis, but rather be a consequence of a more stem-like and intrinsically aggressive AML state (Papaemmanuil *et al.*, 2016).

Of note, a yet unexplored but of potential relevance field under this newly generated knowledge is checkpoint inhibition. Since healthy and leukemic HSCs promote immunosuppression, checkpoint (and tolerance) inhibition efficacy might be affected by this capacity of AMLs . While immunotherapy has proved an extraordinary asset to fight different tumor entities, its effect on AML has remained sparse (Liao *et al.*, 2019; Barrett, 2020; Vago and Gojo, 2020). The immune properties of the interaction described in this thesis, suggest that further *in silico* analyses should be performed in order to understand whether MHC-II expression is related in any way to differences in the outcome of checkpoint inhibition. Importantly, this work opens up new functional immune characteristics of AML and thus, plausible reasons for a diverse immunotherapy outcome. Accordingly, in patients where AML hijacks the HSC tolerance induction might have a greater benefit from these immunosuppressive therapies.

Altogether, while the thoroughly characterized MHC-II-specific bidirectional interaction would serve as a first line of defense against leukemia onset and relapse, it might also be hijacked by full-grown AML as a driver of an immune-privileged niche, in order to avoid its immune clearance. Both mechanisms, would point towards a shared functionality between healthy and leukemic HSCs (Figure 26).

Identification of leukemic and pre-leukemic stem cells by clonal tracking from single-cell transcriptomics

Healthy and pre/leukemic HSCs share many phenotypic and functional characteristics. A clear example would be the previously described ability to interact and modulate the adaptive immune system. In fact, distinguishing them from each other and obtaining valuable functional information to compare them has proved to be a major challenge (Essers and Trumpp, 2010; Pollyea and Jordan, 2017). An improved understanding of leukemic stem cells is crucial to design new therapeutic strategies to target malignant HSCs in order to avoid relapse (Liran I. Shlush *et al.*, 2017)

In the past, other studies have tried to distinguish HSCs and LSCs by single cell mutational tracking from RNA-Seq data (Nam *et al.*, 2019; Petti *et al.*, 2019; van Galen *et al.*, 2019). However, these studies fell short in the confidence by which they could qualify a big proportion of the cells.

To overcome this hurdle, we have made use of mitochondrial variant calling as an additional layer in addition to the RNA-Seq-derived mutational profile (Ludwig *et al.*, 2019; Xu *et al.*, 2019). Combining both, genomic and mitochondrial profiles, has shown to be an extraordinary enhancement for clonality attribution and *de novo* discovery. Furthermore, transcriptomic data allowed us to classify different cells based on their molecular state and cell type. Importantly, when combining the two of them, mechanistic differences between different clones could be further investigated.

While the patient numbers investigated in this study are restricted and patients with a diverse set of mutations have been profiled, this study reveals a new avenue for AML study and understanding. Generating similar data across larger patient cohorts, taking into account disease subtypes or common genetic alterations, would create an extremely powerful dataset. It would also be the first systematic comparison of healthy and pre/malignant HSCs in AML as a whole or in different subtypes. Since conventional therapies fail in eradicating LSCs, the addition of LSC-specific targets would potentially avoid, or at least reduce, relapse rates.

CONCLUSIONS

Healthy and malignant hematopoietic stem cells are immunoregulatory antigen presenting cells

A brief summary of the findings from this part of the thesis is:

- HSCs functionally express MHC-II.
- HSCs activate $CD4^+$ helper T cells in an antigen-dependent manner.
- HSC-activated T cells are tolerogenic, mainly through IL-10 secretion.
- Upon effective antigen presentation, HSCs proliferate and differentiate into MDSC-like cells.
- Continuous antigen presentation ultimately drive HSCs to exhaust.
- Stem-like AMLs express MHC-II and have an adverse prognosis.
- HSC-derived AMLs activate $CD4^+$ helper T cells in a tolerogenic manner.
- The HSC-T cell interaction protects the organism against leukemia onset

In summary, in this thesis we have demonstrated that HSCs are not only passive receivers of immune signals, but active modulators of their microenvironment (Figure 27). A yet unknown HSC function directly controlling adaptive immunity and affecting HSC biology, microenvironment and hematopoiesis has been uncovered. In addition, this mechanism is of major importance against leukemia onset, but might also be exploited by AML in order to avoid immune surveillance. We expect these findings to be of high relevance in future stem cell research and to further broaden our view on how to better target AML.

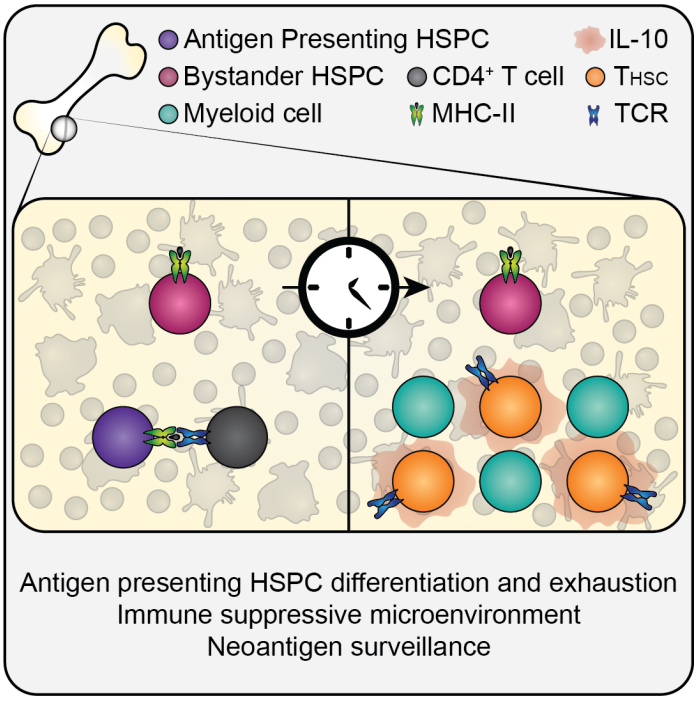

Figure 27. Graphical abstract.
Summary of the findings in this part of the thesis.

Identification of leukemic and pre-leukemic stem cells by clonal tracking from single-cell transcriptomics

A short summary of the findings from this part of the thesis is:

- MutaSeq combines single cell transcriptomics, mutational profiling and mitochondrial variant calling.
- MutaSeq is an effective way to recapitulate clonal architecture in AML.
- Healthy, preleukemic and leukemic HSCs can be distinguished based on clonal origin.

In brief, in this thesis, I have contributed to the development a novel single cell technology called MutaSeq. MutaSeq can at the same unveil the clonal cellular origin and the molecular profile of single cells in AML. MutaSeq allows to confidently unravel the molecular consequences arising from mutational steps, from health to disease. Thus, our approach opens new avenues for the identification of novel targets specific for pre/malignant cells, while sparing healthy HSCs.

MATERIALS

Mouse antibodies		
Reagent	Source	Identifier
Anti-mouse B220 FITC	ThermoFisher	Clone:RA3-6B2
Anti-mouse B220 AF700	ThermoFisher	Clone:RA3-6B2
Anti-mouse B220 APC-Cy7	ThermoFisher	Clone:RA3-6B2
Anti-mouse CD105 BV421	ThermoFisher	Clone:MJ7/18
Anti-mouse CD117 BV711	BioLegend	Clone:2B8
Anti-mouse CD117 PE	ThermoFisher	Clone:2B8
Anti-mouse CD117 PE-Cy5	BioLegend	Clone:2B8
Anti-mouse CD11b FITC	ThermoFisher	Clone:M1/70
Anti-mouse CD11b AF700	ThermoFisher	Clone:M1/70
Anti-mouse CD127 PE	BioLegend	Clone:A7R34
Anti-mouse CD150 PE-Cy5	ThermoFisher	Clone:TC15-12F12.2
Anti-mouse CD16/32 AF700	ThermoFisher	Clone:93
Anti-mouse CD16/32 APC	ThermoFisher	Clone:93
Anti-mouse CD19 APC	BioLegend	Clone:6D5
Anti-mouse CD206 FITC	BioLegend	Clone:C068C2
Anti-mouse CD25 BV785	BioLegend	Clone:PC61
Anti-mouse CD25 APC	BioLegend	Clone:PC61
Anti-mouse CD274 (PD-L1) BV711	BioLegend	Clone:10F.9G2
Anti-mouse CD274 (PD-L1) PE	BioLegend	Clone:10F.9G2
Anti-mouse CD279 (PD-1) APC	ThermoFisher	Clone:J43
Anti-mouse CD34 PE	BD	Clone:RAM34
Anti-mouse CD3e FITC	ThermoFisher	Clone:17A2
Anti-mouse CD3e	BioXCell	Clone:145-2C11
Anti-mouse CD4 BUV805	BD	Clone:GK1.5
Anti-mouse CD4 FITC	ThermoFisher	Clone:GK1.5
Anti-mouse CD4 AF700	ThermoFisher	Clone:GK1.5
Anti-mouse CD4 APC-Cy7	BioLegend	Clone:GK1.5
Anti-mouse CD41 APC	BioLegend	Clone:MWReg30
Anti-mouse CD41 FITC	BD	Clone:MWReg30
Anti-mouse CD44 FITC	ThermoFisher	Clone:IM7
Anti-mouse CD45 Pacific Blue	BioLegend	Clone:30F11
Anti-mouse CD45.1 BUV395	BD	Clone:A20

Anti-mouse CD45.1 BV606	BioLegend	Clone:A20
Anti-mouse CD45.1 PE	ThermoFisher	Clone:A20
Anti-mouse CD45.1 PE-Cy5	ThermoFisher	Clone:A20
Anti-mouse CD45.2 FITC	ThermoFisher	Clone:104
Anti-mouse CD45.2 APC-Cy7	ThermoFisher	Clone:104
Anti-mouse CD48 BUV395	BD	Clone:HM48-1
Anti-mouse CD48 APC	ThermoFisher	Clone:HM48-1
Anti-mouse CD48 Pacific Blue	BioLegend	Clone:HM48-1
Anti-mouse CD69 PE-Cy5	BioLegend	Clone:H1.2F3
Anti-mouse CD8 BUV395	BD	Clone:53-6.7
Anti-mouse CD8 FITC	ThermoFisher	Clone:53-6.7
Anti-mouse CD8 AF700	ThermoFisher	Clone:53-6.7
Anti-mouse CD84 PE	BioLegend	Clone:mCD84.7
Anti-mouse CD90.1 FITC	BioLegend	Clone:OX7
Anti-mouse F4/80 BV421	ThermoFisher	Clone:BM8
Anti-mouse Gr-1 FITC	ThermoFisher	Clone:RA3-6B2
Anti-mouse Gr-1 AF700	ThermoFisher	Clone:RA3-6B2
Anti-mouse Ki67 PE-Cy7	BD	Clone:B56
Anti-mouse Lag3 APC-Cy7	ThermoFisher	Clone:C9B7W
Anti-mouse MHC-II (I-A/I-E)	BioXCell	Clone:M5/114.15.2.
Anti-mouse MHC-II (I-A/I-E) BV785	BioLegend	Clone:M5/114.15.2.
Anti-mouse MHC-II (I-A/I-E) PE	BioLegend	Clone:M5/114.15.2.
Anti-mouse IL-10 PE	BioLegend	Clone:JES5-16E3
Anti-mouse Sca-1 APC-Cy7	BD	Clone:D7
Anti-mouse SiglecF Pacific Blue	BD	Clone:E50-Z440
Anti-mouse SiglecH PE	ThermoFisher	Clone:eBio440c
Anti-mouse TCR-b PE-Cy7	Biolegend	Clone:H57-597
Anti-mouse Ter119 FITC	ThermoFisher	Clone:Ter-119
Anti-mouse Ter119 AF700	ThermoFisher	Clone:Ter-119
Anti-mouse Tim3 APC	BioLegend	Clone:5D12
Anti-mouse I-Ab-Ea FITC	ThermoFisher	Clone:Y-Ae
Anti-mouse I-Ab-Ea Biotin	ThermoFisher	Clone:Y-Ae
Human antibodies		
Reagent	Source	Identifier
Anti-human CD3 BUV395	BD	Clone:UCHT1
Anti-human CD4 APC	BD	Clone:561844
Anti-human CD4 BUV805	ThermoFisher	Clone:SK3

Anti-human CD8 APC	BD	Clone:RPA-T8
Anti-human CD11b APC	BD	Clone:ICRF44
Anti-human CD11c BV605	BD	Clone:563929
Anti-human CD11c Pe-Cy7	BioLegend	Clone:3.9
Anti-human CD19 APC	ThermoFisher	Clone:HIB19
Anti-human CD19 APC-Cy7	BioLegend	Clone:H1B19
Anti-human CD19 BV786	BioLegend	Clone:H1B19
Anti-human CD20 APC	BD	Clone:2H7
Anti-human CD25 PE-Cy7	BioLegend	Clone:BC96
Anti-human CD33 BV421	BioLegend	Clone:WM53
Anti-human CD34 APC-Cy7	ThermoFisher	Clone:H1B19
Anti-human CD38 A700	ThermoFisher	Clone:HIT2
Anti-human CD41a APC	BioLegend	Clone:HIP8
Anti-human CD45 APC	BioLegend	Clone:HI30
Anti-human CD45 PE	ThermoFisher	Clone:HI30
Anti-human CD45RA FITC	BioLegend	Clone:HI100
Anti-human CD45RO FITC	BioLegend	Clone:UCHL1
Anti-human CD49b FITC	BioLegend	Clone:PIE6-C5
Anti-human CD49f PE-Cy7	ThermoFisher	Clone:GoH3
Anti-human CD56 APC	BD	Clone:B159
Anti-human CD56 Alexa Fluor 488	BD	Clone:B159
Anti-human CD56 BV711	BioLegend	Clone:318335
Anti-human CD69 BUV395	BD	Clone:FN50
Anti-human CD90 PE-Cy5	BD	Clone:5E10
Anti-human HLA-DR PE	ThermoFisher	Clone:LN3
Anti-human CD154 PE-Cy5	BioLegend	Clone:24-31
Anti-human CD197 (CCR7) Pacific Blue	BioLegend	Clone:G043H7
Anti-human CD223 (LAG3) BV711	BioLegend	Clone:11C3C65
Anti-human CD235 APC	BD	Clone:HIR2
Anti-human CD274 (PD-L1) BV785	BioLegend	Clone:29E.2A3
Anti-human CD279 (PD1) APC	BioLegend	Clone:EH12.2H7
Anti-human CD366 (TIM3) BV605	BioLegend	Clone:F38-2f2
Bacterial and virus strains		
Virus	Used in	
MCMV-Δm157 (MCMV)	Hirche *et al.*, 2017	

Biological samples	
Sample	From
Human Healthy Bone Marrow Aspirates	Heidelberg University Hospital
Human Peripheral Blood	University Hospital Mannheim
Human AML Bone Marrow Aspirates	AML-SG and SAL biorepositories

Chemicals, peptides and recombinant proteins		
Reagent	Source	Identifier
pI:C	Invivogen	Cat#tlrl-pic
LPS	ThermoFisher	Cat#00-4976-03
IFNα	Miltenyi	Cat#130-093-131
Ovalbumin	Invivogen	Cat#vac-stova
DQ Ovalbumin	Invitrogen	Cat#D12053
Ovalbumin 323-339 peptide	Invivogen	Cat#vac-isq
Ovalbumin 257-264 peptide	Invivogen	Cat#vac-sin
MOG peptide	Genemed Sythesis	Cat#MOG3555-P2-1
Eα peptide (52-68)	Mimotopes	Cat#68827-005
ACK Buffer	Lonza	Cat#10-548E
Sodium pyruvate	Gibco	Cat#11360039
L-Glutamine	Gibco	Cat#25030081
L-arginine	Sigma	Cat#A5006-100G
L-asparagine	Sigma	Cat#A0884-100G
Penicillin/Streptomycin	Sigma	Cat#P4458-100ml
Folic acid	Sigma	Cat#F7876-10G
MEM non-essential amino acids	ThermoFisher	Cat#11140050
MEM vitamin solution	ThermoFisher	Cat#11120052
β-mercaptoethanol	Sigma	Cat# M3148
Cell Trace Violet	ThermoFisher	Cat#C34557
Dynabeads Mouse T-Activator	ThermoFisher	Cat#11452D
CytoStim	Miltenyi	Cat#130-092-172
PepMix CEFX Ultra SuperStim MHC-II Subset Pool	JPT	Cat#PM-CEFX-3
Mouse TPO	PreproTech	Cat#315-14
Mouse SCF	PreproTech	Cat#250-03
CNBr-activated Sepharose	GE Healthcare	Cat#17-0430-01
Trifluoroacetic acid	Merck	Cat#108262

DNAseI	Roche	Cat#4716728001
2',7'-Dichlorofluorescin diacetate	Sigma	Cat#D6883-50MG
DAPI	ThermoFisher	Cat#D1306
Sunflower oil	Sigma	S5007-250ML
Tamoxifen	Sigma	T5648-1G
Human CD3 MicroBeads	Miltenyi	Cat#130-050-101
RNAsin+	Promega	N2611
Triton X-100	Sigma	9002-93-1
Smart-seq2 Oligo-dT primer	Sigma	N/A
dNTP mix	NEB	N0447S
ERCC spike-in mix	Ambion	4456740
5x SMART FS buffer	Takara	N/A
DTT	Takara	N/A
SmartScribe	Takara	639538
Smart-seq2 TSO	Exiqon	N/A
Smart-seq2 ISPCR primer	Sigma	N/A
CleanPCR beads	CleanNA	CPCR-0005
StemSpan SFEM media	Stem Cell Tech.	09650
Human SCF	Peprotech	300-07
Human Flt3-L	Peprotech	300-19
Human TPO	Peprotech	300-18
Human IL-3	Peprotech	200-03
Human IL-6	Peprotech	200-06
Human G-CSF	Peprotech	300-23
Human EPO	Peprotech	100-64
Human M-CSF	Peprotech	300-25
Human GM-CSF	Peprotech	300-03
Human IL-5	Peprotech	200-05
RLT Buffer	Qiagen	79216
ExoI Buffer	NEB	B0293S
ExoI	NEB	M0293S
FastAP	ThermoFisher	EF0651
Ctrl IgG2b	ThermoFisher	Clone:eB149/10H5
Anti-Biotin Streptavidin PE	BioLegend	Clone:B123088

Commercial kits		
Reagent	Source	Identifier
Dynabeads Untouched Mouse CD4 Cells Kit	Invitrogen	Cat#11416D
Cell Stimulation Cocktail (plus protein transport inhibitors)	eBioscience	Cat#00-4975-93
Fixation/Permeabilization Solution Kit	BD	Cat#554714
Arcturus PicoPure RNA Isolation Kit	Invitrogen	Cat#KIT0204
SuperScript VILO cDNA synthesis Kit	Invitrogen	Cat#11754050
PowerUP SybrGreen Mastermix	ThermoFisher	Cat#A25741
RNA 6000 Pico Kit	Agilent	Cat#5067-1513
SMARTer Ultra Low Input RNA Kit	Takara	Cat# 634940
NEBNext ChIP-seq Library Prep Kit for Illumina	NEB	Cat# E6240
Qubit™ dsDNA HS Assay Kit	Invitrogen	Cat# Q32851
SureSelect HS XT Target Enrichment System v6	Agilent	N/A
KAPA HiFi HS Mastermix	Merck	
Mice		
Strain	Source	Identifier
BALB/c	Harlan / Jackson / Taconic	JAX:000651
C57BL/6J		JAX:000664
B6.SJL-Ptprca Pepcb/BoyJ		JAX:002014
NOD.Cg-Prkdc^{scid}IL2rg^{tmWjl}/SzJ	Jackson	JAX:005557
C57BL/6-Tg(CAG-OVA)916Jen/J	Jackson	JAX:005145
C57BL/6-Tg(Tcra2D2,Tcrb2D2)1Kuch/J	Jackson	JAX:006912
B6.Cg-Tg(TcraTcrb)425Cbn/J	Jackson	JAX:004194
C57BL/6-Tg(TcraTcrb)1100Mjb/J	Jackson	JAX:003831
B6.129S2-Il10rbtm1Agt/J	Jackson	JAX:005027
B6.129S(Cg)-Stat1tm1Dlv/J	Durbin *et al.*, 1996	JAX:012606
BALB/c x C57BL/6J	N/A	N/A
B6-Tg(Tal1-cre)42-056Jrg H2-Ab1^{tm1Koni} Gt(ROSA)26Sor$^{tm1(EYFP)Cos}$/Atp	N/A	N/A
H2-Ab1^{tm1Koni} Gt(ROSA)26Sor$^{tm1(EYFP)Cos}$/Atp	N/A	N/A
C57BL/6-FLT3wt/ITD/Mx1-Cre	(Li *et al.*, 2008)	N/A

Mouse oligonucleotides		
Gene	Forward Primer (5' → 3')	Reverse Primer (5' → 3')
ActB	*CTAAGGCCAACCGTGAAAAG*	*ACCAGAGGCATACAGGGACA*
Cd274	*AAATCGTGGTCCCCAAGC*	*TCTGCAGGCGAGGAGACT*
Cd74	*CACCGAGGCTCCACCTAA*	*GCAGGGATGTGGCTGACT*
Ciita	*CTCAGCCACCTTCCCTCA*	*CAGTGATGTTGTTTTGGGACA*
Foxp3	*CATATAAGCAGACAGCTGGGTTT*	*TCTTTCATTTGGTATCCGCTTT*
H2-Aa	*CTCTGATTCTGGGGGTCCT*	*ACCATAGGTGCCTACGTGGT*
H2-Ab1	*GTGGTGCTGATGGTGCTG*	*CCATGAACTGGTACACGAAATG*
H2-Dma	*AGGTCAAATCCCAGTGTCCA*	*AACTCCAGGGGCTTCAGTG*
H2-Dmb1/2	*GGGACCTCTGAGCCCATC*	*GGCTGCAGACACAGAGACCT*
H2-Eb1	*CCTCCAGTGGCTTTGGTC*	*CTGCGTCCCGTTGTAGAAAT*
H2-Oa	*AACACTGGGGCCTGGATAC*	*TCTATGGTGTCCGGTGGTG*
H2-Ob	*CAGAGCTGCTGTGAACATGG*	*CCTCTGGAGGCACATTTCTC*
Havcr2	*TTTTCAGGTCTTACCCTCAACTG*	*CATAAGCATTTTCCAATGACCTT*
Icos	*GCAAACATTCTCCTGGGGTA*	*TGTCAAACCCAGAGAGAGCA*
Il10	*CAGAGCCACATGCTCCTAGA*	*TGTCCAGCTGGTCCTTTGTT*
Lag3	*CACCTGTAGCATCCATCTGC*	*CCAGGTAACCCGAAGGATTT*
Maf	*CCTTCCTCTCCCGAATTTTT*	*CCACGGAGCATTTAACAAGG*
Pdcd1	*TGCAGTTGAGCTGGCAAT*	*GGCTGGGTAGAAGGTGAGG*
Prdm1	*ACGTGTGGGTACGACCTTG*	*CCATGTCCATTTTCATGATCC*
Tigit	*TGCCTTCCTCGCTACAGG*	*TGCAGAGATGTTCCTCTTTGTATC*
Tnfrsf4	*AGGACAGCGGCTACAAGC*	*GGGTCTGCTTTCCAGATAAGGT*

Human oligonucleotides		
Gene	Forward Primer (5' → 3')	Reverse Primer (5' → 3')
ACTB	CCAACCGCGAGAAGATGA	CCAGAGGCGTACAGGGATAG
B2M	TTCTGGCCTGGAGGCTATC	TCAGGAAATTTGACTTTCCATTC
CD226	GCTTTACCGCTGCTACTTGC	TCCAGCCACAAAGAGGGTAT
CD274	GGCATCCAAGATACAAACTCAA	CAGAAGTTCCAATGCTGGATTA
FOXP3	ACCGTGGATGAGCTGGAGT	GCCAGGTGTAGGGTTGGAA
HAVCR2	CTGCAAGCTCCATGTTTTCA	GACCTCCGCTCTGTATTCCA
IL10	TGCCTTCAGCAGAGTGAAGA	GCAACCCAGGTAACCCTTAAA
LAG3	GACCTACACCTGCCATATCCA	CCAAAGGATTTGGGAGTCAC
MAF	AGCGGCTTCCGAGAAAAC	GCGAGTGGGCTCAGTTATG

Software and algorithms	
Tool	From

Quant StudioTM Real-Time PCR Software v1.3	Applied Biosystems
FACSDIVA v8.0	BD
Flowjo v10	TreeStar
Proteome Discoverer v1.3	ThermoFisher
Sequest search engine	ThermoFisher
nSolver Analysis Software	Nanostring
cluster v2.1.0	Maechler *et al.*, 2019
NbClust v3.0	Charrad *et al.*, 2014
R v3.6.2	N/A
ComplexHeatmap v.2.0.0	Gu, Eils and Schlesner, 2016
STAR 2.5.3a	Dobin *et al.*, 2013
SAMtools 1.6	Li *et al.*, 2009
Sambamba Version 0.6.5.	Tarasov *et al.*, 2015
FeatureCounts, Subread version 1.5.3	Liao, Smyth and Shi, 2014
DESeq2	Love, Huber and Anders, 2014
ClusterProfiler	Yu et al., 2012
BWA MEM v0.7.15	Li, 2013
Mutect2 v3.8 and v4.0.9	Cibulskis et al., 2013
ANNOVAR	Wang, Li and Hakonarson, 2010
Primer3	Untergasser et al., 2012
DeepSNV R package	Gerstung et al., 2012
Scanorama	Hie, Bryson and Berger, 2019
Seurat	Stuart et al., 2019
UMAP	Becht et al., 2019
MAST	Finak et al., 2015
Ggplot2 v3.2.1	Wickham, 2009
Pheatmap v1.9.12	N/A
GraphPad Prism v8	GraphPad Software

Table 1. Key materials used in the thesis.

METHODS

Some parts of the text have been taken and/or adapted from the previosly manuscripts (Velten et al., 2021; Hernández-Malmierca et al., under revision) originally co-written by myself (see author contributions for more details).

Sample acquisition and processing

Mouse samples

All animal experiments were approved by the Animal Care and Use Committees of the German Regierungspräsidium Karlsruhe für Tierschutz und Arzneimittelüberwachung (Karlsruhe, Germany), the Harvard Medical Area Standing Committee on Animals, the Brigham and Women's Hospital Institutional Animal Care and Use Committee (Boston, USA) or the Institutional Animal Care and Use Committees (IACUC) of the Dana-Farber Cancer Institute (Boston, USA). All mice were maintained in individually ventilated cages under SPF conditions in the animal facility of the DKFZ (Heidelberg, Germany), the Hale Building for Transformative Medicine of the Brigham and Women's Hospital (Boston, USA) or Dana-Farber Cancer Institute (Boston, USA). Wild type mice (BALB/c, C57BL/6J (CD45.2) and B6.SJL-Ptprca Pepcb/BoyJ (CD45.1)) were purchased from Harlan Laboratories, Taconic or the Jackson Laboratories. NOD.Cg-Prkdc^{scid}IL2rg^{tmWjl}/SzJ (NSG), C57BL/6-Tg(CAG-OVA)916Jen/J (CAG-OVA), C57BL/6-Tg(Tcra2D2,Tcrb2D2)1Kuch/J (2D2) and B6.Cg-Tg(TcraTcrb)425Cbn/J (OT-II) mice were purchased from the Jackson Laboratories. B6.129S(Cg)-Stat1^{tm1Dlv}/J (STAT1$^{-/-}$) and B6.129S2-Il10rb^{tm1Agt}/J (Il10rb$^{-/-}$) have been described before (Durbin *et al.*, 1996; Spencer *et al.*, 1998). B6.129S2-Il10rb^{tm1Agt}/J mice were kindly provided by Dr. Laura Llaó-Cid. C57BL/6-FLT3wt/ITD/Mx1-Cre mice were kindly provided by the group of Prof. Dr. Carsten Müller Tidow. C57BL/6-Tg(TcraTcrb)1100Mjb/J (OT-I) mice were kindly provided by Stephanie Lindner, from the group of Prof. Dr. Rienk Offringa. BALB/cxC57BL/6J F1 and B6-Tg(Tal1-cre)42-056Jrg H2-Ab1t^{m1Koni} Gt(ROSA)26Sor$^{tm1(EYFP)Cos}$/Atp (SclCreERT2 x MHC-II-flox x Rosa26-EYFP-flox) mice were generated in house.

Mouse bone marrow was prepared by crushing femur, tibia, humerus, ilium, sternum and columna vertebralis in PBS (Sigma) supplemented with 2% heat-inactivated FCS (Gibco). Subsequently, cells were filtered through 40µm cell strainers (Falcon) and erythrocyte lysis was performed for 5 min using ACK buffer (Lonza), followed by washing and centrifugation for 5 min at 250 x g. For isolation of HSPCs, cells were incubated in PBS 2% FCS for 15 minutes with antibodies against the lineage markers CD11b (M1/70), Gr-1 (RB6.8C5), CD4 (GK1.5), CD8a (53.6.7), Ter119 (Ter119) and B220 (RA3-6B2) at 4°C. Subsequently, cells were washed

and incubated for 15 minutes with pre-washed anti-rat IgG-coated Dynabeads 4,5µm magnetic polystyrene beads (Invitrogen) in the ratio of 1mL of beads /mouse. Cells expressing lineage markers were depleted using a separation magnet (Invitrogen), followed by staining the remaining lineage-negative cells described below.

Spleen and lymph nodes (inguinal, axial, submandibular, mesenteric) were dissected and homogenized through a 40µm filter into PBS 2% FCS using the plunger of a syringe. Erythrocyte lysis was performed for 5 min using ACK buffer (Lonza). For $CD4^+$ T cell sorts, the Dynabeads Untouched Mouse CD4 Cells Kit (Invitrogen) was used according to the manufacturer's instructions. Enriched cells were stained and isolated by FACS sorting as described below.

Human samples

Peripheral blood and bone marrow samples from healthy donors were obtained from the University Hospital Mannheim and Heidelberg University Hospital after informed written consent. Mononuclear cells were isolated by density gradient centrifugation and stored in liquid nitrogen until further use. All experiments involving human samples were conducted in compliance with the Declaration of Helsinki and approved by and in accordance with regulations and guidelines by the ethics committee of the medical faculty of the University of Heidelberg.

Flow cytometry staining, acquisition and FACS sorting

For flow cytometric analyses and FACS sorting, lineage-depleted, $CD4^+$ T cell enriched or unfractionated cells were stained in PBS 2% FCS for 20 min with corresponding antibodies and washed.

For Y-Ae antibody conjugated with biotin, cells were washed and incubated for another 20 minutes with Streptavidin-PE (ThermoFisher).

For intracellular cytokine staining, cells were stimulated for 4h at 37°C with the Cell Stimulation Cocktail (plus protein transport inhibitors) (eBioscience). After surface staining, cells were fixed, permeabilized and stained using the BD Fixation/Permeabilization Solution Kit (BD Biosciences) according to manufacturer's instructions.

For cell cycle staining, after surface staining, cells were fixed, permeabilized and stained for Ki67 using the BD Fixation/Permeabilization Solution Kit (BD Biosciences) according to manufacturer's instructions, resuspended in wash buffer with DAPI (ThermoFisher).

For reactive oxygen species (ROS) measurement, 2',7'-dichlorofluorescin diacetate (H_2DCFDA) was used as previously described (Alshetaiwi *et al.*, 2020).

Finally, cells were filtered through a 35-40µM filter and acquired by a flow cytometer (LSR II or LSRFortessa, Becton Dickinson) or cell sorter (FACSAria II or FACSAria Fusion, Becton Dickinson) for analysis or sort, respectively. Common gating strategies used in this study to define populations are depicted in Supplementary Figures 3 and 4.

Ex vivo experimental procedures

Murine T cell cocultures

Cells were cultured at 37°C and 5% CO_2 in U-bottom plates in a total volume of 200µL of Dulbecco's Modified Eagle's Medium GlutaMAX (DMEM GlutaMAX, Gibco) supplemented with 10% heat-inactivated Fetal Calf Serum (FCS, Gibco), sodium pyruvate (1.5mM, Gibco), L-glutamine (2mM, Gibco), L-arginine (1x, Sigma), L-asparagine (1x, Sigma), penicillin/streptomycin (100 U/mL, Sigma), folic acid (14µM, Sigma), MEM non-essential amino acids (1x, ThermoFisher), MEM vitamin solution (1x, ThermoFisher) and β-mercaptoethanol (57.2µM, Sigma). Cells were sorted and, when mentioned, labelled with cell trace violet (ThermoFisher) according to manufacturer's instructions. $5x10^4$ naïve $CD4^+$ T cells were cultured with $2x10^4$ DCs, HSPCs or $CD8^+$ T cells, unless stated otherwise. When stated, ovalbumin peptide (323-339) (25µg/mL, Invivogen), full ovalbumin protein (10 mg/mL, Invivogen), DQ-OVA (100µg/mL, Invitrogen), MOG peptide (50µg/mL, Genemed Sythesis), Eα peptide (52-68) (100µg/mL, Mimotopes), LPS (100 ng/mL, ThermoFisher), αMHC-II blocking antibody (10µg/mL, M5/114.15.2, BioXCell) or a control IgG2b antibody (10µg/mL, eB149/10H5, ThermoFisher) were added to the cultures. For transwell experiments, cells were plated as described with additional $2x10^4$ HSPCs plated on 96-well plate inserts with polyester membrane and 1 µm pore size (Corning). For resting of T cells, culture medium was replaced by fresh culture medium in the absence of ovalbumin peptide, followed by culturing for two days. Re-stimulation was performed by addition of Dynabeads Mouse T-Activator (ThermoFisher) according to manufacturer's instructions.

In vitro suppression assay

T_{DCs} and T_{HSCs} were generated by 3 days of culture as described above, rested in the absence of ovalbumin peptide for 2 days and FACS-sorted. Subsequently, 10^5 CTV-labelled naïve bystander $CD4^+$ T cells were cultured with 10^5 $CD19^-CD3^-$ splenocytes and different ratios of *in vitro*-generated T_{HSCs} or T_{DCs}, or freshly purified $CD4^+$ T_{regs} relative to the amount of naïve bystander $CD4^+$ T cells, and anti-CD3 antibody (1 µg/mL,145-2C11, BioXCell). Cells were

analyzed by flow cytometry and proliferation of bystander cells was assessed with the following parameters:

Suppression index = (Sample CTV gMFI) / (No T cell activation CTV gMFI)

Proliferation index = Σ ((# of cells in i) / 2^i *i) / (Σ ((# of cells in i) / 2^i)) - (# of cells in i=0))

Where i = Number of cell divisions, seen by CTV dilution

Human T cell cocultures

Human cells were cultured under the same conditions as murine cells. For T cell interaction assays, $5x10^4$ naïve $CD4^+$ T cells were cultured with $5x10^3$ antigen presenting cells (either DCs, $CD34^+$ HSPCs or additional T cells) from an unrelated donor in the presence or absence of CytoStim (Miltenyi) or PepMix CEFX Ultra SuperStim MHC-II Subset Pool (JPT) according to manufacturer's instructions. All analyses were performed after three days of co-culture.

In vivo experimental procedures

Treatments

To induce inflammatory conditions, mice were injected intraperitoneally with a single dose of 5 mg/kg pI:C (Invivogen), 0.25 mg/kg LPS (ThermoFisher), 500U/g IFNα (Miltenyi) and MCMV (Hirche *et al.*, 2017). For administration of ovalbumin, 500mg/kg of full ovalbumin protein (Invivogen), 500mg/kg of DQ-OVA (Invitrogen), or 12.5mg/kg of ovalbumin 323-339 peptide (Invivogen) was administered. For knock-out induction, 100mg/kg of tamoxifen were resuspended in sunflower oil with ethanol (10%) and injected intraperitoneally once a day for five consecutive days.

Bone marrow transplantation

For mouse stem cell transplantation experiments, HSPCs were transplanted intravenously into lethally irradiated (2x500rad) recipient mice together with 10^5 rescue bone marrow cells. Mice were bled periodically and cells were stained as described above for assessment of engraftment. After 4 months, mice were sacrificed, analyzed for engraftment and 10^6 bone marrow cells were intravenously transplanted into secondary lethally irradiated recipients.

Chimeric transplantation setup

Same number of sorted HSPCs coming from different genetic backgrounds (CAG-OVA vs B6 and MHC-II-floxxRosa26-EYFP-flox vs YFP+MHC- from SclCreERT2xMHC-II-floxxRosa26-EYFP-flox) were intravenously into lethally irradiated (2x500rad) recipient mice together with 10^5 rescue bone marrow cells. $0.5x10^6$ naïve OT-II T cells were co-transplanted either at the same time or 8 weeks afterwards. Mice were bled periodically and cells were stained as described above for assessment of engraftment. After 4 months, mice were sacrificed, analyzed for engraftment and 10^6 bone marrow cells were intravenously transplanted into secondary lethally irradiated recipients that were bled monthly.

Xenotransplantation

The indicated fractions were sorted from human bone marrow aspirates, and 10^5 sorted cells were transplanted intrafemorally into sublethal irradiated (175x1rad) NSG mice. Engraftment of human cells in bone marrow was measured by flow cytometry.

Adoptive co-transfer of OVA-loaded HSCs and antigen-specific T cells

$1.5x10^5$ BM OT-II $CD4^+$ T cells were sorted and intravenously transferred into Ly5.1 mice. LSK cells were isolated as described above and cultured for 12 hours in presence or absence of ovalbumin peptide (50µg/mL) in culture medium supplemented with TPO (50 ng/mL, PreproTech) and SCF (50 ng/mL, PreproTech) at 37°C, 5% CO_2 levels. Subsequently, cells were washed and (10^5 cells per mouse) adoptively transferred into the recipient mice from above. After three days, mice were sacrificed and the BM was isolated for flow cytometric analysis of HSPC-derived cells.

In vivo T cell suppression assay

For the *in vivo* suppression assay, T_{DCs} and T_{HSCs} were generated as described above and FACS sorted at day 3 of the co-culture. Subsequently, $1.5x10^5$ cells were adoptively transferred intravenously together with 10^6 CTV-labelled naïve OT-II $CD4^+$ T cells into naive mice. One day post transfer, mice were injected with ovalbumin peptide and LPS as described above, and splenic T cells were analyzed after 3 days via flow cytometry. The proliferation index was calculated as described above.

MLL-AF9 leukemia model

LSK or GMP cells were sorted and transduced with an MLL-AF9 construct and transplanted into sublethally irradiated C57BL/6J mice (Taconic) as previously described (Krivtsov *et al.*,

2006, 2013). One month post-transplant, mice were sacrificed and leukemic GFP^+ cells were sorted and co-cultured with naïve OT-II T cells as described above. For *in vivo* relevance of leukemic-T cell antigen-specific interactions, $0.5x10^6$ naïve OT-II T cells were co-transplanted either at the same time or 2 weeks afterwards and mice were bled weekly and sacrificed when disease burden was compromising animal health.

Immunopeptidomics

Isolation of MHC ligands

$2.5x10^7$-$5x10^7$ splenocytes ($CD3^-$), T cells ($CD3^+$) or HSPCs (Lineage-cKit+) were sorted and snap frozen. The MHC class II molecules were isolated using standard immunoaffinity purification (Falk *et al.*, 1991; Kowalewski and Stevanović, 2013). In brief, snap-frozen primary samples were lysed in 10 mM CHAPS/PBS (AppliChem) with 1× protease inhibitor (Roche). For the immunoprecipitation of MHC class II–peptide complexes, the monoclonal antibody M5/114.15.2 (eBioscience) covalently linked to CNBr-activated Sepharose were used (GE Healthcare). MHC–peptide complexes were eluted by repeated addition of 0.2% TFA (trifluoroacetic acid, Merck). Eluted MHC ligands were purified by ultrafiltration using centrifugal filter units (Amicon). Peptides were desalted using ZipTip C18 pipette tips (Millipore), eluted in 35 µl 80% acetonitrile (Merck)/0.2% TFA, vacuum-centrifuged and resuspended in 25 µl of 1% acetonitrile/0.05% TFA and samples stored at − 20 °C until LC–MS/MS analysis.

Analysis of MHC ligands by LC–MS/MS

Isolated peptides were separated by reversed-phase liquid chromatography (nano-UHPLC, UltiMate 3000 RSLCnano; ThermoFisher) and analyzed in an online-coupled Orbitrap Fusion Lumos mass spectrometer (ThermoFisher). Samples were analyzed in three technical replicates and sample shares of 33% trapped on a 75 µm × 2 cm trapping column (Acclaim PepMap RSLC; Thermo Fisher) at 4 µl/min for 5.75 min. Peptide separation was performed at 50 °C and a flow rate of 175 nl/min on a 50 µm × 25 cm separation column (Acclaim PepMap RSLC; Thermo Fisher) applying a gradient ranging from 2.4 to 32.0% of acetonitrile over the course of 90 min. Samples were analyzed on the Orbitrap Fusion Lumos implementing a top-speed CID method with survey scans at 120k resolution and fragment detection in the Orbitrap (OTMS2) at 60 k resolution. A mass range of 300–1500 *m/z* was analyzed with charge states ≥ 2 selected for fragmentation.

Database search and spectral annotation

LC-MS/MS results were processed using Proteome Discoverer (v.1.3; ThermoFisher) to perform database search using the Sequest search engine (ThermoFisher) and the murine proteome as reference database annotated by the UniProtKB/Swiss-Prot (http://www.uniprot.org), status February 2014 containing 20,270 ORFs. The search combined data of three technical replicates, was not restricted by enzymatic specificity and oxidation of methionine residues was allowed as dynamic modification. Precursor mass tolerance was set to 5 ppm, and fragment mass tolerance to 0.02 Da. False discovery rate was estimated using the Percolator node (Käll *et al.*, 2007) and was limited to 5%. Peptide length was limited to 12–25 aminoacids of length.

Quantitative Polymerase Chain Reaction (qPCR)

For qPCR analyses, cells were directly sorted into RNA lysis buffer (Arcturus PicoPure RNA Isolation Kit (Invitrogen), incubated for 30 min at 42°C and processed for cDNA synthesis using SuperScript VILO cDNA synthesis kit (Invitrogen) according to manufacturer's instructions. The newly synthesized cDNA was diluted 1:10 in RNase free H_2O and 6 µL were mixed in technical triplicates in 384-well plates with 0.5 µl of forward and reverse primer (10 µM) (Table S1 and S2) and 7 µl PowerUP SybrGreen Mastermix (ThermoFisher). Program: 50°C for 2 minutes, 95°C for 10 minutes and 40 cycles of 95°C for 15 seconds, 60°C 1 minute. Primers were designed to be intron spanning whenever possible using the Universal ProbeLibrary Assay Design Center (Roche) and purchased from Sigma Aldrich. Experiments were performed on the ViiA7 System (ThermoFisher) and analysis of gene amplification curves was performed using the Quant StudioTM Real-Time PCR Software v1.3 (Applied Biosystems). RNA expression was normalized to the housekeeper genes *Gapdh/Actb* for murine and *B2M/ACTB* for human gene expression analysis. Relative expression levels are depicted in $2^{-\Delta Ct}$ values, ΔCt = (geoMean Housekeeper Ct) - (gene of interest Ct).

NanoString and RNA-Seq gene expression analysis

After 3 days of co-culture with $2.5x10^3$ (NanoString) or $2x10^4$ (RNA-Seq) HSPCs or $2x10^4$ DCs, $CD4^+$ T cells were FACS-sorted and lysed in RLT Buffer (Qiagen) with 1% β-mercaptoethanol (Sigma). For NanoString, RNA was hybridized with the PanCancer Mouse Immune Profiling CodeSet provided by NanoString Technologies. The barcodes were counted on an nCounter Digital Analyzer. The obtained raw data was analyzed using the nSolver Analysis Software. For RNA-Seq, the SmartSeq2 protocol was followed (Picelli *et al.*, 2013, 2014) and sequenced on an Illumina NextSeq 550 (75bp high-output). Differential expression between samples was

tested using the R/Bioconductor package DESeq2 (Love, Huber and Anders, 2014). GSEA was run with the R/Bioconductor package clusterProfiler (Yu *et al.*, 2012).

EuroFlow analysis of diagnostic AML samples

Diagnostic bone marrow aspirates of AML patients were analyzed using the EuroFlow panels (van Dongen *et al.*, 2012) at the Heidelberg University Hospital, Germany. AML blast cells were gated in FlowJo as $CD45^{+}$ excluding $CD45^{high}SSC^{low}$ healthy lymphoid cells, and geometric mean fluorescence intensities (gMFIs) for all surface markers were exported. Before z-score scaling the data, values larger than the 95^{th} percentile and smaller than the 5^{th} percentile were considered to be outliers and adjusted to the 95^{th} or 5^{th} percentile, respectively. The data was partitioned into 4 clusters by PAM (partitioning around medoids) clustering using the R package cluster v2.1.0 (Maechler *et al.*, 2019), after determining the best number of clusters using NbClust v3.0 (Charrad *et al.*, 2014). Heatmap visualizations of the data were done using the R/Bioconductor package ComplexHeatmap v.2.0.0 (Gu, Eils and Schlesner, 2016). Stem-, Mono-, and Granulo-indices were calculated by adding the scaled gMFIs of the respective signature for each patient and min-max feature scaling each index between patients: Stem-index = CD34 and CD117, Mono-index = CD14, CD64, CD300e and CD45, Granulo-index = CD35, CD15, CD16 and SSC-A.

RNA-sequencing of diagnostic *DNMT3A* and *NPM1* mutant AML samples

RNA isolation from primary AML samples

DNMT3A and *NPM1* mutant AML patient samples were selected from AML-SG and SAL biorepositories. AML BM samples were freshly thawed in IMDM supplemented with 10% FCS and 20 U/ml DNAseI (Roche). $CD3^{+}$ cells were depleted using human CD3 MicroBeads (Miltenyi). 10,000-20,000 $CD3^{-}$cells were collected in Arcturus PicoPure Extraction Buffer (Applied Biosystems). RNA was extracted with Arcturus PicoPure RNA Isolation Kit (Applied Biosystems) according to manufacturer's instructions. RNA quality was assessed with a Bioanalyzer (Agilent) using Agilent RNA 6000 Pico Kit (Agilent).

RNA-Seq libraries preparation

3ng of total RNA was used for RNA-Seq library preparation. cDNA production was performed using SMARTer Ultra Low Input RNA Kit (Takara) according to manufacturer's instructions. DNA libraries were produced using NEBNext ChIP-seq Library Prep Kit for Illumina (New England BioLabs). Libraries quality check was performed using Qubit™ dsDNA HS Assay Kit

(Invitrogen) and Agilent High Sensitivity DNA Kit for Bioanalyzer (Agilent). Libraries were sequenced with Illumina HiSeq2000 v4 (125 bp PE).

RNA-Seq analysis

Bcl2fastq2 2.20 was used for base calling. Reads were trimmed for adapter sequences and aligned to the 1000 Genomes Phase 2 assembly of the Genome Reference Consortium human genome (build 37, version hs37d5) with STAR 2.5.3a (Dobin *et al.*, 2013) and the following parameters: alignIntronMax 500,000, alignMatesGapMax 500,000, outSAMunmapped Within, outFilterMultimapNmax 1, outFilterMismatchNmax 3, outFilterMismatchNoverLmax 0.3, sjdbOverhang 50, chimSegmentMin 15, chimScoreMin 1, chimScoreJunctionNonGTAG 0, chimJunctionOverhangMin 15. GENCODE gene annotation (GENCODE Release 19) was used for building the index. BAM files were generated using SAMtools 1.6 (Li *et al.*, 2009) and duplicates were marked with Sambamba Version 0.6.5 (Tarasov *et al.*, 2015). Raw counts were generated using featureCounts, Subread version 1.5.3 (Liao, Smyth and Shi, 2014). For calculation of normalized counts, mtRNA, tRNA, rRNA as well as all transcripts from the Y- and X-chromosome were removed and subsequently normalization was performed in analogy to TPM (transcripts per million). Differential expression between ER and LTR samples was conducted using the R/Bioconductor package DESeq2 (Love, Huber and Anders, 2014). Log2 fold changes were used for GSEA with the R/Bioconductor package clusterProfiler (Yu *et al.*, 2012). Median normalized counts were used as cut-off between subgroups of high and low expression.

Statistical analysis and representation

Flow cytometric analyses were performed in FlowJo (BD). Bioinformatic analyses were performed in R, and visualized in R or GraphPad Prism (v8.4.2, GraphPad Software). One- or two-way ANOVA, or Kruskal-Wallis tests were performed as discovery tests wherever necessary. Only when the discovery test was significant, post-hoc two-tailed t-tests or Mann-Whitney tests were performed based on normality of the data. In case of multiple comparisons, p-values were corrected by the Benjamini-Hochberg false discovery rate of 5% and q-values were subsequently used to indicate significance. Significance is depicted as: no significance = ns, $P<0.05$ *, $P<0.01$ **, $P<0.001$ ***, $P<0.0001$ **** according to statistical tests indicated in each figure legend.

MutaSeq

Deep exome sequencing and target selection

For exome sequencing, DNA was extracted from $9x10^3$ flow sorted $CD34^+$ cells (for CD34+ leukemias: P1, P3) or total bone marrow. Healthy controls were a buccal swap (P1), FACS-sorted $CD45^-$ $CD105^+$ MSCs (P3) or in vitro expanded MSCs (P2 and P4) (Schallmoser *et al.*, 2008). Sequencing libraries were constructed using the SureSelect HS XT Target Enrichment System v6 (Agilent), and a mean on-exon sequencing coverage of at least >70X was obtained for each patient. Genomic alignments were performed using BWA MEM v0.7.15 (Li, 2013) and cancer variants were identified using Mutect2 v3.8 (P1 and P3) and v4.0.9 (P2 and P4) (Cibulskis *et al.*, 2013), following the GATK best practice recommendations. Variants were annotated using ANNOVAR (Wang, Li and Hakonarson, 2010). Output from Mutect2 was filtered to remove variants that did not overlap with known genes. The final list of candidate variants included only those with allele frequencies (AF) greater than 4% in the cancer exome sample and with an AF four-fold larger than in the healthy exome sample. Finally, the candidates for targeting were hand-selected from this list with a focus on cancer relevant genes, highly expressed genes, and potential sub-clonal markers.

Single-cell cultures

Bone Marrow mononuclear cells from patient P1 were stained and Lin- or Lin-CD34+ single cells were index-sorted into ultra-low attachment 96-well plates (Corning) containing 100µL StemSpan SFEM media. Media was supplemented with penicillin/streptomycin (100ng/mL), L-glutamine (100ng/mL) and the following human cytokines: SCF (20ng/mL), Flt3-L (20ng/mL), TPO (50ng/mL), IL-3 (20ng/mL), IL-6 (20ng/mL), G-CSF (20ng/mL), EPO (40ng/mL), IL-5 (20ng/mL), M-CSF (20ng/mL), GM-CSF (50ng/mL). After 21 days at 5% CO_2 and 37°C, colonies were imaged by microscopy, and processed as detailed in the following.

Targeted DNA sequencing by nested PCR amplification

Single-cell derived colonies were transferred into 50µL buffer RLT. Cleanup was performed using CleanPCR beads at a 1.8x volume ratio and eluted in 20µL 10mM Tris-HCl pH 7.8. 4.5µL were transferred to a PCR plate containing 7.5µL Kapa HiFi HS mastermix and 3 µL of a pool of all outer primers (each primer at 0.5µM) were added, followed by a PCR program of 98°C 3', 30 cycles of [98°C, 20'', 63°C, 60'', 72°C 10''] and 72°C, 5' and subsequent enzymatic cleanup with 2.5µL 10x ExoI buffer, 0.4µL ExoI and 0.4µL FastAP, 30' incubation at 37°C and 5' inactivation at 95°C. Afterwards, 1µL was transferred to a PCR tube containing 5.9µL water, 7.5µL Kapa HiFi HS mastermix and 0.6µL of a pool of all inner primers (each primer at 0.5µM),

followed by a PCR program of 98°C 3’, 15 cycles of [98°C, 20’’, 65°C, 15’’, 72°C 30’’], 72°C, 5’ and enzymatic cleanup as above. 1µL was then transferred into a PCR with Nextera indexing primers (Hennig *et al.*, 2018) and amplified with 98°C 3’, 10 cycles of [98°C, 20’’, 60°C, 15’’, 72°C 30’’] and 72°C, 5’.

MutaSeq and mitoClone

For specific technical and bioinformatic details, please refer to (Velten *et al.*, 2021).

CONTRIBUTIONS

This thesis has been proof-read and corrected by **Dr. Simon Haas**, **Isabel Barriuso Ortega** and **Dominik Vonficht** with input from **Shubhankar Sood**.

Healthy and malignant hematopoietic stem cells are immunoregulatory antigen presenting cells

First and foremost, the data generation of many different experiments presented in this section is the result of intense and productive collaboration with the MSc students that have been under my supervision in this project. Chronologically, **Sophie-Luise Landua**, **Dominik Vonficht**, **Elise van der Salm**, **Mohamed Mahmoud**, **Christine Trautmann** and **Alina Bolhagen**.

Throughout this section, bioinformatic support and analysis was performed by **Florian Grünschläger**. Likewise, experimental and conceptual support was provided by **Dominik Vonficht**. Additionally, assistance with mouse housing, crossing and genotyping was provided by **Adriana Przybylla**.

The RNA used for qPCRs in Figure 7 was generated by **Dr. Simon Haas**, **Alexandra Schnell** and **Dr. Christoph Hirche**. Also **Dr. Christoph Hirche** together with **Franziska Pilz** were crucial setting up and following up the MHC-II FACS-sorted primary and secondary transplantations. Immunopeptidomics were executed, analyzed and the respective method section was performed by **Dr. Michael Ghosh**, in the laboratory of **Dr. Stefan Stevanovic**. Nanostring, intracellular staining and 2D2 experiments to better characterize T_{HSCs} were performed by **Dr. Vijay Kuchroo** and **Alexandra Schnell**, in the laboratory of **Dr. Vijay Kuchroo**. Hemap analysis was done by **Claudia Robens**. **Dr. Simon Raffel** provided the human healthy and diseased bone marrow samples and **Corinna Klein** performed xenograft injections**.** RNA-Seq for AML comparison between ER and LTR patients was performed and analyzed by **Dr. Nádia Correia**, **Dr. Elisa Donato** and **Carolin Andresen**. MLL-AF9 experiments were perfomed by **Dr. Hannah Uckelmann** and **Alexandra Schnell** in a joint effort from the laboratories of **Dr. Scott Armstron** and **Dr. Vijay Kuchroo**. Statistical guidance was given by **Dr. Dr. Daniel Hübschmann**.

Additional technical and/or conceptual assistance was provided by **Shubhankar Sood**, **Jasper Panten**, **Simon Renders**, **Franziska Pilz** and **Dr. Raphael Lutz**.

Dr. Simon Haas and **Prof. Dr. Andreas Trumpp** were instrumental with major guidance on the project shape and direction.

Identification of leukemic and pre-leukemic stem cells by clonal tracking from single-cell transcriptomics

Above all, **Dr. Lars Velten** and **Dr. Simon Haas** designed and coordinated the project presented in this section of the thesis.

Dr. Simon Raffel provided with AML samples and extraordinarily valuable translational input. **Dr. Malte Paulsen**, **Daniel Leonce** and **Jennifer Milbank** assisted on the technical side of FACS sorting and MutaSeq performance and optimization. **Dr. Lars Velten** and **Benjamin Story,** from the laboratory of **Prof. Dr. Lars Steinmetz,** were the responsible minds behind an amazing bioinformatic effort. The figures, figure legends and methods derived from the bioinformatic analysis were also performed by them. **Aykut Demir** provided extra experimental assistance in the last stages of this project.

As in the previous section, **Dr. Simon Haas** and **Prof. Dr. Andreas Trumpp** were instrumental with major guidance on the project shape and direction.

ACKNOWLEDGEMENTS

I cannot reinforce enough how and for how many reasons I am grateful to **Simon Haas**. You not only gave me the chance to perform the PhD in the greatest atmosphere, but to be part of the beginning of what will be one of the most successful labs out there. Thanks for growing as a supervisor and a mentor with me, for adapting to my scientific mood swings and to my quite "unprofessional" way of being. It was always great to randomly walk into your office and engage in a long conversation about science or personal matters, and your guidance in both aspects has been invaluable to me. But mostly, I want to thank you for becoming a friend along this way, science and outings were unique with "Bossito" around.

I would like to thank **Andreas Trumpp** for his lab, his institute and his working atmosphere. I am proud to have called myself a member of HI-STEM and to have worked with you. Thank you for the extremely helpful and educational insights into the "dos and don'ts" of how to orient a project and how to make it more appealing, among other very valuable conversations. I must say, I am very grateful to you for giving me the chance to do a PhD, but also for sharing some beers with you ('Mentoring the Next Generation: Andreas Trumpp', 2018).

Next, I want to thank all the master students that I have been honored to supervise throughout this PhD. Each of you, have made not only substantial scientific contributions, but have added tons of your personality and time into this story and have taught me way more than you would expect.

Sophie-Luise Landua, your enthusiasm was contagious. We began this project together and we spent so many hours and great conversations sorting that I still tell those stories and cannot avoid smiling. Thank you!

Dominik Vonficht, you came from "far across the sea" with great recommendations and thus, many doubts of their veracity from my side. You did not only make my doubts look foolish, but exceeded what they said about you. You are an insatiable worker and the most positive person I have had the pleasure to work with. Thank you!

Elise van der Salm, your constancy to overcome hurdles was inspirational. I admire your devotion to learn what is needed and beyond. But I admire even more that you always do it with a smile in your face. Thank you!

Mohamed Mahmoud, Mr. Tenacity, but also Mr. Stubbornness (in the best possible way). Your ideas were amazing and so was your passion to defend them. You always made me think harder to catch up with your suggestions and your huge deal of hard work. Thank you!

Christine Trautmann, your attitude in the work environment is needed and should be mandatory in every lab. Always nice to talk to you, always nice to work with you. Thank you!

Alina Bolhagen, since day one you have shocked me. There was no day where you were unprepared and there was no question you were not able to answer. Such was the case that I feel that I could not teach you much, but having you as a peer was extraordinary. Thank you!

I want to take a moment from you, reading this, to acknowledge the sacrifice of animal lives done for research. While this little fragment will not compensate the **1655 mice** implicated in this work, it is my wish that our findings will be of help to inspire and improve other lives in the future. Thank you to all of those little helpers that have made a huge impact and to whom I can only be grateful and hope to have given the best treatment possible.

Along those lines, I want to thank **Adriana Przybylla** for helping me on a daily basis dealing with mice and with the mouse house, and for helping me out to a massive extent scientifically and personally. Having you in the lab was a great support in many aspects and you made my PhD smooth (and realistic). In addition, I can only say good words about the **Technician Team** in HI-STEM and the core facilities of **animal housing** and **flow cytometry**. Without them, this work would have not been possible.

Regarding smoothness of the PhD, I must mention **Dagmar Wolf**. I cannot overstate in any way how fundamental she has been every single time paperwork showed up and how appreciated was her sense of humor and deft touch while dealing with my stress regarding it.

I want to also acknowledge the people that have made of my working environment and the (small and with not much personality) city of Heidelberg, a second home. They have eventually turned into my adopted and oddly charming family.

Shubhankar Sood, every day since we shared a room during the selection, I have been trying to figure out whether I like you or not. Also, every day we have shared inside or outside of the lab has been packed with laughter and with brotherhood. I would have not been able to make it through the bad times without your support, but also the good times would have not been as great without our complicity. **Andrea Barnert**, we started this together and we are finishing it together too. It has been a pleasure to share with you our ins and outs within the lab, to grow together and to grow a wonderful friendship. To the both of you, thank you for walking the path with me, but mostly, thank you for supporting and pulling me up along the way.

Dominik Vonficht and **Florian Grünschläger**, you went from outstanding master students to outstanding friends. Of course, I could not separate you even in this section of the thesis. You two have set very high couple goals as a pack, but separate you have been the greatest lab (and life) colleagues I could ask for. **Domi**, thank you for the chilling, for the “gossiiiip”, for the

talking, for the sport chitchat, for the pizza and for millions of other things. But mostly, thank you for how "EAAAASY" things are with you. "**Abuelo" Flori**, if it was not because of you, I would be under tons of German bureaucracy, my worst nightmare. I would also be experiencing 20% of the things I have experienced with and because of you. Thank you for sharing, for listening, for your valuable advice and support, for the drinks and for millions of other things. But mostly, thank you for your sense of humor while dealing with all my stupid jokes and answering back to them. To the both of you, thank you for always being there and for our overwhelming comradery and friendship.

Jasper Panten, my dearest colleague, thank you for all the back and forth, thank you for the laughter and thank you for being you. You are truly my toughest to achieve friendship, but surely one that is worth an extra effort for.

Simon Renders, my personal internal reviewer and the person that has pushed me the most scientifically. Sharing time with you in the lab was always fun, and sharing it together in Hydra was a bliss. Special mention to the other "**Party Crew**" members (**Alessia**, **Becky**, **Ben**, **Elsa**, **Kadi**, **Kim** and **Margit**). They are all brilliant scientists and amazing people who made of this experience the most special scientific occasion in my life.

Rebecca Wagner, **Becky**, thank you for being a breath of fresh air in every situation. Your refreshing sense of humor and constant and contagious good mood has made me smile and laugh when I less expected to do so.

Franzi Pilz, always there both professionally and personally. You have taught me about Germany and about Frühlingsfest and throughout that process I have learnt that you are a wonderful human being.

Felix Geist, I cannot reinforce enough how much of a support system you have been to deal with the PhD, but also to show me the light at the end of the tunnel. It is always great and inspiring to be around you.

To all of you, but also to those that were a part of the lunch group, coffee breaks, the "Fun office" and other social activities (**Chris**, **Paula**, **Vera**, **Khwab**, **Jenny**, **Anders**, **Viktoria**, **Matea** and **Joel**, among many others), thank you for making me feel at home at many homesick moments.

Paula Argos Vélez, gracias por todos los buenos momentos que hemos tenido en el piso y fuera de él. Por todas las cervezas, partidas de cosas y por todos los ratos en los que por un momento olvidaba que estábamos hasta arriba con el doctorado.

Juan Díaz Miyar, tú eres en parte responsable de que yo acabara aquí (sí, te culpo y culparé por ello). Pero también eres la persona que más veces me ha rescatado de la mala leche y del aburrimiento durante mis dos primeros años aquí. Has sido la persona con la que he tenido el privilegio de convivir y que ha hecho que cada día fuese como quedar con un amigo al que llevas tiempo sin ver. También quien me ha sacado de mi zona de confort con más frecuencia. Pero, sobre todo, gracias por ser durante ya diez años un gran apoyo y gracias por seguir siéndolo en la distancia.

Por ultimo no quiero terminar este agradecimiento sin mencionar a las tres personas más importantes en mi vida. Sin su apoyo, sin sus ánimos y sin su cariño constantes e incondicionales no estaría escribiendo esto y habría tirado la toalla hace mucho tiempo. Por tanto quiero agradecerles a ellos por encima de todo este logro, ya que son tan partícipes de él como yo mismo.

Isabel Barriuso Ortega, no tengo palabras ni espacio suficiente para agradecerte lo que has hecho por esta tesis y lo que es más importante, por mí. Tu mirada crítica me impulsa constantemente a esforzarme por mejorar y tu apoyo me ayuda a levantarme y no ver el fracaso cuando no lo consigo. Gracias por acompañarme en mi montaña rusa, llena de picos de euforia e hiperactividad y caídas de apatía y mal humor. Pero sobre todo, gracias por siempre hacerlo calmada y sonriendo (aunque quieras tirarme por la ventana en los picos y los valles). Eres la mejor compañía que podría imaginar.

El último lugar se lo reservo a mis padres, **Federico José Hernández Navarro** y **María Victoria Malmierca Benito**. Durante toda mi vida habéis sido los artífices de mi formación personal, educativa y profesional. Nadie me ha enseñado tanto, ni a nadie le debo tanto como a vosotros. Habéis sido vosotros quienes más han creído en mí. Cuando me he encontrado con rechazos, falta de oportunidades o fracasos, siempre estabais allí para levantarme, para apoyarme, para ser mis mecenas, para todo. Gracias a vosotros y vuestras enseñanzas soy quien soy y no podría estar más agradecido por ello.

De ti, **Fede**, quiero destacar tu paciencia infinita. Tu manera de lidiar con los problemas, uno a uno y dedicándoles el tiempo que haga falta. Tu saber estar y sentido del humor constantes. Tu devoción y capacidad de sacrificio. Tu tutela y enseñanzas eternas, yendo desde las trivialidades más pequeñas en los deportes que practicaba hasta las cosas más importantes de la vida. Pero sobre todo, por todos los momentos que seguimos disfrutando juntos.

De ti, **Madre**, no puedo más que asombrarme y agradecerte tu inmenso amor y cariño (y tu comida). Tu capacidad crítica y objetiva, que aún a día de hoy me hacen crecer. Tu resiliencia, resistencia y adaptabilidad a todo lo que viene. El entusiasmo y valor con el que afrontas cada

nuevo reto o aventura. Pero sobre todo, la pasión con la que vives y (me) contagias las cosas que te gustan.

Gracias a ambos por llevarme de la mano en este largo camino, por vuestra ayuda en cada paso, por vuestro apoyo en cada traspiés y por siempre estar ahí para mí. Sois los mejores padres y amigos con los que se puede soñar y no hay día que no me sienta un privilegiado por haber nacido donde he nacido.

I feel proud to have reached this point, but I feel even prouder of how and with whom I have reached it.

Me siento orgulloso de haber llegado aquí, pero me siento más orgulloso aún de cómo y con quién lo he hecho.

SUPPLEMENTARY MATERIAL

Supplementary figures

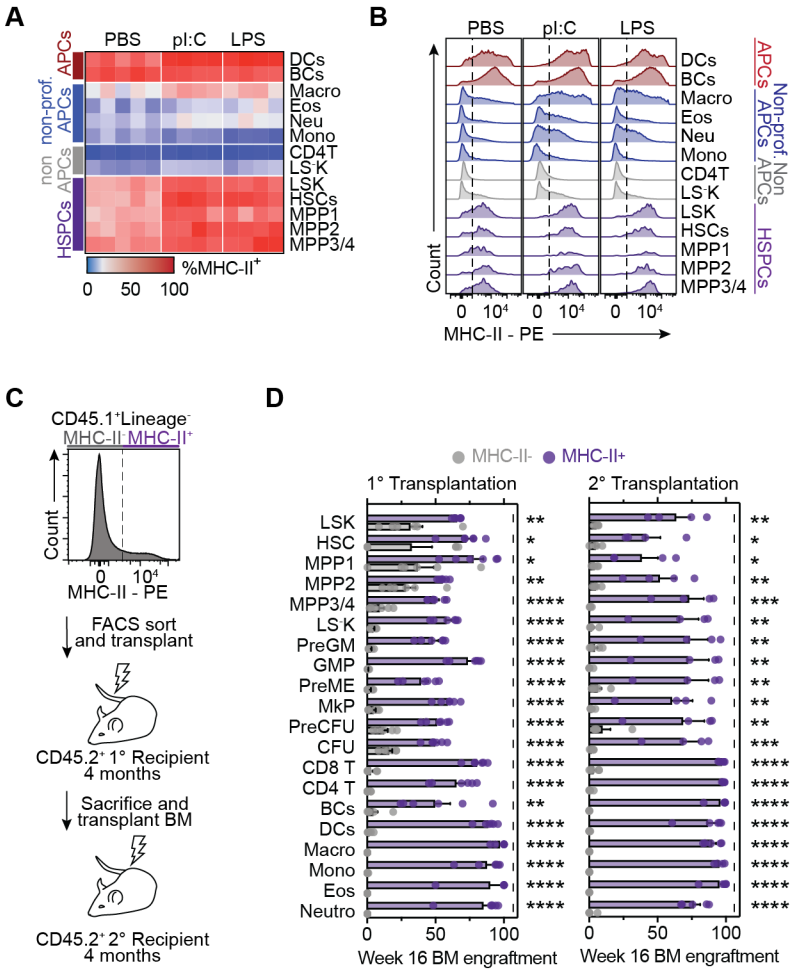

Supplementary Figure 1. MHC-II expression and regulation in mouse HSPCs.
(**A** and **B**) MHC-II surface measurements by flow cytometry of indicated populations at homeostasis or 24 hours post LPS or pI:C treatment. Representative histograms with dashed lines indicating thresholds for gating (**B**). Heatmap summarizing MHC-II surface (**A**), *n=4-5*. (**C**) Experimental design corresponding to Figure 7F and Supplementary Figure 1D. (**D**) Bone marrow engraftment levels of transplanted MHC-II bone marrow populations across different mature and progenitor cell types at the endpoint of the primary (left, 4 months post primary) and secondary (right, 4 months post-secondary) transplantations, *n=4-6*. Individual values are depicted in **A** and means and SEM are depicted **D**. No significance = ns, P<0.05 *, P<0.01 **, P<0.001 ***, P<0.0001 ****. One-way ANOVA (**D**) was performed as discovery test, followed by unpaired two-tailed t-tests as post-hoc tests. In case of multiple comparisons, p-values were corrected according to Benjamini-Hochberg.

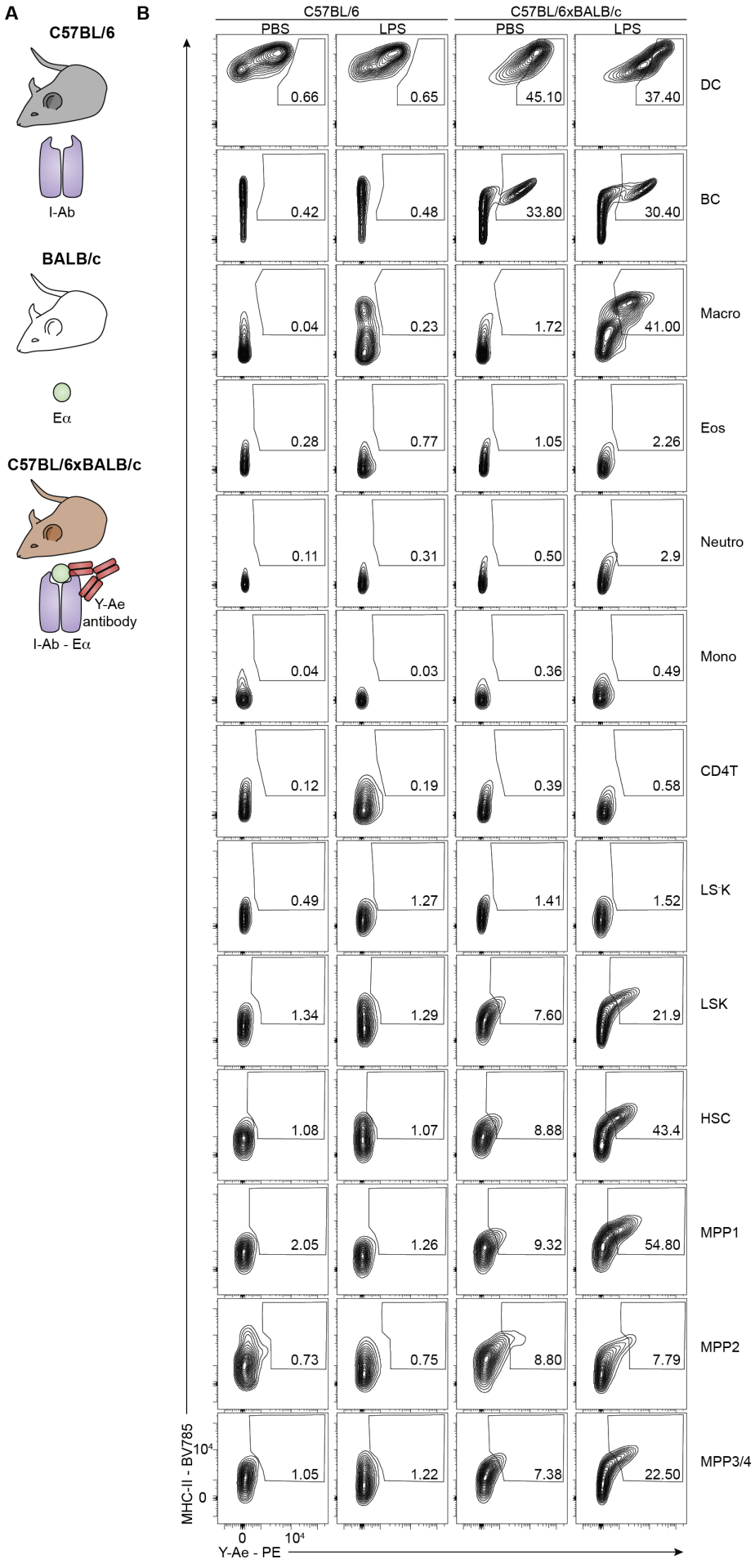
A
C57BL/6
I-Ab
BALB/c
Eα
C57BL/6xBALB/c
Y-Ae antibody
I-Ab - Eα
B
C57BL/6
C57BL/6xBALB/c
PBS
LPS
PBS
LPS
DC
0.66
0.65
45.10
37.40
BC
0.42
0.48
33.80
30.40
Macro
0.04
0.23
1.72
41.00
Eos
0.28
0.77
1.05
2.26
Neutro
0.11
0.31
0.50
2.9
Mono
0.04
0.03
0.36
0.49
CD4T
0.12
0.19
0.39
0.58
LS-K
0.49
1.27
1.41
1.52
LSK
1.34
1.29
7.60
21.9
HSC
1.08
1.07
8.88
43.4
MPP1
2.05
1.26
9.32
54.80
MPP2
0.73
0.75
8.80
7.79
MPP3/4
1.05
1.22
7.38
22.50
MHC-II - BV785
10⁴
0
0
10⁴
Y-Ae - PE

Supplementary Figure 2. Self-presentation experimental approach.
(**A**) Schematic illustration related Figure 8D and E and supplementary figure 2B. The presence of the I-A^d haplotype and Eα peptide in each of the used mouse strains and ability of Y-Ae antibody to bind only the combination of both is displayed. (**B**) Representative flow cytometry plots of in vivo antigen presentation assay of Figure 8D and E. Numbers represent percentages of cells inside the gates. The Y-Ae antibody was used to measure presentation of Eα via MHC-II in C57BL/6xBALB/c mice and control C57BL/6 mice 24 hours post PBS or LPS injection. Boxes indicate quantified populations.

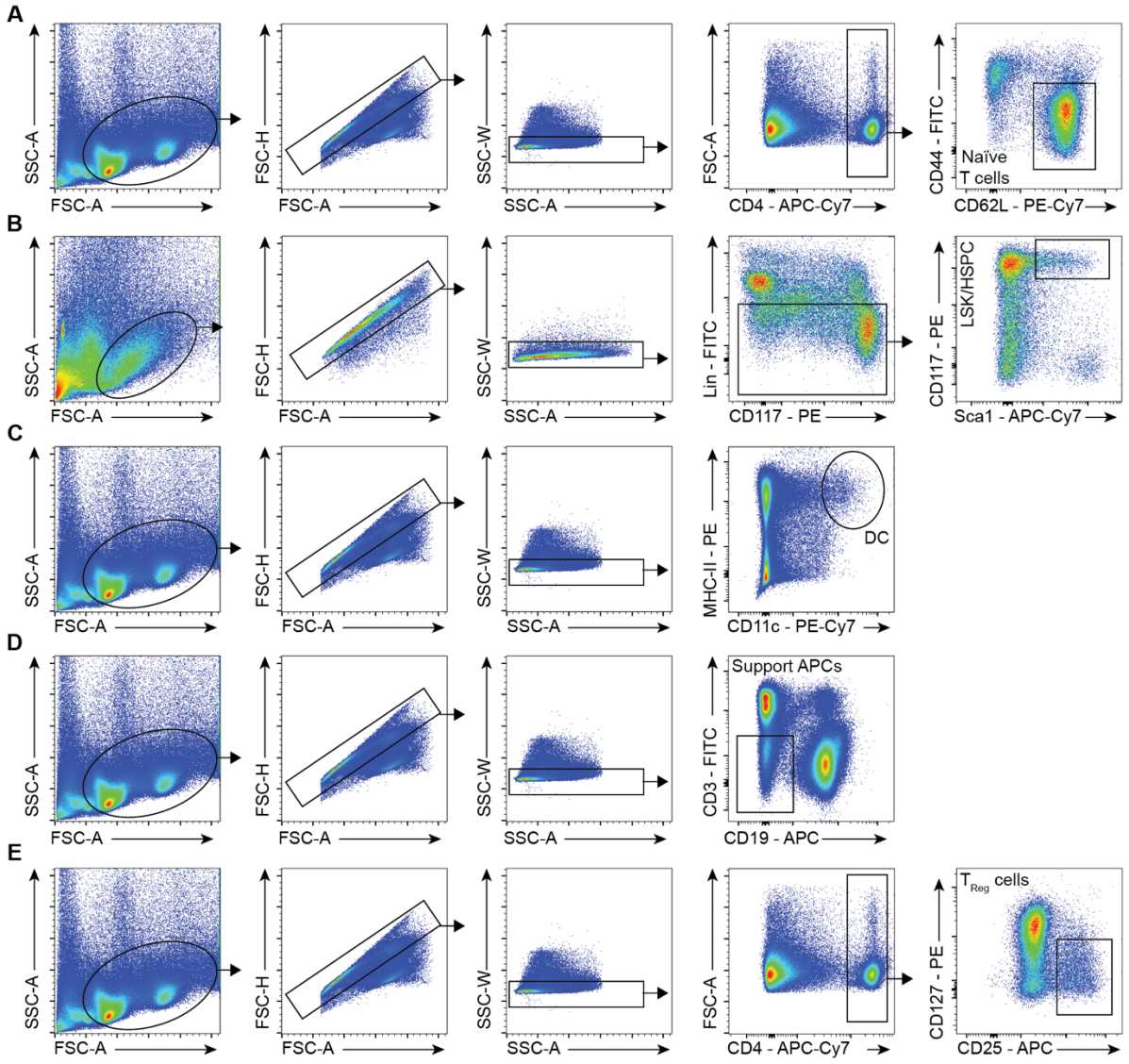

Supplementary Figure 3. Flow cytometry gating strategies I.
(**A**) Murine naïve $CD4^+$ T cells. (**B**) Murine HSPCs/LSKs. (**C**) Murine dendritic Cells. (**D**) Murine splenocytes for *in vitro* suppression assay. (**E**) Murine Treg cells for *in vitro* suppression assay.

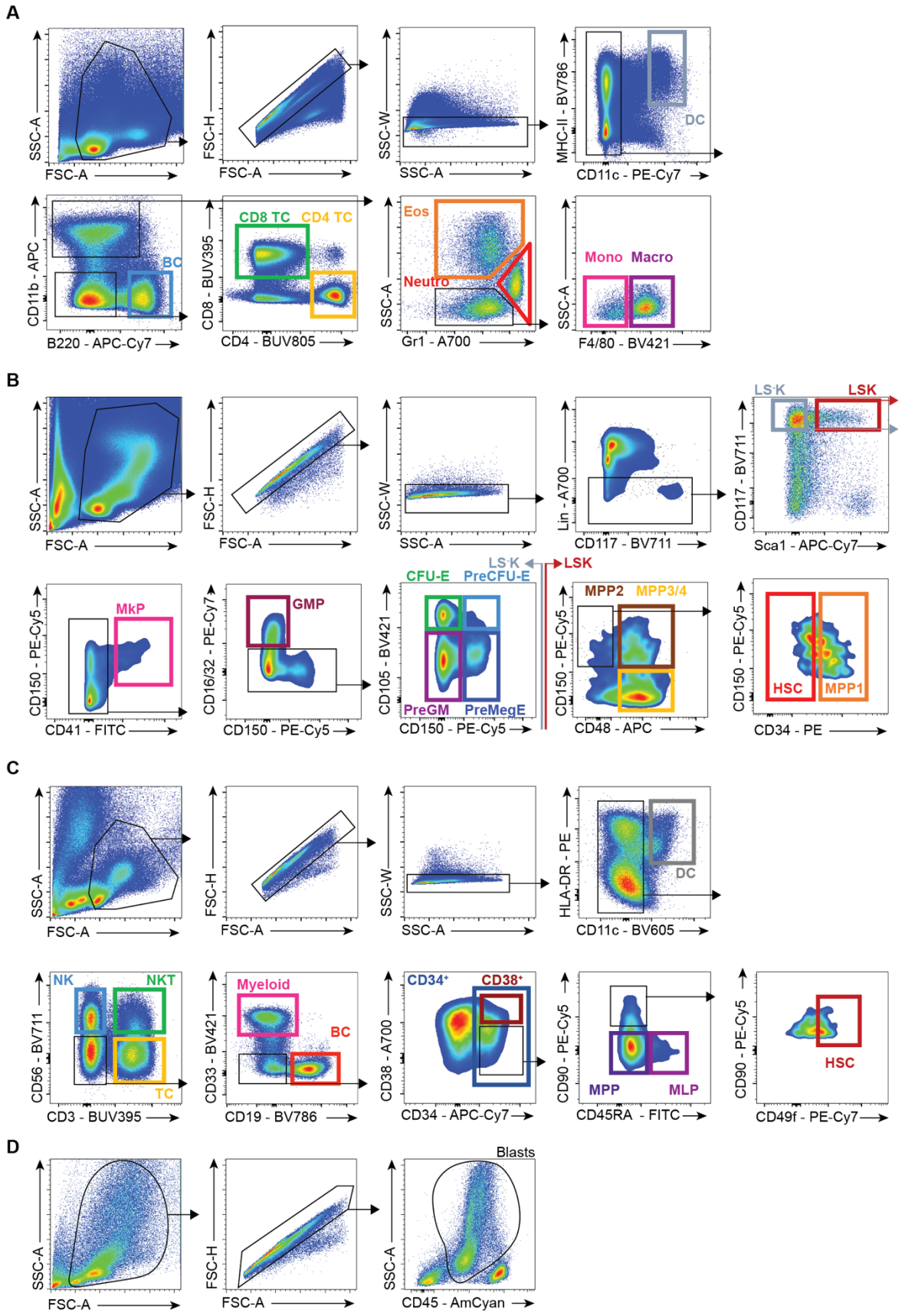

Supplementary Figure 4. Flow cytometry gating strategies II.
(**A**) Murine mature cell populations gated for different analyses in blood, spleen and bone marrow. (**B**) Murine stem and progenitor populations gated for different analyses and sorts. (**C**) Human mature and

stem and progenitor gating strategies for analyses and sorts throughout the study. (**D**) Gating strategy for human AML blasts cells in the EuroFlow panels.

List of abbreviations

AA ..... Aplastic Anemia
AD ..... Allelic Dropout
AF ..... Allele Frequency
AML ..... Acute Myeloid Leukemia
APC ..... Antigen Presenting Cell
APL ..... Acute Promyelocytic Leukemia
BC ..... B Cell
BCR ..... B Cell Receptor
CBL ..... Casitas B-lineage Lymphoma
CHIP ..... Clonal Hematopoiesis of Indeterminate Potential
CIITA ..... Class II major histocompatibility complex Transactivator
CLIP ..... Class II invariant chain-associated peptide
CS ..... CytoStim
CTV ..... CellTrace Violet
DC ..... Dendritic Cell
DNMT3A ..... DNA (cytosine-5)-methyltransferase 3A
ER ..... Early Remission
FLT3 ..... Fms Related Receptor Tyrosine Kinase 3
FDR ..... False Discovery Rate
FPR ..... False Positive Rate
gMFI ..... Geometric Mean Fluorescence Intensity
GMP ..... Granulocyte-Monocyte Progenitor
GSEA ..... Gene Set Enrichment Analysis
GVHD ..... Graft-Versus-Host Disease
GVL ..... Graft-Versus-Leukemia
HLA ..... Human Leukocyte Antigen
HSC ..... Hematopoietic Stem Cell
HSPC ..... Hematopoietic Stem and Progenitor Cell
IDH ..... Isocitrate dehydrogenase
IF ..... Intrafemoral
IFN ..... Interferon
IL ..... Interleukin
IL2R/CD25 ..... Interleukin 2 Receptor
IP ..... Intraperitoneal
ITD ..... Internal tandem duplication
iTreg ..... Induced Regulatory T cell

IV..... Intravenous
KO ..... Knock-Out
LOH ..... Loss of Heterozygosity
LPS ..... Lipopolysaccharide
LSC ..... Leukemic Stem cell
LSK ..... Lineage$^-$Sca-1$^+$cKit$^+$
LTR ..... Long Term Remission
MDSC ..... Myeloid Derived Suppressive Cell
MEP..... Megakaryocyte Erythroid Progenitor
MFI..... Mean Fluorescence Intensity
MHC..... Major Histocompatibility Complex
MLL/KMT2A ..... Histone-lysine N-methyltransferase 2A
MPP ..... Multipotent Progenitor
mt ..... Mitochondrial genome
NES..... Normalized Enrichment Score
NK ..... Natural Killer
NPM1 ..... Nucleophosmin
nTreg..... Natural Regulatory T cell
nuc ..... Nuclear genome
OVA..... Ovalbumin
pI:C..... Polyinosinic:polycytidylic acid
PP..... (MHC-II-restricted) Peptide Pool
ROS ..... Reactive Oxigen Species
sc..... Single Cell
seq ..... Sequencing
Tam ..... Tamoxifen
TC..... T Cell
TCR..... T Cell Receptor
T_{DC} ..... Dendritic cell-activated T cell
Th ..... Helper T cell
T_{HSC}..... Hematopoietic Stem Cell-activated T cell
TLRs..... Toll-Like Receptors
Tr1..... Type 1 Regulatory T cell
Treg ..... Regulatory T cell
VAF..... Variant Allele Frequency
WT ..... Wild Type
YFP ..... Yellow Fluorescent Protein

Table of figures

Main

Supplementary

References

Adams, P. D., Jasper, H. and Rudolph, K. L. (2015) 'Aging-Induced Stem Cell Mutations as Drivers for Disease and Cancer', *Cell Stem Cell*, 16(6), pp. 601–612. doi: 10.1016/j.stem.2015.05.002.

Aiden, E. L. and Casellas, R. (2015) 'Somatic Rearrangement in B Cells: It's (Mostly) Nuclear Physics', *Cell*, 162(4), pp. 708–711. doi: 10.1016/j.cell.2015.07.034.

Akira, S., Uematsu, S. and Takeuchi, O. (2006) 'Pathogen Recognition and Innate Immunity', *Cell*, 124(4), pp. 783–801. doi: 10.1016/j.cell.2006.02.015.

Ali, M. A. E. and Park, C. Y. (2020) 'A new view of hematopoiesis during inflammation', *Blood*, 136(10), pp. 1117–1118. doi: 10.1182/blood.2020006887.

Ali, N. *et al.* (2017) 'Regulatory T Cells in Skin Facilitate Epithelial Stem Cell Differentiation', *Cell*. Elsevier Inc., 169(6), pp. 1119-1129.e11. doi: 10.1016/j.cell.2017.05.002.

Alshetaiwi, H. *et al.* (2020) 'Defining the emergence of myeloid-derived suppressor cells in breast cancer using single-cell transcriptomics', *Science Immunology*, 5(44), p. eaay6017. doi: 10.1126/sciimmunol.aay6017.

Alspach, E. *et al.* (2019) 'MHC-II neoantigens shape tumour immunity and response to immunotherapy.', *Nature*. Springer US, 574(February). doi: 10.1038/s41586-019-1671-8.

Alt, F. W. *et al.* (1992) 'VDJ recombination', *Immunology Today*, 13(8), pp. 306–314. doi: 10.1016/0167-5699(92)90043-7.

Arpaia, N. *et al.* (2015) 'A Distinct Function of Regulatory T Cells in Tissue Protection', *Cell*. Elsevier Inc., 162(5), pp. 1078–1089. doi: 10.1016/j.cell.2015.08.021.

Asada, N., Takeishi, S. and Frenette, P. S. (2017) 'Complexity of bone marrow hematopoietic stem cell niche', *International Journal of Hematology*. Springer Japan. doi: 10.1007/s12185-017-2262-9.

Baccin, C. *et al.* (2020) 'Combined single-cell and spatial transcriptomics reveal the molecular, cellular and spatial bone marrow niche organization', *Nature Cell Biology*, 22(1), pp. 38–48. doi: 10.1038/s41556-019-0439-6.

Baldridge, M. T. *et al.* (2010) 'Quiescent haematopoietic stem cells are activated by IFN-γ in response to chronic infection', *Nature*. Nature Publishing Group, 465(7299), pp. 793–797. doi: 10.1038/nature09135.

Barnden, M. J. *et al.* (1998) 'Defective TCR expression in transgenic mice constructed using cDNA-based α- and β-chain genes under the control of heterologous regulatory elements', *Immunology and Cell Biology*, 76(1), pp. 34–40. doi: 10.1046/j.1440-1711.1998.00709.x.

Barrett, A. J. (2020) 'Acute myeloid leukaemia and the immune system: implications for immunotherapy', *British Journal of Haematology*, 188(1), pp. 147–158. doi:

10.1111/bjh.16310.

Beatty, G. L. and Gladney, W. L. (2015) 'Immune Escape Mechanisms as a Guide for Cancer Immunotherapy', *Clinical Cancer Research*, 21(4), pp. 687–692. doi: 10.1158/1078-0432.CCR-14-1860.

Becht, E. *et al.* (2019) 'Dimensionality reduction for visualizing single-cell data using UMAP', *Nature Biotechnology*, 37(1), pp. 38–44. doi: 10.1038/nbt.4314.

Berard, M. and Tough, D. F. (2002) 'Qualitative differences between naïve and memory T cells.', *Immunology*, 106(2), pp. 127–38. doi: 10.1046/j.1365-2567.2002.01447.x.

Berlin, C. *et al.* (2015) 'Mapping the HLA ligandome landscape of acute myeloid leukemia: a targeted approach toward peptide-based immunotherapy', *Leukemia*, 29(3), pp. 647–659. doi: 10.1038/leu.2014.233.

Bettelli, E. *et al.* (2003) 'Myelin Oligodendrocyte Glycoprotein–specific T Cell Receptor Transgenic Mice Develop Spontaneous Autoimmune Optic Neuritis', *Journal of Experimental Medicine*, 197(9), pp. 1073–1081. doi: 10.1084/jem.20021603.

Bill, M. *et al.* (2020) 'Mutations associated with a 17-gene leukemia stem cell score and the score's prognostic relevance in the context of the European LeukemiaNet classification of acute myeloid leukemia', *Haematologica*, 105(3), pp. 721–729. doi: 10.3324/haematol.2019.225003.

Biton, M. *et al.* (2018) 'T Helper Cell Cytokines Modulate Intestinal Stem Cell Renewal and Differentiation', *Cell*. Elsevier Inc., 175(5), pp. 1307-1320.e22. doi: 10.1016/j.cell.2018.10.008.

Blanpain, C. and Fuchs, E. (2009) 'Epidermal homeostasis: a balancing act of stem cells in the skin', *Nature Reviews Molecular Cell Biology*, 10(3), pp. 207–217. doi: 10.1038/nrm2636.

Boettcher, S. and Manz, M. G. (2017) 'Regulation of Inflammation- and Infection-Driven Hematopoiesis', *Trends in Immunology*, 38(5), pp. 345–357. doi: 10.1016/j.it.2017.01.004.

Bonilla, F. A. and Oettgen, H. C. (2010) 'Adaptive immunity', *Journal of Allergy and Clinical Immunology*, 125(2), pp. S33–S40. doi: 10.1016/j.jaci.2009.09.017.

Bourdely, P. *et al.* (2020) 'Transcriptional and Functional Analysis of CD1c+ Human Dendritic Cells Identifies a CD163+ Subset Priming CD8+CD103+ T Cells', *Immunity*, 53(2), pp. 335-352.e8. doi: 10.1016/j.immuni.2020.06.002.

Bowman, R. L., Busque, L. and Levine, R. L. (2018) 'Clonal Hematopoiesis and Evolution to Hematopoietic Malignancies', *Cell Stem Cell*. Elsevier Inc., 22(2), pp. 157–170. doi: 10.1016/j.stem.2018.01.011.

Brennecke, P. *et al.* (2015) 'Single-cell transcriptome analysis reveals coordinated ectopic gene-expression patterns in medullary thymic epithelial cells', *Nature Immunology*, 16(9), pp. 933–941. doi: 10.1038/ni.3246.

ten Broeke, T., Wubbolts, R. and Stoorvogel, W. (2013) 'MHC Class II Antigen Presentation by

Dendritic Cells Regulated through Endosomal Sorting', *Cold Spring Harbor Perspectives in Biology*, 5(12), pp. a016873–a016873. doi: 10.1101/cshperspect.a016873.

Broudy, V. C. and Fitchen, J. H. (1986) 'Class II MHC Antigens and Hematopoiesis', in *HLA Class II Antigens*. Berlin, Heidelberg: Springer Berlin Heidelberg, pp. 386–401. doi: 10.1007/978-3-642-70367-6_22.

Broxmeyer, H. E. *et al.* (2002) 'Th1 cells regulate hematopoietic progenitor cell homeostasis by production of Oncostatin M', *Immunity*, 16(6), pp. 815–825. doi: 10.1016/S1074-7613(02)00319-9.

Burzyn, D. *et al.* (2013) 'A Special Population of Regulatory T Cells Potentiates Muscle Repair', *Cell*. Elsevier Inc., 155(6), pp. 1282–1295. doi: 10.1016/j.cell.2013.10.054.

Charrad, M. *et al.* (2014) 'Nbclust: An R package for determining the relevant number of clusters in a data set', *Journal of Statistical Software*. American Statistical Association, 61(6), pp. 1–36. doi: 10.18637/jss.v061.i06.

Chavakis, T., Mitroulis, I. and Hajishengallis, G. (2019) 'Hematopoietic progenitor cells as integrative hubs for adaptation to and fine-tuning of inflammation', *Nature Immunology*. Springer US, 20(7), pp. 802–811. doi: 10.1038/s41590-019-0402-5.

Chen, A., Hu, S. and Wang, Q.-F. (2019) 'Tumor heterogeneity of acute myeloid leukemia: insights from single-cell sequencing', *Blood Science*, 1(1), pp. 73–76. doi: 10.1097/BS9.0000000000000015.

Chen, L. and Flies, D. B. (2013) 'Molecular mechanisms of T cell co-stimulation and co-inhibition', *Nature Reviews Immunology*, 13(4), pp. 227–242. doi: 10.1038/nri3405.

Cheng, M. and Anderson, M. S. (2018) 'Thymic tolerance as a key brake on autoimmunity', *Nature Immunology*. Springer US, 19(July), p. 1. doi: 10.1038/s41590-018-0128-9.

Chihara, N. *et al.* (2018) 'Induction and transcriptional regulation of the co-inhibitory gene module in T cells', *Nature*, 558(7710), pp. 454–459. doi: 10.1038/s41586-018-0206-z.

Cho, B. K. *et al.* (1999) 'Functional differences between memory and naive CD8 T cells', *Proceedings of the National Academy of Sciences*, 96(6), pp. 2976–2981. doi: 10.1073/pnas.96.6.2976.

Christopher, M. J. *et al.* (2018) 'Immune Escape of Relapsed AML Cells after Allogeneic Transplantation', *New England Journal of Medicine*, 379(24), pp. 2330–2341. doi: 10.1056/NEJMoa1808777.

Chu, S. H. *et al.* (2012) 'FLT3-ITD Knockin Impairs Hematopoietic Stem Cell Quiescence/Homeostasis, Leading to Myeloproliferative Neoplasm', *Cell Stem Cell*, 11(3), pp. 346–358. doi: 10.1016/j.stem.2012.05.027.

Cibulskis, K. *et al.* (2013) 'Sensitive detection of somatic point mutations in impure and heterogeneous cancer samples', *Nature Biotechnology*, 31(3), pp. 213–219. doi: 10.1038/nbt.2514.

Clevers, H. (2013) 'The Intestinal Crypt, A Prototype Stem Cell Compartment', *Cell*, 154(2), pp. 274–284. doi: 10.1016/j.cell.2013.07.004.

Clevers, H. (2015) 'What is an adult stem cell?', *Science*, 350(6266), pp. 1319–1320. doi: 10.1126/science.aad7016.

Collison, L. W. *et al.* (2007) 'The inhibitory cytokine IL-35 contributes to regulatory T-cell function', *Nature*, 450(7169), pp. 566–569. doi: 10.1038/nature06306.

Collison, L. W. *et al.* (2010) 'IL-35-mediated induction of a potent regulatory T cell population', *Nature Immunology*. Nature Publishing Group, 11(12), pp. 1093–1101. doi: 10.1038/ni.1952.

Corces-Zimmerman, M. R. *et al.* (2014) 'Preleukemic mutations in human acute myeloid leukemia affect epigenetic regulators and persist in remission', *Proceedings of the National Academy of Sciences*, 111(7), pp. 2548–2553. doi: 10.1073/pnas.1324297111.

Corthay, A. (2006) 'A Three-cell Model for Activation of Naïve T Helper Cells', *Scandinavian Journal of Immunology*, 64(2), pp. 93–96. doi: 10.1111/j.1365-3083.2006.01782.x.

Costello, R. *et al.* (1999) 'The immunophenotype of minimally differentiated acute myeloid leukemia (AML-M0): reduced immunogenicity and high frequency of CD34+/CD38− leukemic progenitors', *Leukemia*, 13(10), pp. 1513–1518. doi: 10.1038/sj.leu.2401519.

Crane, G. M., Jeffery, E. and Morrison, S. J. (2017) 'Adult haematopoietic stem cell niches', *Nature Reviews Immunology*. Nature Publishing Group, 17(9), pp. 573–590. doi: 10.1038/nri.2017.53.

Curtsinger, J. M. and Mescher, M. F. (2010) 'Inflammatory cytokines as a third signal for T cell activation', *Current Opinion in Immunology*, 22(3), pp. 333–340. doi: 10.1016/j.coi.2010.02.013.

Dang, L., Jin, S. and Su, S. M. (2010) 'IDH mutations in glioma and acute myeloid leukemia.', *Trends in molecular medicine*, 16(9), pp. 387–97. doi: 10.1016/j.molmed.2010.07.002.

Dempsey, P. W., Vaidya, S. A. and Cheng, G. (2003) 'The Art of War: Innate and adaptive immune responses', *Cellular and Molecular Life Sciences (CMLS)*, 60(12), pp. 2604–2621. doi: 10.1007/s00018-003-3180-y.

Deng, X.-Z. *et al.* (2018) 'Associations between the HLA-A/B/DRB1 polymorphisms and aplastic anemia: evidence from 17 case–control studies', *Hematology*, 23(3), pp. 154–162. doi: 10.1080/10245332.2017.1375064.

Dent, A. L. and Kaplan, M. H. (2008) 'T cell regulation of hematopoiesis', *Frontiers in Bioscience*, 13, pp. 6229–6236.

Dey, S. S. *et al.* (2015) 'Integrated genome and transcriptome sequencing of the same cell', *Nature Biotechnology*, 33(3), pp. 285–289. doi: 10.1038/nbt.3129.

Dhaliwal, J. S. *et al.* (2011) 'Susceptibility to aplastic anemia is associated with HLA-DRB1*1501 in an aboriginal population in Sabah, Malaysia', *Human Immunology*. Elsevier Inc., 72(10), pp.

889–892. doi: 10.1016/j.humimm.2011.06.013.

Dobin, A. *et al.* (2013) 'STAR: ultrafast universal RNA-seq aligner', *Bioinformatics*, 29(1), pp. 15–21. doi: 10.1093/bioinformatics/bts635.

van Dongen, J. J. M. *et al.* (2012) 'EuroFlow antibody panels for standardized n-dimensional flow cytometric immunophenotyping of normal, reactive and malignant leukocytes', *Leukemia*, 26(9), pp. 1908–1975. doi: 10.1038/leu.2012.120.

Doulatov, S. *et al.* (2012) 'Hematopoiesis: A Human Perspective', *Cell Stem Cell*. Elsevier Inc., 10(2), pp. 120–136. doi: 10.1016/j.stem.2012.01.006.

Driessens, G., Kline, J. and Gajewski, T. F. (2009) 'Costimulatory and coinhibitory receptors in anti-tumor immunity', *Immunological Reviews*, 229(1), pp. 126–144. doi: 10.1111/j.1600-065X.2009.00771.x.

Dunn, G. P. *et al.* (2002) 'Cancer immunoediting: from immunosurveillance to tumor escape', *Nature Immunology*, 3(11), pp. 991–998. doi: 10.1038/ni1102-991.

Durbin, J. E. *et al.* (1996) 'Targeted Disruption of the Mouse Stat1 Gene Results in Compromised Innate Immunity to Viral Disease', *Cell*, 84(3), pp. 443–450. doi: 10.1016/S0092-8674(00)81289-1.

Eaves, C. (2015) 'Hematopoietic stem cells: concepts, definitions, and the new reality', *Blood*, 125(17), pp. 2605–2614. doi: 10.1182/blood-2014-12-570200.Lessons.

Ebrahim, E. K. *et al.* (2016) 'FLT3 internal tandem duplication mutation, cMPL and CD34 expressions predict low survival in acute myeloid leukemia patients', *Annals of Clinical and Laboratory Science*, 46(6), pp. 592–600.

Eppert, K. *et al.* (2011) 'Stem cell gene expression programs influence clinical outcome in human leukemia', *Nature medicine*. Nature Publishing Group, 17(9), pp. 1086–1093. doi: 10.1038/nm.2415.

Espin-Palazon, R. *et al.* (2018) 'Proinflammatory Signals as Fuel for the Fire of Hematopoietic Stem Cell Emergence', *Trends in Cell Biology*. Elsevier Ltd, 28(1), pp. 58–66. doi: 10.1016/j.tcb.2017.08.003.

Essers, M. A. G. *et al.* (2009) 'IFNα activates dormant haematopoietic stem cells in vivo', *Nature*. Nature Publishing Group, 458(7240), pp. 904–908. doi: 10.1038/nature07815.

Essers, M. A. G. and Trumpp, A. (2010) 'Targeting leukemic stem cells by breaking their dormancy', *Molecular Oncology*. Elsevier B.V, 4(5), pp. 443–450. doi: 10.1016/j.molonc.2010.06.001.

Falini, B. *et al.* (2019) 'IDH1-R132 changes vary according to NPM1 and other mutations status in AML.', *Leukemia*, 33(4), pp. 1043–1047. doi: 10.1038/s41375-018-0299-2.

Falk, K. *et al.* (1991) 'Allele-specific motifs revealed by sequencing of self-peptides eluted from MHC molecules', *Nature*, 351(6324), pp. 290–296. doi: 10.1038/351290a0.

Falkenburg, J. H. F. *et al.* (1984) 'Polymorphic and Monomorphic HLA-DR Determinants on Human Hematopoietic Progenitor Cells', *Blood*, 63(5), pp. 1125–1132.

Falkenburg, J. H. F. *et al.* (1985) 'Human Hematopoietic Progenitor Cells in Long-Term Cultures Express HLA-DR Antigens and Lack HLA-DQ Antigens', *Journal of Experimental Medicine*, 162(October), pp. 1359–1369.

Fathman, C. G. and Lineberry, N. B. (2007) 'Molecular mechanisms of CD4+ T-cell anergy', *Nature Reviews Immunology*, 7(8), pp. 599–609. doi: 10.1038/nri2131.

Feuerer, M. *et al.* (2003) 'Bone marrow as a priming site for T-cell responses to blood-borne antigen', *Nature Medicine*, 9(9), pp. 1151–1157. doi: 10.1038/nm914.

Filbin, M. G. *et al.* (2018) 'Developmental and oncogenic programs in H3K27M gliomas dissected by single-cell RNA-seq', *Science*, 360(6386), pp. 331–335. doi: 10.1126/science.aao4750.

Finkielsztein, A. *et al.* (2015) 'Human megakaryocyte progenitors derived from hematopoietic stem cells of normal individuals are MHC class II-expressing professional APC that enhance Th17 and Th1/Th17 responses', *Immunology Letters*. Elsevier B.V., 163(1), pp. 84–95. doi: 10.1016/j.imlet.2014.11.013.

Fitchen, J. H., Foon, K. A. and Cline, M. J. (1981) 'The Expression of Histocompatibility-2 Antigens on Hemopoietic Stem Cells', *New England Journal of Medicine*, 305(1). doi: 10.1056/NEJM198107023050104.

Fitzgerald, K. A. and Kagan, J. C. (2020) 'Toll-like Receptors and the Control of Immunity', *Cell*, 180(6), pp. 1044–1066. doi: 10.1016/j.cell.2020.02.041.

Francisco, L. M. *et al.* (2009) 'PD-L1 regulates the development, maintenance, and function of induced regulatory T cells', *The Journal of Experimental Medicine*, 206(13), pp. 3015–3029. doi: 10.1084/jem.20090847.

Fujisaki, J. *et al.* (2011) 'In vivo imaging of Treg cells providing immune privilege to the haematopoietic stem-cell niche', *Nature*, 474(7350), pp. 216–219. doi: 10.1038/nature10160.

van Galen, P. *et al.* (2019) 'Single-Cell RNA-Seq Reveals AML Hierarchies Relevant to Disease Progression and Immunity', *Cell*. Elsevier Inc., 0(0), pp. 1265-1281.e24. doi: 10.1016/j.cell.2019.01.031.

Gasteiger, G. *et al.* (2017) 'Cellular Innate Immunity: An Old Game with New Players', *Journal of Innate Immunity*, 9(2), pp. 111–125. doi: 10.1159/000453397.

Gebe, J. A. *et al.* (2001) 'T Cell Selection and Differential Activation on Structurally Related HLA-DR4 Ligands', *The Journal of Immunology*, 167(6), pp. 3250–3256. doi: 10.4049/jimmunol.167.6.3250.

Genovese, G. *et al.* (2014) 'Clonal Hematopoiesis and Blood-Cancer Risk Inferred from Blood DNA Sequence', *New England Journal of Medicine*, 371(26), pp. 2477–2487. doi: 10.1056/NEJMoa1409405.

Germain, R. N. (1994) 'MHC-dependent antigen processing and peptide presentation: Providing ligands for T lymphocyte activation', *Cell*, 76(2), pp. 287–299. doi: 10.1016/0092-8674(94)90336-0.

Gerritsen, M. *et al.* (2019) 'RUNX1 mutations enhance self-renewal and block granulocytic differentiation in human in vitro models and primary AMLs', *Blood Advances*, 3(3), pp. 320–332. doi: 10.1182/bloodadvances.2018024422.

Giampaolo, S. *et al.* (2017) 'Interleukin-2-regulatory T cell axis critically regulates maintenance of hematopoietic stem cells', *Oncotarget*, 8(18), pp. 29625–29642. doi: 10.18632/oncotarget.16377.

Giustacchini, A. *et al.* (2017) 'Single-cell transcriptomics uncovers distinct molecular signatures of stem cells in chronic myeloid leukemia', *Nature Medicine*, 23(6), pp. 692–702. doi: 10.1038/nm.4336.

Godkin, A. J. *et al.* (2001) 'Naturally Processed HLA Class II Peptides Reveal Highly Conserved Immunogenic Flanking Region Sequence Preferences That Reflect Antigen Processing Rather Than Peptide-MHC Interactions', *The Journal of Immunology*, 166(11), pp. 6720–6727. doi: 10.4049/jimmunol.166.11.6720.

Goodnow, C. C. *et al.* (2005) 'Cellular and genetic mechanisms of self tolerance and autoimmunity', *Nature*, 435(7042), pp. 590–597. doi: 10.1038/nature03724.

Greaves, M. (2016) 'Leukaemia "firsts" in cancer research and treatment', *Nature Reviews Cancer*, 16(3), pp. 163–172. doi: 10.1038/nrc.2016.3.

Griffin, J. D. *et al.* (1983) 'Surface marker analysis of acute myeloblastic leukemia: identification of differentiation-associated phenotypes.', *Blood*, 62(3), pp. 557–63.

Gu, Z., Eils, R. and Schlesner, M. (2016) 'Complex heatmaps reveal patterns and correlations in multidimensional genomic data', *Bioinformatics*, 32(18), pp. 2847–2849. doi: 10.1093/bioinformatics/btw313.

Guermonprez, P. *et al.* (2002) 'Antigen Presentation and T Cell Stimulation by Dendritic Cells', *Annual Review of Immunology*, 20(1), pp. 621–667. doi: 10.1146/annurev.immunol.20.100301.064828.

Gupta, P. K. *et al.* (2019) 'The pursuit of transplantation tolerance : new mechanistic insights', *Cellular & Molecular Immunology*. Springer US, (January). doi: 10.1038/s41423-019-0203-7.

Haas, S. *et al.* (2015) 'Inflammation-Induced Emergency Megakaryopoiesis Driven by Hematopoietic Stem Cell-like Megakaryocyte Progenitors', *Cell Stem Cell*, 17(4), pp. 422–434. doi: 10.1016/j.stem.2015.07.007.

Haas, S., Trumpp, A. and Milsom, M. D. (2018) 'Causes and Consequences of Hematopoietic Stem Cell Heterogeneity', *Cell Stem Cell*, 22(5), pp. 627–638. doi: 10.1016/j.stem.2018.04.003.

Hanahan, D. and Weinberg, R. A. (2011) 'Hallmarks of cancer: The next generation', *Cell*. Elsevier Inc., 144(5), pp. 646–674. doi: 10.1016/j.cell.2011.02.013.

Hay, S. B. *et al.* (2018) 'The Human Cell Atlas bone marrow single-cell interactive web portal', *Experimental Hematology*. Elsevier Inc., 68, pp. 51–61. doi: 10.1016/j.exphem.2018.09.004.

Hennig, B. P. *et al.* (2018) 'Large-Scale Low-Cost NGS Library Preparation Using a Robust Tn5 Purification and Tagmentation Protocol', *G3: Genes|Genomes|Genetics*, 8(1), pp. 79–89. doi: 10.1534/g3.117.300257.

Henri, S. *et al.* (2010) 'CD207+ CD103+ dermal dendritic cells cross-present keratinocyte-derived antigens irrespective of the presence of Langerhans cells', *The Journal of Experimental Medicine*, 207(1), pp. 189–206. doi: 10.1084/jem.20091964.

Hepworth, M. R. *et al.* (2013) 'Innate lymphoid cells regulate CD4+ T-cell responses to intestinal commensal bacteria.', *Nature*, 498(7452), pp. 113–7. doi: 10.1038/nature12240.

Hérault, A. *et al.* (2017) 'Myeloid progenitor cluster formation drives emergency and leukaemic myelopoiesis', *Nature*. Nature Publishing Group, 544(7648), pp. 53–58. doi: 10.1038/nature21693.

Hie, B., Bryson, B. and Berger, B. (2019) 'Efficient integration of heterogeneous single-cell transcriptomes using Scanorama', *Nature Biotechnology*, 37(6), pp. 685–691. doi: 10.1038/s41587-019-0113-3.

Hilligan, K. L. and Ronchese, F. (2020) 'Antigen presentation by dendritic cells and their instruction of CD4+ T helper cell responses', *Cellular & Molecular Immunology*. Springer US, 17(6), pp. 587–599. doi: 10.1038/s41423-020-0465-0.

Hiltbold, E. M. and Roche, P. A. (2002) 'Trafficking of MHC class II molecules in the late secretory pathway', *Current Opinion in Immunology*, 14(1), pp. 30–35. doi: 10.1016/S0952-7915(01)00295-3.

Hirahara, K. *et al.* (2012) 'Interleukin-27 Priming of T Cells Controls IL-17 Production In trans via Induction of the Ligand PD-L1', *Immunity*, 36(6), pp. 1017–1030. doi: 10.1016/j.immuni.2012.03.024.

Hirata, Y. *et al.* (2018) 'CD150highBone Marrow Tregs Maintain Hematopoietic Stem Cell Quiescence and Immune Privilege via Adenosine', *Cell Stem Cell*. Elsevier Inc., 22(3), pp. 445-453.e5. doi: 10.1016/j.stem.2018.01.017.

Hirche, C. *et al.* (2017) 'Systemic Virus Infections Differentially Modulate Cell Cycle State and Functionality of Long-Term Hematopoietic Stem Cells In Vivo', *Cell Reports*, 19(11), pp. 2345–2356. doi: 10.1016/j.celrep.2017.05.063.

Hirsch, R. *et al.* (1989) 'Effects of in vivo administration of anti-CD3 monoclonal antibody on T cell function in mice.', *The Journal of Immunology*, 140(11), pp. 3766–3772.

Hoebe, K., Janssen, E. and Beutler, B. (2004) 'The interface between innate and adaptive immunity', *Nature Immunology*, 5(10), pp. 971–974. doi: 10.1038/ni1004-971.

Hosen, N. *et al.* (2007) 'CD96 is a leukemic stem cell-specific marker in human acute myeloid leukemia', *Proceedings of the National Academy of Sciences of the United States of America*,

104(26), pp. 11008–11013. doi: 10.1073/pnas.0704271104.

Inaba, M. and Yamashita, Y. M. (2012) 'Asymmetric Stem Cell Division: Precision for Robustness', *Cell Stem Cell*, 11(4), pp. 461–469. doi: 10.1016/j.stem.2012.09.003.

Jaiswal, S. *et al.* (2014) 'Age-related clonal hematopoiesis associated with adverse outcomes.', *The New England journal of medicine*, 371(26), pp. 2488–98. doi: 10.1056/NEJMoa1408617.

Jakubzick, C. V., Randolph, G. J. and Henson, P. M. (2017) 'Monocyte differentiation and antigen-presenting functions', *Nature Reviews Immunology*. Nature Publishing Group, 17(6), pp. 349–362. doi: 10.1038/nri.2017.28.

Jan, M. *et al.* (2011) 'Prospective separation of normal and leukemic stem cells based on differential expression of TIM3, a human acute myeloid leukemia stem cell marker', *Proceedings of the National Academy of Sciences*. National Academy of Sciences, 108(12), pp. 5009–5014. doi: 10.1073/pnas.1100551108.

Janossy, G. *et al.* (1978) 'Cell sorter analysis of leukaemia-associated antigens on human myeloid precursors', *Nature*, 276(5684), pp. 176–178. doi: 10.1038/276176a0.

Jurewicz, M. M. and Stern, L. J. (2019) 'Class II MHC antigen processing in immune tolerance and inflammation', *Immunogenetics*. Immunogenetics, 71(3), pp. 171–187. doi: 10.1007/s00251-018-1095-x.

Käll, L. *et al.* (2007) 'Semi-supervised learning for peptide identification from shotgun proteomics datasets', *Nature Methods*, 4(11), pp. 923–925. doi: 10.1038/nmeth1113.

Kambayashi, T. and Laufer, T. M. (2014) 'Atypical MHC class II-expressing antigen-presenting cells: can anything replace a dendritic cell?', *Nature Reviews Immunology*, 14(11), pp. 719–730. doi: 10.1038/nri3754.

Kaplan, M. H. *et al.* (2011) 'STAT3-dependent IL-21 production from T helper cells regulates hematopoietic progenitor cell homeostasis', *Blood*, 117(23), pp. 6198–6202. doi: 10.1182/blood-2011-02-334367.

Katagiri, T. *et al.* (2011) 'Frequent loss of HLA alleles from hematopoietic stem cells in patients with hepatitis-associated aplastic anemia', *Blood*, 118 (21)(December), pp. 6601–6610. doi: 10.1182/blood-2011-07-365189.

Keir, M. E. *et al.* (2008) 'PD-1 and Its Ligands in Tolerance and Immunity', *Annual Review of Immunology*, 26, pp. 677–704. doi: 10.1146/annurev.immunol.26.021607.090331.

King, K. Y. and Goodell, M. A. (2011) 'Inflammatory modulation of HSCs: viewing the HSC as a foundation for the immune response', *Nature Reviews Immunology*. Nature Publishing Group, 11(10), pp. 685–692. doi: 10.1038/nri3062.

Klein, L., Robey, E. A. and Hsieh, C. (2019) 'Central CD4+ T cell tolerance: deletion versus regulatory T cell differentiation', *Nature Reviews Immunology*. Springer US, 19(1), pp. 7–18. doi: 10.1038/s41577-018-0083-6.

Klimmeck, D. *et al.* (2014) 'Transcriptome-wide Profiling and Posttranscriptional Analysis of Hematopoietic Stem/Progenitor Cell Differentiation toward Myeloid Commitment', *Stem Cell Reports*. The Authors, 3(5), pp. 858–875. doi: 10.1016/j.stemcr.2014.08.012.

Klobuch, S. *et al.* (2020) 'HLA-DPB1 Reactive T Cell Receptors for Adoptive Immunotherapy in Allogeneic Stem Cell Transplantation.', *Cells*, 9(5). doi: 10.3390/cells9051264.

Kobayashi, K. S. and van den Elsen, P. J. (2012) 'NLRC5: a key regulator of MHC class I-dependent immune responses', *Nature Reviews Immunology*, 12(12), pp. 813–820. doi: 10.1038/nri3339.

Kohlmann, A. *et al.* (2010) 'Gene expression profiling in AML with normal karyotype can predict mutations for molecular markers and allows novel insights into perturbed biological pathways', *Leukemia*, 24(6), pp. 1216–1220. doi: 10.1038/leu.2010.73.

Kordasti, S. *et al.* (2016) 'Deep phenotyping of Tregs identifies an immune signature for idiopathic aplastic anemia and predicts response to treatment', *Blood*, 128(9), pp. 1193–1205. doi: 10.1182/blood-2016-03-703702.

Korniotis, S. *et al.* (2020) 'Mobilized Multipotent Hematopoietic Progenitors Stabilize and Expand Regulatory T Cells to Protect Against Autoimmune Encephalomyelitis', *Frontiers in Immunology*, 11(December), pp. 1–13. doi: 10.3389/fimmu.2020.607175.

Kowalewski, D. J. and Stevanović, S. (2013) 'Biochemical Large-Scale Identification of MHC Class I Ligands', in *Methods Mol Biol*, pp. 145–157. doi: 10.1007/978-1-62703-218-6_12.

Kreso, A. and Dick, J. E. (2014) 'Evolution of the cancer stem cell model', *Cell Stem Cell*. Elsevier Inc., 14(3), pp. 275–291. doi: 10.1016/j.stem.2014.02.006.

Krivtsov, A. V *et al.* (2006) 'Transformation from committed progenitor to leukaemia stem cell initiated by MLL-AF9', *Nature*, 442(7104), pp. 818–822. doi: 10.1038/nature04980.

Krivtsov, A. V *et al.* (2013) 'Cell of origin determines clinically relevant subtypes of MLL-rearranged AML.', *Leukemia*, 27(4), pp. 852–60. doi: 10.1038/leu.2012.363.

Kumánovics, A., Takada, T. and Lindahl, K. F. (2003) 'Genomic Organization of the Mammalian MHC', *Annual Review of Immunology*, 21(1), pp. 629–657. doi: 10.1146/annurev.immunol.21.090501.080116.

Kuswanto, W. *et al.* (2016) 'Poor Repair of Skeletal Muscle in Aging Mice Reflects a Defect in Local, Interleukin-33-Dependent Accumulation of Regulatory T Cells', *Immunity*. Elsevier Inc., 44(2), pp. 355–367. doi: 10.1016/j.immuni.2016.01.009.

Kwak, K., Akkaya, M. and Pierce, S. K. (2019) 'B cell signaling in context', *Nature Immunology*, 20(8), pp. 963–969. doi: 10.1038/s41590-019-0427-9.

de la Guardia, R. D. *et al.* (2020) 'Bone marrow clonogenic myeloid progenitors from NPM1-mutated AML patients do not harbor the NPM1 mutation: Implication for the cell-of-origin of NPM1+ AML', *Genes*, 11(1), pp. 1–5. doi: 10.3390/genes11010073.

Lee, J. H., Wang, C. and Kim, C. H. (2009) 'FoxP3+ regulatory T cells restrain splenic extramedullary myelopoiesis via suppression of hemopoietic cytokine-producing T cells.', *Journal of Immunology*, 183(10), pp. 6377–6386. doi: 10.4049/jimmunol.0901268.

Lennon-Duménil, A.-M. *et al.* (2002) 'A closer look at proteolysis and MHC-class-II-restricted antigen presentation', *Current Opinion in Immunology*, 14(1), pp. 15–21. doi: 10.1016/S0952-7915(01)00293-X.

Ley, T. J. *et al.* (2013) 'Genomic and Epigenomic Landscapes of Adult De Novo Acute Myeloid Leukemia', *New England Journal of Medicine*, 368(22), pp. 2059–2074. doi: 10.1056/NEJMoa1301689.

Li, H. *et al.* (2009) 'The Sequence Alignment/Map format and SAMtools', *Bioinformatics*, 25(16), pp. 2078–2079. doi: 10.1093/bioinformatics/btp352.

Li, H. (2013) 'Aligning sequence reads, clone sequences and assembly contigs with BWA-MEM'.

Li, L. *et al.* (2008) 'Knock-in of an internal tandem duplication mutation into murine FLT3 confers myeloproliferative disease in a mouse model', *Blood*, 111(7), pp. 3849–3858. doi: 10.1182/blood-2007-08-109942.

Li, P. *et al.* (2014) 'Th2 lymphocytes migrating to the bone marrow under high-altitude hypoxia promote erythropoiesis via activin A and interleukin-9', *Experimental Hematology*. ISEH - International Society for Experimental Hematology, 42(9), pp. 804–815. doi: 10.1016/j.exphem.2014.04.007.

Liao, D. *et al.* (2019) 'A review of efficacy and safety of checkpoint inhibitor for the treatment of acute myeloid leukemia', *Frontiers in Pharmacology*, 10(JUN), pp. 1–11. doi: 10.3389/fphar.2019.00609.

Liao, Y., Smyth, G. K. and Shi, W. (2014) 'featureCounts: an efficient general purpose program for assigning sequence reads to genomic features', *Bioinformatics*, 30(7), pp. 923–930. doi: 10.1093/bioinformatics/btt656.

Liggett, L. A. and Sankaran, V. G. (2020) 'Unraveling Hematopoiesis through the Lens of Genomics', *Cell*, 182(6), pp. 1384–1400. doi: 10.1016/j.cell.2020.08.030.

Liu, S. *et al.* (2016) 'Association of Human Leukocyte Antigen DRB1*15 and DRB1*15:01 Polymorphisms with Response to Immunosuppressive Therapy in Patients with Aplastic Anemia: A Meta-Analysis', *PLOS ONE*. Edited by J. Devaney, 11(9), p. e0162382. doi: 10.1371/journal.pone.0162382.

Love, M. I., Huber, W. and Anders, S. (2014) 'Moderated estimation of fold change and dispersion for RNA-seq data with DESeq2', *Genome Biology*, 15(12), p. 550. doi: 10.1186/s13059-014-0550-8.

Ludwig, L. S. *et al.* (2019) 'Lineage Tracing in Humans Enabled by Mitochondrial Mutations and Single-Cell Genomics', *Cell*, 176(6), pp. 1325-1339.e22. doi: 10.1016/j.cell.2019.01.022.

Luo, Y. *et al.* (2018) 'M1 and M2 macrophages differentially regulate hematopoietic stem cell self-renewal and ex vivo expansion', *Blood Advances*, 2(8), pp. 859–870. doi: 10.1182/bloodadvances.2018015685.

Macaulay, I. C. *et al.* (2015) 'G&T-seq: parallel sequencing of single-cell genomes and transcriptomes', *Nat Methods*, 12(6), pp. 519–522. doi: 10.1038/nmeth.3370.

Maciejewski, J. P. *et al.* (1996) 'A severe and consistent deficit in marrow and circulating primitive hematopoietic cells (long-term culture-initiating cells) in acquired aplastic anemia.', *Blood*, 88(6), pp. 1983–91.

Maechler, M. *et al.* (2019) 'cluster: Cluster Analysis Basics and Extensions. R package version 2.1.0.'

Majeti, R., Chao, M. P., *et al.* (2009) 'CD47 Is an Adverse Prognostic Factor and Therapeutic Antibody Target on Human Acute Myeloid Leukemia Stem Cells', *Cell*. Elsevier Ltd, 138(2), pp. 286–299. doi: 10.1016/j.cell.2009.05.045.

Majeti, R., Becker, M. W., *et al.* (2009) 'Dysregulated gene expression networks in human acute myelogenous leukemia stem cells', *Proceedings of the National Academy of Sciences of the United States of America*, 106(9), pp. 3396–3401. doi: 10.1073/pnas.0900089106.

Malikic, S. *et al.* (2019) 'PhISCS: a combinatorial approach for subperfect tumor phylogeny reconstruction via integrative use of single-cell and bulk sequencing data', *Genome Research*, 29(11), pp. 1860–1877. doi: 10.1101/gr.234435.118.

Man, Y. *et al.* (2021) 'Hematopoietic Stem Cell Niche During Homeostasis, Malignancy, and Bone Marrow Transplantation', *Frontiers in Cell and Developmental Biology*, 9. doi: 10.3389/fcell.2021.621214.

Mardis, E. R. *et al.* (2009) 'Recurring mutations found by sequencing an acute myeloid leukemia genome.', *The New England Journal of Medicine*, 361(11), pp. 1058–66. doi: 10.1056/NEJMoa0903840.

Matatall, K. A. *et al.* (2014) 'Type II Interferon Promotes Differentiation of Myeloid-Biased Hematopoietic Stem Cells', *STEM CELLS*, 32(11), pp. 3023–3030. doi: 10.1002/stem.1799.

McCormick, P. J., Martina, J. A. and Bonifacino, J. S. (2005) 'Involvement of clathrin and AP-2 in the trafficking of MHC class II molecules to antigen-processing compartments', *Proceedings of the National Academy of Sciences*, 102(22), pp. 7910–7915. doi: 10.1073/pnas.0502206102.

Meacham, C. E. and Morrison, S. J. (2013) 'Tumour heterogeneity and cancer cell plasticity.', *Nature*, 501(7467), pp. 328–37. doi: 10.1038/nature12624.

Mellins, E. D. and Stern, L. J. (2014) 'HLA-DM and HLA-DO, key regulators of MHC-II processing and presentation', *Current Opinion in Immunology*. Elsevier Ltd, 26(1), pp. 115–122. doi: 10.1016/j.coi.2013.11.005.

Méndez-Ferrer, S. *et al.* (2020) 'Bone marrow niches in haematological malignancies', *Nature Reviews Cancer*, 20(5), pp. 285–298. doi: 10.1038/s41568-020-0245-2.

'Mentoring the Next Generation: Andreas Trumpp' (2018) *Cell Stem Cell*, 23(3), pp. 326–328. doi: 10.1016/j.stem.2018.08.004.

Merad, M. *et al.* (2013) 'The Dendritic Cell Lineage: Ontogeny and Function of Dendritic Cells and Their Subsets in the Steady State and the Inflamed Setting', *Annual Review of Immunology*, 31(1), pp. 563–604. doi: 10.1146/annurev-immunol-020711-074950.

Mercier, F. E., Ragu, C. and Scadden, D. T. (2012) 'The bone marrow at the crossroads of blood and immunity', *Nature Reviews Immunology*. Nature Publishing Group, 12(1), pp. 49–60. doi: 10.1038/nri3132.

Meredith, M. *et al.* (2015) 'Aire controls gene expression in the thymic epithelium with ordered stochasticity', *Nature Immunology*, 16(9), pp. 942–949. doi: 10.1038/ni.3247.

Miale, T. D. *et al.* (1982) 'Surface Ia-Like Expression and MLR-Stimulating Capacity of Human Leukemic Myeloblasts: Implications for Immunotherapy and Prognosis', *Acta Haematologica*, 68(1), pp. 3–13. doi: 10.1159/000206941.

Miraki-Moud, F. *et al.* (2013) 'Acute myeloid leukemia does not deplete normal hematopoietic stem cells but induces cytopenias by impeding their differentiation.', *Proceedings of the National Academy of Sciences of the United States of America*, 110(33), pp. 13576–81. doi: 10.1073/pnas.1301891110.

Mojsilovic, S. *et al.* (2015) 'Interleukin-17 and its implication in the regulation of differentiation and function of hematopoietic and mesenchymal stem cells', *Mediators of Inflammation*, 2015. doi: 10.1155/2015/470458.

Monteiro, J. P. *et al.* (2005) 'Normal hematopoiesis is maintained by activated bone marrow CD4+ T cells', *Blood*, 105(4), pp. 1484–1491. doi: 10.1182/blood-2004-07-2856.

Morrison, S. J. and Kimble, J. (2006) 'Asymmetric and symmetric stem-cell divisions in development and cancer', *Nature*, 441(7097), pp. 1068–1074. doi: 10.1038/nature04956.

Morrison, S. J. and Spradling, A. C. (2008) 'Stem Cells and Niches: Mechanisms That Promote Stem Cell Maintenance throughout Life', *Cell*, 132(4), pp. 598–611. doi: 10.1016/j.cell.2008.01.038.

Murphy, D. B. *et al.* (1989) 'A novel MHC class II epitope expressed in thymic medulla but not cortex', *Nature*, 338(6218), pp. 765–768. doi: 10.1038/338765a0.

Murry, C. E. and Keller, G. (2008) 'Differentiation of Embryonic Stem Cells to Clinically Relevant Populations: Lessons from Embryonic Development', *Cell*, 132(4), pp. 661–680. doi: 10.1016/j.cell.2008.02.008.

Mutis, T. *et al.* (1997) 'HLA Class II Restricted T-Cell Reactivity to a Developmentally Regulated Antigen Shared by Leukemic Cells and CD34+ Early Progenitor Cells', *Blood*, 90(3), pp. 1083–1090. doi: 10.1182/blood.V90.3.1083.1083_1083_1090.

Mutis, T. *et al.* (1998) 'CD80-Transfected Acute Myeloid Leukemia Cells Induce Primary Allogeneic T-Cell Responses Directed at Patient Specific Minor Histocompatibility Antigens and

Leukemia-Associated Antigens', *Blood*, 92(5), pp. 1677–1684. doi: 10.1182/blood.V92.5.1677.417k14_1677_1684.

Naik, S. *et al.* (2018) 'Two to Tango: Dialog between Immunity and Stem Cells in Health and Disease', *Cell*. Elsevier Inc., 175(4), pp. 908–920. doi: 10.1016/j.cell.2018.08.071.

Nakao, S. *et al.* (1994) 'Identification of a specific HLA class II haplotype strongly associated with susceptibility to cyclosporine-dependent aplastic anemia', *Blood*, 84(12), pp. 4257–4261. doi: 10.1182/blood.V84.12.4257.bloodjournal84124257.

Nam, A. S. *et al.* (2019) 'Somatic mutations and cell identity linked by Genotyping of Transcriptomes', *Nature*, 571(7765), pp. 355–360. doi: 10.1038/s41586-019-1367-0.

Neefjes, J. *et al.* (2011) 'Towards a systems understanding of MHC class I and MHC class II antigen presentation', *Nature Reviews Immunology*. Nature Publishing Group, 11(12), pp. 823–836. doi: 10.1038/nri3084.

Netea, M. G. *et al.* (2020) 'Defining trained immunity and its role in health and disease', *Nature Reviews Immunology*, 20(6), pp. 375–388. doi: 10.1038/s41577-020-0285-6.

Neumuller, R. A. and Knoblich, J. A. (2009) 'Dividing cellular asymmetry: asymmetric cell division and its implications for stem cells and cancer', *Genes & Development*, 23(23), pp. 2675–2699. doi: 10.1101/gad.1850809.

Newman, R. A. *et al.* (1983) 'Differential expression of HLA-DR and DR-linked determinants on human leukemias and lymphoid cells', *European Journal of Immunology*, 13(2), pp. 172–176. doi: 10.1002/eji.1830130215.

Newman, R. A. and Greaves, M. F. (1982) 'Characterization of HLA-DR antigens on leukaemic cells', *Clinical and Experimental Immunology*, 50(1), pp. 41–50.

Ng, S. W. K. *et al.* (2016) 'A 17-gene stemness score for rapid determination of risk in acute leukaemia', *Nature*. Nature Publishing Group, 540(7633), pp. 433–437. doi: 10.1038/nature20598.

Nimer, S. D. *et al.* (1994) 'An increased HLA DR2 frequency is seen in aplastic anemia patients.', *Blood*, 84(3), pp. 923–7.

Novershtern, N. *et al.* (2011) 'Densely Interconnected Transcriptional Circuits Control Cell States in Human Hematopoiesis', *Cell*. Elsevier Inc., 144(2), pp. 296–309. doi: 10.1016/j.cell.2011.01.004.

Nowak, J. *et al.* (2013) 'Potential link between MHC-self-peptide presentation and hematopoiesis; the analysis of HLA-DR expression in CD34-positive cells and self-peptide presentation repertoires of MHC molecules associated with paroxysmal nocturnal hemoglobinuria', *Cell Biochemistry and Biophysics*, 65(3), pp. 321–333. doi: 10.1007/s12013-012-9435-1.

Ogawa, M. and Matsunaga, T. (1999) 'Humoral regulation of hematopoietic stem cells', *Annals of the New York Academy of Sciences*, 872, pp. 17–24. doi: 10.1111/j.1749-

6632.1999.tb08449.x.

Okumura, N., Tsuji, K. and Nakahata, T. (1992) 'Changes in cell surface antigen expressions during proliferation and differentiation of human erythroid progenitors', *Blood*, 80(3), pp. 642–650. doi: 10.1182/blood.v80.3.642.bloodjournal803642.

Oliphant, C. J. *et al.* (2014) 'MHCII-mediated dialog between group 2 innate lymphoid cells and CD4+ T cells potentiates type 2 immunity and promotes parasitic helminth expulsion', *Immunity*. The Authors, 41(2), pp. 283–295. doi: 10.1016/j.immuni.2014.06.016.

Orkin, S. H. and Zon, L. I. (2008) 'Hematopoiesis: An Evolving Paradigm for Stem Cell Biology', *Cell*, 132, pp. 631–644. doi: 10.1016/j.cell.2008.01.025.

Pabst, C. *et al.* (2016) 'GPR56 identifies primary human acute myeloid leukemia cells with high repopulating potential in vivo.', *Blood*, 127(16), pp. 2018–2027. doi: 10.1182/blood-2015-11-683649.

Palucka, K. and Banchereau, J. (1999) 'Dendritic cells: a link between innate and adaptive immunity.', *Journal of clinical immunology*, 19(1), pp. 12–25. doi: 10.1023/a:1020558317162.

Papaemmanuil, E. *et al.* (2016) 'Genomic Classification and Prognosis in Acute Myeloid Leukemia', *New England Journal of Medicine*, 374(23), pp. 2209–2221. doi: 10.1056/NEJMoa1516192.

Paul, F. *et al.* (2015) 'Transcriptional Heterogeneity and Lineage Commitment in Myeloid Progenitors', *Cell*. Elsevier Inc., 163(7), pp. 1663–1677. doi: 10.1016/j.cell.2015.11.013.

Pellin, D. *et al.* (2019) 'A comprehensive single cell transcriptional landscape of human hematopoietic progenitors', *Nature Communications*, 10(1), p. 2395. doi: 10.1038/s41467-019-10291-0.

Petti, A. A. *et al.* (2019) 'A general approach for detecting expressed mutations in AML cells using single cell RNA-sequencing', *Nature Communications*, 10(1), p. 3660. doi: 10.1038/s41467-019-11591-1.

Picelli, S. *et al.* (2013) 'Smart-seq2 for sensitive full-length transcriptome profiling in single cells', *Nature Methods*, 10(11), pp. 1096–1098. doi: 10.1038/nmeth.2639.

Picelli, S. *et al.* (2014) 'Full-length RNA-seq from single cells using Smart-seq2', *Nature Protocols*, 9(1), pp. 171–181. doi: 10.1038/nprot.2014.006.

Pierini, A. *et al.* (2017) 'Foxp3+ regulatory T cells maintain the bone marrow microenvironment for B cell lymphopoiesis', *Nature Communications*. Nature Publishing Group, 8(1), p. 15068. doi: 10.1038/ncomms15068.

Pietras, E. M. *et al.* (2016) 'Chronic interleukin-1 exposure drives haematopoietic stem cells towards precocious myeloid differentiation at the expense of self-renewal', *Nature Cell Biology*, 18(6), pp. 607–618. doi: 10.1038/ncb3346.

Pietras, E. M. (2017) 'Inflammation: a key regulator of hematopoietic stem cell fate in health

and disease', *Blood*, 130(15), pp. 1693–1698. doi: 10.1182/blood-2017-06-780882.

Pinho, S. and Frenette, P. S. (2019) 'Haematopoietic stem cell activity and interactions with the niche', *Nature Reviews Molecular Cell Biology*. Springer US, 20(5), pp. 303–320. doi: 10.1038/s41580-019-0103-9.

Platten, M. *et al.* (2021) 'A vaccine targeting mutant IDH1 in newly diagnosed glioma', *Nature*, 592(7854), pp. 463–468. doi: 10.1038/s41586-021-03363-z.

Pollyea, D. A. and Jordan, C. T. (2017) 'Therapeutic targeting of acute myeloid leukemia stem cells', *Blood*. American Society of Hematology, 129(12), pp. 1627–1635. doi: 10.1182/blood-2016-10-696039.

Pölönen, P. *et al.* (2019) 'Hemap: An Interactive Online Resource for Characterizing Molecular Phenotypes across Hematologic Malignancies', *Cancer Research*, 79(10), pp. 2466–2479. doi: 10.1158/0008-5472.CAN-18-2970.

Post, Y. and Clevers, H. (2019) 'Defining Adult Stem Cell Function at Its Simplest: The Ability to Replace Lost Cells through Mitosis', *Cell Stem Cell*, 25(2), pp. 174–183. doi: 10.1016/j.stem.2019.07.002.

Price, P. W. and Cerny, J. (1999) 'Characterization of CD4+ T cells in mouse bone marrow. I. Increased activated/memory phenotype and altered TCR Vbeta repertoire.', *European journal of immunology*, 29(3), pp. 1051–1056. doi: 10.1002/(SICI)1521-4141(199903)29:03<1051::AID-IMMU1051>3.0.CO;2-Y.

Raffel, S. *et al.* (2017) 'BCAT1 restricts αkG levels in AML stem cells leading to IDHmut-like DNA hypermethylation', *Nature*. Nature Publishing Group, 551(7680), pp. 384–388. doi: 10.1038/nature24294.

Rathinam, C. *et al.* (2010) 'Myeloid leukemia development in c-Cbl RING finger mutant mice is dependent on FLT3 signaling', *Cancer Cell*. Elsevier Inc., 18(4), pp. 341–352. doi: 10.1016/j.ccr.2010.09.008.

Rehman, S. *et al.* (2009) 'The Frequency of HLA Class I and II Alleles in Pakistani Patients with Aplastic Anemia', *Immunological Investigations*, 38(8), pp. 812–819. doi: 10.3109/08820130903271415.

Reinhardt, R. L. *et al.* (2001) 'Visualizing the generation of memory CD4 T cells in the whole body', *Nature*, 410(6824), pp. 101–105. doi: 10.1038/35065111.

Riether, C., Schürch, C. M. and Ochsenbein, A. F. (2015) 'Regulation of hematopoietic and leukemic stem cells by the immune system', *Cell Death & Differentiation*, 22(2), pp. 187–198. doi: 10.1038/cdd.2014.89.

Robinson, J. *et al.* (1981) 'Expression of cell-surface HLA-DR, HLA-ABC and glycophorin during erythroid differentiation', *Nature*, 289(5793), pp. 68–71. doi: 10.1038/289068a0.

Roche, P. A. and Furuta, K. (2015) 'The ins and outs of MHC class II-mediated antigen processing and presentation', *Nature Reviews Immunology*. Nature Publishing Group, 15(4),

pp. 203–216. doi: 10.1038/nri3818.

Rock, K. L., Reits, E. and Neefjes, J. (2016) 'Present Yourself ! By MHC Class I and MHC Class II Molecules', *Trends in Immunology*. Elsevier Ltd, 37(11), pp. 724–737. doi: 10.1016/j.it.2016.08.010.

Rodriguez-Meira, A. *et al.* (2019) 'Unravelling Intratumoral Heterogeneity through High-Sensitivity Single-Cell Mutational Analysis and Parallel RNA Sequencing', *Molecular Cell*, 73(6), pp. 1292-1305.e8. doi: 10.1016/j.molcel.2019.01.009.

Roerden, M., Nelde, A. and Walz, J. S. (2019) 'Neoantigens in Hematological Malignancies-Ultimate Targets for Immunotherapy?', *Frontiers in immunology*, 10, p. 3004. doi: 10.3389/fimmu.2019.03004.

Roncarolo, M. G. *et al.* (2018) 'The Biology of T Regulatory Type 1 Cells and Their Therapeutic Application in Immune-Mediated Diseases', *Immunity*. Elsevier Inc., 49(6), pp. 1004–1019. doi: 10.1016/j.immuni.2018.12.001.

Di Rosa, F. and Gebhardt, T. (2016) 'Bone Marrow T Cells and the Integrated Functions of Recirculating and Tissue-Resident Memory T Cells', *Frontiers in Immunology*, 7(51). doi: 10.3389/fimmu.2016.00051.

Rossant, J. and Tam, P. P. L. (2017) 'New Insights into Early Human Development: Lessons for Stem Cell Derivation and Differentiation', *Cell Stem Cell*, 20(1), pp. 18–28. doi: 10.1016/j.stem.2016.12.004.

Rudensky, A. Y. *et al.* (1991) 'On the complexity of self', *Nature*, 353(6345), pp. 660–662. doi: 10.1038/353660a0.

Russell, J. L. and Engh, G. J. (1979) 'The Expression of Histocompatibility-2 Antigens on Hemopoietic Stem Cells', *Tissue Antigens*, 13. doi: http://doi.wiley.com/10.1111/j.1399-0039.1979.tb01135.x.

Rutten, C. E. *et al.* (2013) 'Patient HLA-DP-specific CD4+ T cells from HLA-DPB1-mismatched donor lymphocyte infusion can induce graft-versus-leukemia reactivity in the presence or absence of graft-versus-host disease.', *Biology of blood and marrow transplantation : journal of the American Society for Blood and Marrow Transplantation*, 19(1), pp. 40–8. doi: 10.1016/j.bbmt.2012.07.020.

Sakaguchi, S. *et al.* (2008) 'Regulatory T Cells and Immune Tolerance', *Cell*, 133(5), pp. 775–787. doi: 10.1016/j.cell.2008.05.009.

Sato, K. *et al.* (2003) 'Regulatory dendritic cells protect mice from murine acute graft-versus-host disease and leukemia relapse', *Immunity*, 18(3), pp. 367–379. doi: 10.1016/S1074-7613(03)00055-4.

Sauntharajah, Y. *et al.* (2002) 'HLA-DR15 (DR2) is overrepresented in myelodysplastic syndrome and aplastic anemia and predicts a response to immunosuppression in myelodysplastic syndrome', *Blood*, 100(5), pp. 1570–1574. doi: 10.1182/blood.V100.5.1570.h81702001570_1570_1574.

Scadden, D. T. (2006) 'The stem-cell niche as an entity of action', *Nature*, 441(7097), pp. 1075–1079. doi: 10.1038/nature04957.

Schallmoser, K. *et al.* (2008) 'Rapid Large-Scale Expansion of Functional Mesenchymal Stem Cells from Unmanipulated Bone Marrow Without Animal Serum', *Tissue Engineering Part C: Methods*, 14(3), pp. 185–196. doi: 10.1089/ten.tec.2008.0060.

Schatz, D. G. and Ji, Y. (2011) 'Recombination centres and the orchestration of V(D)J recombination', *Nature Reviews Immunology*, 11(4), pp. 251–263. doi: 10.1038/nri2941.

Scheinberg, P. and Young, N. S. (2012) 'How I treat acquired aplastic anemia', *Blood*, 120(6), pp. 1185–1196. doi: 10.1182/blood-2011-12-274019.

Schenkel, J. M. and Masopust, D. (2014) 'Tissue-resident memory T cells', *Immunity*. Elsevier Inc., 41(6), pp. 886–897. doi: 10.1016/j.immuni.2014.12.007.

Schneider, E. *et al.* (1997) 'Hematopoietic changes induced by a single injection of anti-CD3 monoclonal antibody into normal mice.', *Stem cells*, 15(2), pp. 154–160.

Schroeder, T. (2010) 'Hematopoietic Stem Cell Heterogeneity: Subtypes, Not Unpredictable Behavior', *Cell Stem Cell*, 6(3), pp. 203–207. doi: 10.1016/j.stem.2010.02.006.

Schumacher, T. *et al.* (2014) 'A vaccine targeting mutant IDH1 induces antitumour immunity', *Nature*, 512(7514), pp. 324–327. doi: 10.1038/nature13387.

Sharma, P. and Allison, J. P. (2015) 'Immune Checkpoint Targeting in Cancer Therapy: Toward Combination Strategies with Curative Potential', *Cell*, 161(2), pp. 205–214. doi: 10.1016/j.cell.2015.03.030.

Sharpe, A. H. and Pauken, K. E. (2018) 'The diverse functions of the PD1 inhibitory pathway', *Nature Reviews Immunology*, 18(3), pp. 153–167. doi: 10.1038/nri.2017.108.

Shimazu, T. *et al.* (2012) 'CD86 is expressed on murine hematopoietic stem cells and denotes lymphopoietic potential', *Blood*, 119(21), pp. 4889–4897. doi: 10.1182/blood-2011-10-388736.

Shlush, L. I. *et al.* (2014) 'Identification of pre-leukaemic haematopoietic stem cells in acute leukaemia', *Nature*. Nature Publishing Group, 506(7488), pp. 328–333. doi: 10.1038/nature13038.

Shlush, Liran I *et al.* (2017) 'Tracing the origins of relapse in acute myeloid leukaemia to stem cells', *Nature*. Nature Publishing Group, 547(7661), pp. 104–108. doi: 10.1038/nature22993.

Sieff, C. *et al.* (1982) 'Changes in Cell Surface Antigen Expression During Hemopoietic Differentiation', *Blood*, 60(3).

Siracusa, F. *et al.* (2017) 'Nonfollicular reactivation of bone marrow resident memory CD4 T cells in immune clusters of the bone marrow', *Proceedings of the National Academy of Sciences*, pp. 1–6. doi: 10.1073/pnas.1715618115.

Solomou, E. E., Keyvanfar, K. and Young, N. S. (2006) 'T-bet, a Th1 transcription factor, is up-regulated in T cells from patients with aplastic anemia', *Blood*, 107(10), pp. 3983–3991. doi: 10.1182/blood-2005-10-4201.

Spencer, S. D. *et al.* (1998) 'The Orphan Receptor CRF2-4 Is an Essential Subunit of the Interleukin 10 Receptor', *Journal of Experimental Medicine*, 187(4), pp. 571–578. doi: 10.1084/jem.187.4.571.

Sperling, A. S., Gibson, C. J. and Ebert, B. L. (2016) 'The genetics of myelodysplastic syndrome: from clonal haematopoiesis to secondary leukaemia', *Nature Reviews Cancer*. Nature Publishing Group, advance on(1), pp. 5–19. doi: 10.1038/nrc.2016.112.

Spranger, S. and Gajewski, T. F. (2018) 'Mechanisms of Tumor Cell–Intrinsic Immune Evasion', *Annual Review of Cancer Biology*, 2(1), pp. 213–228. doi: 10.1146/annurev-cancerbio-030617-050606.

Steensma, D. P. *et al.* (2015) 'Clonal hematopoiesis of indeterminate potential and its distinction from myelodysplastic syndromes', *Blood*, 126(1), pp. 9–16. doi: 10.1182/blood-2015-03-631747.

Steimle, V. *et al.* (1993) 'Complementation cloning of an MHC class II transactivator mutated in hereditary MHC class II deficiency (or bare lymphocyte syndrome)', *Cell*, 75(1), pp. 135–146. doi: 10.1016/S0092-8674(05)80090-X.

Steimle, V. *et al.* (1994) 'Regulation of MHC class II expression by interferon-γ mediated by the transactivator gene CIITA', *Science*, 265(5168), pp. 106–109. doi: 10.1126/science.8016643.

Steinman, R. M. (2007) 'Dendritic cells: Understanding immunogenicity', *European Journal of Immunology*, 37(SUPPL. 1), pp. 53–60. doi: 10.1002/eji.200737400.

Su, H. *et al.* (2017) 'The biological function and significance of CD74 in immune diseases', *Inflammation Research*, 66(3), pp. 209–216. doi: 10.1007/s00011-016-0995-1.

Sun, J. C., Beilke, J. N. and Lanier, L. L. (2009) 'Adaptive immune features of natural killer cells', *Nature*, 457(7229), pp. 557–561. doi: 10.1038/nature07665.

Sweeney, C. and Vyas, P. (2019) 'The Graft-Versus-Leukemia Effect in AML.', *Frontiers in oncology*, 9, p. 1217. doi: 10.3389/fonc.2019.01217.

Szer, J. *et al.* (1985) 'Failure of autologous marrow reconstitution after cytolytic treatment of marrow with anti-Ia monoclonal antibody', *Blood*, 65(4), pp. 819–822. doi: 10.1182/blood.v65.4.819.bloodjournal654819.

Tajbakhsh, S. (2003) 'Stem cells to tissue: molecular, cellular and anatomical heterogeneity in skeletal muscle', *Current Opinion in Genetics & Development*, 13(4), pp. 413–422. doi: 10.1016/S0959-437X(03)00090-X.

Tang, Q. and Bluestone, J. A. (2008) 'The Foxp3+ regulatory T cell: a jack of all trades, master of regulation', *Nature Immunology*, 9(3), pp. 239–244. doi: 10.1038/ni1572.

Tarasov, A. *et al.* (2015) 'Sambamba: fast processing of NGS alignment formats', *Bioinformatics*, 31(12), pp. 2032–2034. doi: 10.1093/bioinformatics/btv098.

Tikhonova, A. N. *et al.* (2019) 'The bone marrow microenvironment at single-cell resolution', *Nature*, 569(7755), pp. 222–228. doi: 10.1038/s41586-019-1104-8.

Tober, J. *et al.* (2018) 'Maturation of hematopoietic stem cells from prehematopoietic stem cells is accompanied by up-regulation of PD-L1', *Journal of Experimental Medicine*, 215(2), pp. 645–659. doi: 10.1084/jem.20161594.

Toffalori, C. *et al.* (2019) 'Immune signature drives leukemia escape and relapse after hematopoietic cell transplantation', *Nature Medicine*. Springer US, 25(4), pp. 603–611. doi: 10.1038/s41591-019-0400-z.

Tokoyoda, K. *et al.* (2009) 'Professional Memory CD4+ T Lymphocytes Preferentially Reside and Rest in the Bone Marrow', *Immunity*, 30(5), pp. 721–730. doi: 10.1016/j.immuni.2009.03.015.

Trumpp, A., Essers, M. and Wilson, A. (2010) 'Awakening dormant haematopoietic stem cells', *Nature Reviews Immunology*. Nature Publishing Group, 10(3), pp. 201–209. doi: 10.1038/nri2726.

Trumpp, A. and Wiestler, O. D. (2008) 'Mechanisms of Disease: Cancer stem cells-targeting the evil twin', *Nature Clinical Practice Oncology*, 5(6), pp. 337–347. doi: 10.1038/ncponc1110.

Turvey, S. E. and Broide, D. H. (2010) 'Innate immunity', *Journal of Allergy and Clinical Immunology*, 125(2), pp. S24–S32. doi: 10.1016/j.jaci.2009.07.016.

Uckelmann, H. J. *et al.* (2020) 'Therapeutic targeting of preleukemia cells in a mouse model of NPM1 mutant acute myeloid leukemia', *Science*, 367(6477), pp. 586–590. doi: 10.1126/science.aax5863.

Urbieta, M. *et al.* (2010) 'Hematopoietic progenitor cell regulation by CD4+CD25+ T cells', *Blood*, 115(23), pp. 4934–4943. doi: 10.1182/blood-2009-04-218826.

Vago, L. and Gojo, I. (2020) 'Immune escape and immunotherapy of acute myeloid leukemia', *Journal of Clinical Investigation*, 130(4), pp. 1552–1564. doi: 10.1172/JCI129204.

Velten, L. *et al.* (2017) 'Human haematopoietic stem cell lineage commitment is a continuous process without discrete progenitor populations', *Nature Cell Biology*, 19(4). doi: 10.1038/ncb3493.

Velten, L. *et al.* (2021) 'Identification of leukemic and pre-leukemic stem cells by clonal tracking from single-cell transcriptomics', *Nature Communications*, 12(1), p. 1366. doi: 10.1038/s41467-021-21650-1.

Vono, M. *et al.* (2017) 'Neutrophils acquire antigen presentation capacity to memory CD4+ T cells in vitro and ex vivo', *Blood*, 129(14), p. blood-2016-10-744441. doi: 10.1182/blood-2016-10-744441.

Walter, D. *et al.* (2015) 'Exit from dormancy provokes DNA-damage-induced attrition in haematopoietic stem cells', *Nature*, 520(7548), pp. 549–552. doi: 10.1038/nature14131.

Wang, J. C. Y. and Dick, J. E. (2005) 'Cancer stem cells: Lessons from leukemia', *Trends in Cell Biology*, 15(9), pp. 494–501. doi: 10.1016/j.tcb.2005.07.004.

Wang, K., Li, M. and Hakonarson, H. (2010) 'ANNOVAR: functional annotation of genetic variants from high-throughput sequencing data', *Nucleic Acids Research*, 38(16), pp. e164–e164. doi: 10.1093/nar/gkq603.

Wei, Q. and Frenette, P. S. (2018) 'Niches for Hematopoietic Stem Cells and Their Progeny', *Immunity*. Elsevier Inc., 48(4), pp. 632–648. doi: 10.1016/j.immuni.2018.03.024.

Welch, J. S. *et al.* (2012) 'The origin and evolution of mutations in acute myeloid leukemia', *Cell*, 150(2), pp. 264–278. doi: 10.1016/j.cell.2012.06.023.

Wieczorek, M. *et al.* (2017) 'Major Histocompatibility Complex (MHC) Class I and MHC Class II Proteins: Conformational Plasticity in Antigen Presentation', *Frontiers in Immunology*, 8. doi: 10.3389/fimmu.2017.00292.

Wilson, A. *et al.* (2008) 'Hematopoietic Stem Cells Reversibly Switch from Dormancy to Self-Renewal during Homeostasis and Repair', *Cell*, 135(6), pp. 1118–1129. doi: 10.1016/j.cell.2008.10.048.

Wilson, C. B., Rowell, E. and Sekimata, M. (2009) 'Epigenetic control of T-helper-cell differentiation', *Nature Reviews Immunology*, 9(2), pp. 91–105. doi: 10.1038/nri2487.

Xie, M. *et al.* (2014) 'Age-related mutations associated with clonal hematopoietic expansion and malignancies.', *Nature medicine*. Nature Publishing Group, 20(12), pp. 1472–8. doi: 10.1038/nm.3733.

Xing, Y. and Hogquist, K. A. (2012) 'T-Cell Tolerance : Central and Peripheral', *CSH Perspectives*, pp. 1–16.

Xu, J. *et al.* (2019) 'Single-cell lineage tracing by endogenous mutations enriched in transposase accessible mitochondrial DNA', *eLife*, 8. doi: 10.7554/eLife.45105.

Yamashita, M. *et al.* (2020) 'Dysregulated haematopoietic stem cell behaviour in myeloid leukaemogenesis', *Nature Reviews Cancer*. Springer US, 20(July). doi: 10.1038/s41568-020-0260-3.

Yang, L. *et al.* (2016) 'DNMT3A Loss Drives Enhancer Hypomethylation in FLT3-ITD-Associated Leukemias', *Cancer Cell*, 29(6), pp. 922–934. doi: 10.1016/j.ccell.2016.05.003.

Ye, M. *et al.* (2015) 'Hematopoietic Differentiation Is Required for Initiation of Acute Myeloid Leukemia', *Cell Stem Cell*. Elsevier Inc., 17(5), pp. 611–623. doi: 10.1016/j.stem.2015.08.011.

Young, A. L. *et al.* (2016) 'Clonal haematopoiesis harbouring AML-associated mutations is ubiquitous in healthy adults', *Nature Communications*. Nature Publishing Group, 7, pp. 1–7. doi: 10.1038/ncomms12484.

Young, N. S. (2018) 'Aplastic Anemia', *New England Journal of Medicine*, 379(17), pp. 1643–1656. doi: 10.1056/NEJMra1413485.

Young, R. A. (2011) 'Control of the Embryonic Stem Cell State', *Cell*, 144(6), pp. 940–954. doi: 10.1016/j.cell.2011.01.032.

Youngblood, B., Hale, J. S. and Ahmed, R. (2013) 'T-cell memory differentiation: Insights from transcriptional signatures and epigenetics', *Immunology*, 139(3), pp. 277–284. doi: 10.1111/imm.12074.

Yu, G. *et al.* (2012) 'clusterProfiler: an R Package for Comparing Biological Themes Among Gene Clusters', *OMICS: A Journal of Integrative Biology*, 16(5), pp. 284–287. doi: 10.1089/omi.2011.0118.

Yunis, J. J. *et al.* (1989) 'Differential expression of MHC class II antigens in myelomonocytic leukemia cell lines', *Blood*, 73(4), pp. 931–937. doi: 10.1182/blood.v73.4.931.bloodjournal734931.

Zeng, H. *et al.* (2015) 'Type 1 regulatory T cells: a new mechanism of peripheral immune tolerance', *Cellular and Molecular Immunology*, 12(5), pp. 566–571. doi: 10.1038/cmi.2015.44.

Zhang, N. and Bevan, M. J. (2011) 'CD8+ T Cells: Foot Soldiers of the Immune System', *Immunity*, 35(2), pp. 161–168. doi: 10.1016/j.immuni.2011.07.010.

Zhang, P. *et al.* (2018) 'Eomesodermin Promotes the Development of Type-1 Regulatory T (TR1) Cells', *Science Immunology*, 2(10). doi: 10.1126/sciimmunol.aah7152.Eomesodermin.

Zhao, X. *et al.* (2020) 'Interactions of Hematopoietic Stem Cells with Bone Marrow Niche', in, pp. 21–34. doi: 10.1007/7651_2020_298.

Zhu, J. and Paul, W. E. (2008) 'CD4 T cells: fates, functions, and faults', *Blood*, 112(5), pp. 1557–1569. doi: 10.1182/blood-2008-05-078154.

Zhu, J. and Paul, W. E. (2010) 'Peripheral CD4+ T-cell differentiation regulated by networks of cytokines and transcription factors', *Immunological Reviews*, 238(1), pp. 247–262. doi: 10.1111/j.1600-065X.2010.00951.x.

Zink, F. *et al.* (2017) 'Clonal hematopoiesis, with and without candidate driver mutations, is common in the elderly', *Blood*, 130(6), pp. 742–752. doi: 10.1182/blood-2017-02-769869.

Zou, L. *et al.* (2004) 'Bone Marrow Is a Reservoir for CD4 + CD25 + Regulatory T Cells that Traffic through CXCL12/CXCR4 Signals', *Cancer Research*, 64(22), pp. 8451–8455. doi: 10.1158/0008-5472.CAN-04-1987.